ACS MEASUREMENT SCIENCE Au
AN OPEN ACCESS JOURNAL OF THE AMERICAN CHEMICAL SOCIETY

pubs.acs.org/measureau
Review

Advances in Bioelectrode Design for Developing Electrochemical Biosensors

Nabajyoti Kalita,[¶] Sudarshan Gogoi,[¶] Shelley D. Minteer,[*] and Pranab Goswami[*]

Cite This: ACS Meas. Sci. Au 2023, 3, 404–433
Read Online
ACCESS | Metrics & More | Article Recommendations

ABSTRACT: The critical performance factors such as selectivity, sensitivity, operational and storage stability, and response time of electrochemical biosensors are governed mainly by the function of their key component, the bioelectrode. Suitable design and fabrication strategies of the bioelectrode interface are essential for realizing the requisite performance of the biosensors for their practical utility. A multifaceted attempt to achieve this goal is visible from the vast literature exploring effective strategies for preparing, immobilizing, and stabilizing biorecognition elements on the electrode surface and efficient transduction of biochemical signals into electrical ones (i.e., current, voltage, and impedance) through the bioelectrode interface with the aid of advanced materials and techniques. The commercial success of biosensors in modern society is also increasingly influenced by their size (and hence portability), multiplexing capability, and coupling in the interface of the wireless communication technology, which facilitates quick data transfer and linked decision-making processes in real-time in different areas such as healthcare, agriculture, food, and environmental applications. Therefore, fabrication of the bioelectrode involves careful selection and control of several parameters, including biorecognition elements, electrode materials, shape and size of the electrode, detection principles, and various fabrication strategies, including microscale and printing technologies. This review discusses recent trends in bioelectrode designs and fabrications for developing electrochemical biosensors. The discussions have been delineated into the types of biorecognition elements and their immobilization strategies, signal transduction approaches, commonly used advanced materials for electrode fabrication and techniques for fabricating the bioelectrodes, and device integration with modern electronic communication technology for developing electrochemical biosensors of commercial interest.

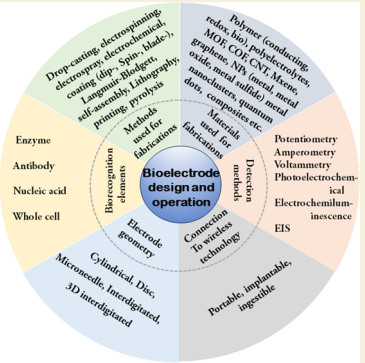

KEYWORDS: *bioelectrode fabrication, biorecognition elements, nanomaterials, lithographic techniques, 3D printing, electrode geometry, wireless technology, miniaturized biosensor*

1. INTRODUCTION

The bioelectrode is a key component of various electrochemical biosensors as it governs the critical performance factors of these devices.[1] As the name implies, the bioelectrode primarily constitutes a biological material, widely known as the biorecognition element and a solid conductive electrode substrate. The biorecognition element is kept in close conjunction (usually immobilized) with the electrode to transduce the substrate-dependent biochemical signal occurring over the bioelectrode surface to a measurable electrical signal (voltage, current, etc.).[2] An effective interaction between the biorecognition element and the underneath electrode substrate is essential to generate and amplify the response signal. Additionally, the interactive physicochemical environment should offer a conducive environment to the labile biorecognition elements for a better shelf life and operational stability of the constructs.[1] Therefore, the bioelectrode interface's design is critical to improving the performance factors such as selectivity, sensitivity, response time, stability, and reproducibility of the fabricated device that eventually contribute to the commercial success of the developed device.[3] Different emerging and advanced materials, such as smart and nanomaterials and conductive and biocompatible polymers, are used along with the biorecognition elements to fabricate the bioelectrode for improving its aforesaid performance factors.

Research articles focusing on different aspects of electrochemical biosensors, such as applications and challenges,[4] carbonaceous nanomaterials,[5] nanomaterials in enzyme-based electrochemical biosensors[6] are numerous. However, this review emphasizes the progress in developing bioelectrodes, encompassing various critical aspects of their design and fabrication. We have also attempted to cover the aspects of device miniaturization, multiplex analyses, and its coupling to

Received: August 1, 2023
Revised: September 26, 2023
Accepted: September 27, 2023
Published: October 27, 2023

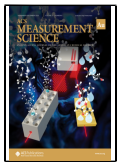

modern communication technology for on-site and remote-control applications.

2. BIORECOGNITION ELEMENTS AND SIGNAL TRANSDUCTION

2.1. Biorecognition Elements

The specificity of the bioelectrode primarily stems from the strong and selective affinity and catalytic activity between the biorecognition element and the target analyte.[7,8] However, some supporting materials in the bioelectrode, such as ion selective membrane, also contribute specificity to the developed biosensors.[9] Common mechanisms involved in biosensing are selective catalysis of the analyte (by enzyme, organelle, cells, and deoxyribozymes) or selective binding of the analyte (by antibody, aptamer, etc.) by the biorecognition element. However, other mechanisms based on enzyme inhibition, reactivation, and logic gates have also been explored.[10] Based on their origin, biorecognition elements may be classified into natural, pseudonatural and synthetic origin.[7] Naturally occurring biorecognition elements include enzymes, antibodies, subcellular components (i.e., organelles), etc., which leverage the naturally evolved physiological interactions to achieve analyte specificity. Synthetic biorecognition elements are artificially engineered species that mimic the physiologically defined interactions of their natural counterparts (e.g., molecularly imprinted polymers). Pseudonatural biorecognition elements are artificially engineered supramolecular modalities consisting of natural subunits that have both natural and synthetic characteristics (e.g., aptamers, enzymes engineered through directed evolution or site direct mutagenesis, metabolically engineered microbes, etc.). All of these biorecognition elements are associated with varied performance characteristics such as selectivity, sensitivity, signal reproducibility, and reusability. Depending upon the requirements, a trade-off is made between these parameters while selecting the most suitable one for optimum results. Some of the conventional and emerging biorecognition elements are briefly described below.

2.1.1. Enzymes. Enzymes are a widely used biorecognition elements due to their substrate specificity and catalytic efficiency.[11] The first reported biosensor electrode was based on glucose oxidase (GOx), the most studied enzyme system in biosensors.[2,12] In electrochemical biosensors, redox enzymes are used as recognition elements. However, nonredox enzymes are also occasionally coupled to redox enzymes or independently used over the electrode to improve the biocatalytic process and to generate the desired redox entity for the specific response signals.[13] The redox current produced during electrocatalytic detection of the analyte is interrogated using mostly amperometric/voltammetric techniques. There are mainly three approaches to detecting the target analyte using an electrochemical enzyme-based biosensor: (a) electrocatalytic monitoring of substrate consumption or product formation,)b) electrocatalytic recycling of a redox mediator, and (c) direct electron transfer (DET) from the redox center to the electrode surface. These approaches are also correspondingly termed as first, second and third generation biosensors as these are evolved through the process of development in steps to eliminate drawbacks.[3] Although second generation biosensors are more advantageous than the first generation, the leaching susceptibility of soluble mediators is one of its major disadvantages. However, various alternative approaches have been explored to fix the issue. For example, Hatada et al. reported a glucose biosensor utilizing amine-reactive phenazine ethosulfate-modified FAD-dependent glucose dehydrogenase. The electrons generated by the substrate oxidation transferred from the cofactor to the electrode via the enzyme-attached mediator through a quasi-DET process; hence, the biosensor was termed a 2.5th generation.[14]

Studies based on third generation enzyme-based biosensors were reviewed by Das et al.[3] Third generation amperometric biosensors require lower applied potentials, compared to the first and second generations, and hence, specificity is less affected by electroactive interferents. However, all the redox enzymes do not support DET, as the employed enzyme's nature and architecture crucially affect the DET. Further, it depends on the surface properties and the structure of the electrode. Until now, several enzymes capable of DET have been reported, e.g., P450 cytochromes, oxidases, peroxidases with single or more than one prosthetic group, and genetically engineered fusion enzymes. Haem prosthetic group-containing enzymes, e.g., peroxidases, are promising for the application in third generation biosensors. They efficiently catalyze the H_2O_2 conversion, hence can be used for its detection, and are often used in various electrochemical biosensors as a part of a bienzymatic system in combination with H_2O_2-producing enzymes, where peroxidase's DET ability is exploited.[15,16] Among various peroxidases, horseradish, tobacco, peanut, soybean, and sweet potato peroxidases are reported to support DET.[17] Copper-containing oxidases such as laccase and bilirubin oxidases have also demonstrated their ability for DET.[17] These enzymes, however, find more applications in biofuel cells as cathodic biocatalysts due to their efficiency in oxygen reduction reactions.[17,18] On the other hand, the DET ability of the widely used glucose oxidase is under debate.[19] Multicofactor enzymes possess more than one prosthetic group. In many cases, multicofactor enzymes are linked with a cytochrome domain and the catalytic group to guide the electron transfer. Lower redox potential associated with the heme domain and efficient interdomain electron transfer makes them suitable candidates for third generation biosensors. Several multicofactor enzyme-based third generation biosensors have been reported; examples include cellobiose dehydrogenase,[20] FAD-dependent fructose dehydrogenase,[21] sulfite oxidase.[22] However, naturally occurring DET in multicofactor enzymes is limited. Therefore, approaches such as protein engineering and fusion of redox enzymes with electron transfer enzymes like cytochromes have been explored.[23] Bollella and Katz discussed different methodologies for effective DET.[24]

2.1.2. Antibodies. Antibodies are widely used biorecognition elements to develop immunosensors. The idea of using them as a recognition element stems from specific affinity interactions between the antibody and the antigen. Using antibody as the capturing probe, a number of clinically relevant biomarkers were detected through electrochemical interrogation. Usually they utilize immobilized antibodies over the electrode surface. The target antigen−antibody binding events could be monitored using electrochemical signal transduction methods either in a label-free format or using a signal-generating molecule.[25] However, compared to the label-free format, the sandwich format utilizing labels offers better sensitivity.[26,27] For example, Yu et al. demonstrated an electrochemical immunosensor-based detection of prostate-

https://doi.org/10.1021/acsmeasuresciau.3c00034
ACS Meas. Sci. Au 2023, 3, 404−433

specific antigens using a labeling approach in human serum. The obtained results were ±5% accuracy compared to the standard ELISA results.[26]

Although, the electrochemical immunosensors show promising results, their lower shelf life, high production cost, and difficulty in regenerating the immunosensors are a few major obstacles compared to newly evolved aptasensors. Besides, the bigger size of the antibodies limits its use in field effect transistor (FET)-based biosensors. In this context, antibody fragments have also been explored as biorecognition elements. Immobilization of antigen-binding fragments instead of the whole antibody increased the sensitivity of the FET biosensor.[28] Using antigen-binding fragments instead of the whole antibody yields increased surface densities and more specific orientations, enhancing the sensitivity and lowering a biosensor's detection limit. However, the immobilization process is complex compared to the whole antibodies.[29,30] Besides, antibody single chain variable fragments (scFvs) have also been explored as an alternative to monoclonal antibodies for biosensor applications. For example, Grewal et al. exploited nanoyeast−scFv to detect *Entamoeba histolytica* cyst antigens.[31] A review by Crivianu-Gaita et al. discussed the comparison of aptamers, antibody fragments and, antibody scFv in the context of biorecognition elements.[32]

2.1.3. Whole Cells. Whole cell-based biosensors are widely used for environmental monitoring using mainly bacteria and yeasts, and to a lesser extent algae.[33] Though not as sensitive as molecular-recognition-based sensors, in general, these cell-based sensors can be genetically engineered to detect a series of complex responses within a living cell. The performance of such types of biosensors depends on the reporter genes and the regulatory protein associated with the promoters. The regulatory protein interacts with the target and induces the expression of the reporter gene that ultimately results in a measurable output.[34,35] Usage of whole cell-based biosensors for gathering information related to pharmacology, cell physiology, toxicology, etc. of a sample are available. Herbicide detection based on the cyanobacteria *Anabaena variabilis* was reported by exploiting the ability of herbicides to inhibit photosynthesis.[36] Genetically engineered *Escherichia coli* and *Salmonella typhimurium* TA1535 based electrochemical biosensor platform has been demonstrated for the detection of genotoxicants nalidixic acid (NA) and 2-amino-3-methylimidazo[4,5-*f*]quinoline (IQ), respectively.[37] Similarly, the detection of As(III) and Hg(II) in contaminated water was reported using engineered *E. coli*,[38] where the expression level of the *lacZ* gene increases in the presence of the target that resulted in the synthesis of the reporter protein, *β*-galactosidase. There are several other reports of using whole cells-based electrochemical biosensors for the detection of heavy metals and toxins in contaminated water.[39,40,34]

2.1.4. Nucleic Acids. Nucleic acid-based biorecognition probes (mostly DNA) offer several advantages owing to their small size, high chemical and thermal stability, easy chemical modification, programmable structure, and scalable production. The hybridization ability of a nucleic acid can be exploited for developing genosensors. Once the target gene sequence is known, a single-stranded DNA probe could be designed and attached to a sensor surface, where hybridization of the target and the probe occurs in the presence of the target. This event can be monitored in a reagentless manner by tagging one end of the probe with a redox-active label. After the hybridization, the change in the redox current is measured to quantify the specific target DNA sequence.[41−43] Based on this approach, various electrochemical genosensors have been developed.[44−46] Peptide nucleic acids (PNAs) and locked nucleic acids (LNAs) offer improved hybridization properties over nucleic acids and have also been explored as biorecognition element.[47]

Recently, CRISPR (clustered regularly interspaced short palindromic repeats)-based biosensors have received special attention. CRISPR are found in prokaryotic genomes. They, along with RNA-guided nucleases (CrRNA-Cas enzymes), can provide a novel CRISPR/Cas biosensing platform with the potential to revolutionize the biosensing technology.[48] Among several available CRISPR/Cas conjugates, CRISPR/Cas12a and CRISPR/Cas13a that belong to the single multidomain protein systems (under the class 2 category) are frequently used to develop biosensors. The collateral activity of the Cas systems is widely employed for nucleic acid detections. Due to gene editing ability and extreme sensitivity and programmability, CRISPR/Cas systems emerge as tools for biosensing of a variety of biological entities such as nucleic acids, toxins, and viruses in a variety of sample environments. Recently CRISPR/Cas systems have been integrated into electrochemical sensing interfaces resulting E-CRISPRs.[49] Bruch et al. have reported the use of CRISPR/Cas13a for target amplification-free detection of pediatric medulloblastoma biomarkers, viz., miRNA-19b and miRNA-20a from a miRNA-17-92 cluster using a microfluidic channel-engraved multiplexed electrochemical sensing platform.[50,51] The mechanism of the detection method is illustrated in Figure 1. In another report,

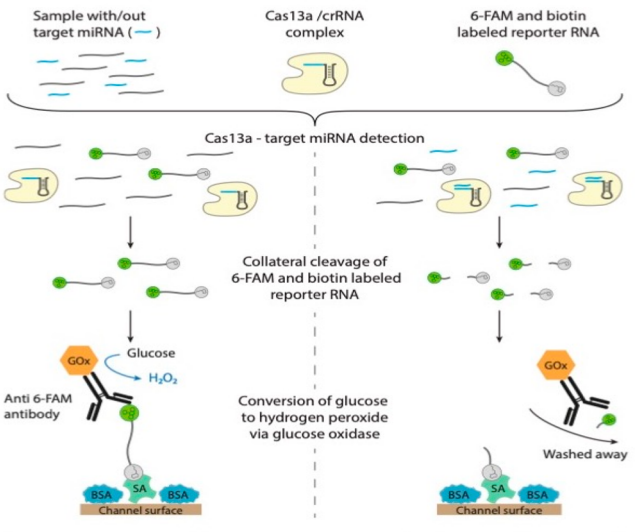

Figure 1. Mechanism of CRISPR-based detection of miRNA. Reprinted with permission under a Creative Commons CC BY License from ref 50. Copyright 2021 Elsevier.

an E-CRISPR was used for cocaine detection using CRISPR/Cas-12a and a terminal signal amplifier, deoxynucleotidyl transferase.[52] In the presence of cocaine, the CRISPR/Cas12a system remains inactive and the complementary strand does not extend. Consequently, the electrode surface remains crowded, preventing the penetration of the redox couple ($Fe(CN)_6^{2+/3+}$) to the interface, resulting in a diminished redox signal.

DNA aptamers are another class of functional nucleic acids that can be used as a recognition probe for a wide range of

https://doi.org/10.1021/acsmeasuresciau.3c00034
ACS Meas. Sci. Au 2023, 3, 404−433

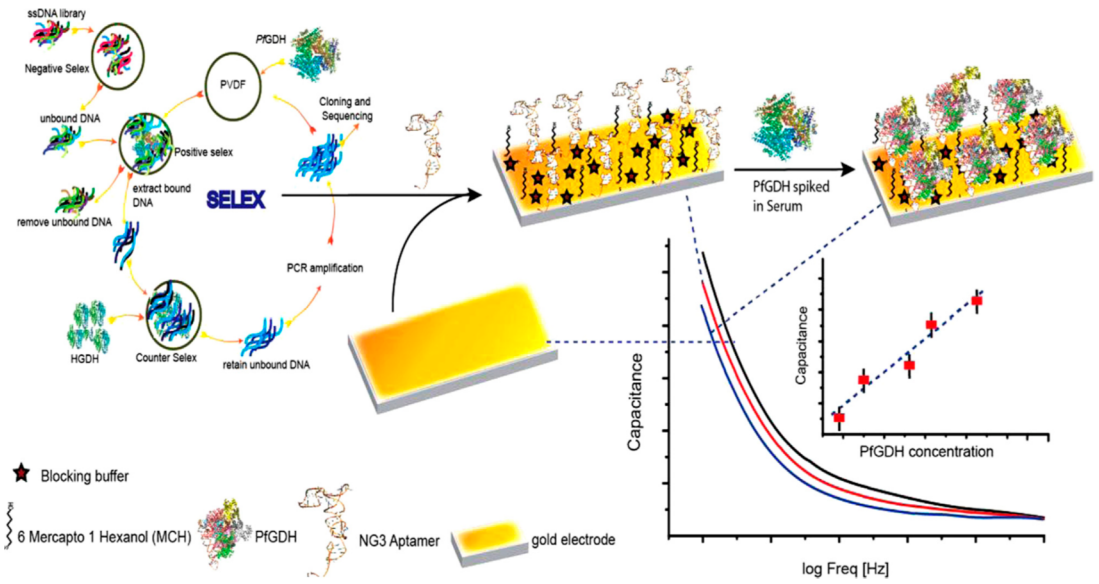

Figure 2. Fabrication of bioelectrode for *P. falciparum* biomarker (PfGDH) detection following nonfaradic EIS. Reprinted from ref 60. Copyright 2018, with permission from Elsevier.

targets such as metal ions, small molecules, proteins, and whole cells.[53] They possess high selectivity and affinity toward the target, comparable to that of antibodies, and therefore sometimes referred to as "chemical antibodies". Additionally, they possess several important characteristics that make them suitable biorecognition elements. For example, unlike antibodies, they can be chemically synthesized in vitro and easily modified with reporter molecules. Besides, they are thermally stable and easy to use for large-scale production at low cost. They are usually selected from a DNA library through an interactive in vitro selection process, termed SELEX (systemic evolution of ligands through exponential enrichment). The selected aptamer is attached to the electrode surface for target detection.[54] On the other hand, unlike enzyme-based biosensors that largely rely on the enzymatic conversion of the target, electrochemical aptamer-based biosensors can function independently of the target-specific reactivity, and they utilize the flexible nature of the aptamers. On target binding, they show a binding-induced conformational change that significantly affects the electron transfer rate, reflecting the target concentration. Due to this ability, the aptamer-based electrochemical biosensors are more generalizable to a wide range of targets. Apart from this strategy (conformational changes upon target binding), different approaches, such as strand displacement, metallization, electrodeposition, etc., have been reported for aptamer-based electrochemical detection.[55]

Xiao et al. reported an electrochemical aptasensor for thrombin detection where methylene blue (MB) labeled thrombin aptamer was immobilized on an electrode.[56] The flexible conformation of the aptamer enables close proximity of the MB (redox label) and the electrode in the absence of the target and hence can show voltametric response. Upon target binding, the aptamer assembles into a G-quadruplex structure, which shields the electron transfer between the MB and the electrode. This in turn attenuates the voltammetric signal. Although, the sensor was characterized by features such as reagentless, reusable, and selective, it suffered from limitations because of its "signal off" architecture. This issue was overcome by introducing a MB-labeled short oligonucleotide.[57] This introduction results in a DNA duplex where the MB tagged nucleotide hybridizes the thrombin-binding portion of the aptamer on the upper dsDNA part and the sequences linking the aptamer to the electrode. The rigid duplex structure prevents interaction between the MB and the electrode, which turns off the amperometric signal. Presence of thrombin, however, triggers dehybridization of the upper dsDNA part. This target-induced strand displacement increases the flexibility of the MB-tagged oligonucleotide, and the interaction between the MB and the electrode become possible.

Aptamers showed promising results in FET-based biosensing that are otherwise challenging with antibody-based FET biosensing. There are some inherent limitations with FET-based detections. In high ionic concentrations (e.g., in physiological conditions), the response of the FET toward target charged species get impeded by ionic screening, which is characterized by the Debye screening length. As the ionic strength increases, Debye screening length decreases, which implies lower sensitivity. Besides, detection of small molecules having fewer or no charge insignificantly affect the transconductance of the FET making indistinguishable binding event.[58] Different ways have been explored to tackle these issues; one of them is to use aptamer as biorecognition element. Indeed, aptamer-based FETs are regarded more promising for detection in high ionic concentrations in comparison to immunoFET. It is because of the small size of aptamers which are mostly under the Debye length, compared to that of the bulky antibodies.[59] Therefore, the target capturing occurs under the Debye screening length and results in detectable signal. The ability of the aptamers to undergo conformational change can be utilized for sensing small and electroneutral molecules. Nakatsuka et al. demonstrated an aptamer-based FET that overcome the issue of Debye screening for small molecule sensing.[58] Here, aptamers having a stem-loop structure were exploited to detect charged and electroneutral targets by changing its conformation. The attached aptamer assembly alters the charge on the FET surface and upon target binding influences the charge distribution on the surface. An aptasensor for a *Plasmodium falciparum* biomarker, *P. falciparum* glutamate dehydrogenase

https://doi.org/10.1021/acsmeasuresciau.3c00034
ACS Meas. Sci. Au 2023, 3, 404−433

(PfGDH), following nonfaradic electrochemical impedance spectroscopy (EIS) has been reported;[60] the detection approach is depicted in Figure 2.

Aptamers have also been explored for in vivo biosensing, although they are still in the infant stage. Unlike enzymes, aptamers can function without relying on the target's reactivity and can selectively work in situ in the living body.[61] The ability of aptamer-based biosensors for real-time and multihour measurement of four drugs in the bloodstream of awake, ambulatory rats was demonstrated.[62] This was a significant demonstration in the context of the technological development of personalized medicine that requires knowledge of patient-specific pharmacokinetics. A recent review by Downs et al. discussed the opportunities and challenges of electrochemical aptamer-based sensors.[61]

2.2. Signals in Electrochemical Biosensors

In electrochemical biosensors, three principal sources of analytical signal, namely, current, potential, and charge, are utilized.[63] Various experimental methods are possible with these signals for extracting information about a system.[64] These methods may be divided into two main categories (Figure 3): (i) bulk methods where properties of the bulk

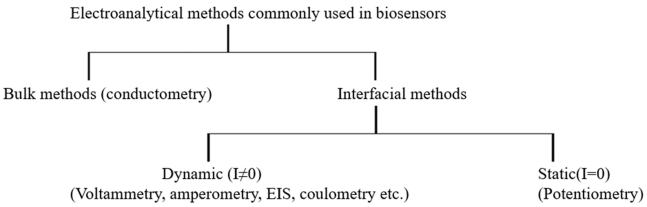

Figure 3. Classification of commonly used electroanalytical techniques for biosensors.

solution (e.g., conductivity) are measured and (ii) interfacial methods where events at the electrode−electrolyte solution interface are measured.[65] The measurement in interfacial methods can be performed (i) under static equilibrium conditions involving zero current, (e.g., potentiometry), and (ii) in dynamic conditions involving nonzero current (e.g., voltammetry, amperometry etc.). Both methods require at least two electrodes. During the static measurements, the potential between the two electrodes is measured, which can be related to the analyte concentration using the Nernst equation. Dynamic methods involve the measurement of current by controlling the potential (known as the controlled-potential technique) or vice versa (controlled-current technique), and its biosensing application seems to be limited. In the controlled potential technique, the current response is correlated to the analyte concentration. The resulting current is a combination of two components: the faradaic component (which represents the redox events occurring at the interface (follows Faraday's law)) and the nonfaradaic component (which does not follow Faraday's law); thus, $I_{Total} = I_{Faradaic} + I_{Nonfaradaic}$. Many factors may contribute to the nonfaradaic component. One of them is charging the electrical double layer during dynamic measurements.[63,66] During electrochemical measurements, minimization of this component is sought.

2.2.1. Theory of Heterogeneous Electron Transfer. To realize the electron transfer between the electrode and reacting species in solution, two main approaches are widely used, the Butler−Volmer (BV) model and the Marcus−Hush (MH) theory.[67] The BV model describes the oxidation and reduction rate constants using three independent parameters E_f^0 (formal potential), k_0 (standard heterogeneous rate constant), and α (or β) (transfer coefficient), through the eqs 1 and 2, and the net reduction current I, is given by $I \propto k_{red} - k_{ox}$.[68,69] Here k_{ox} and k_{red} represent rate constants for oxidation and reduction, respectively, and R, T, and F bear the usual meanings. The equations imply that the reduction or oxidation rate constants are exponentially related to the applied potential E. Although not universally applicable, the BV model has been used by electrochemists over the past decades to successfully describe the kinetics of many electrochemical systems.

$$k_{ox} = k_0 \exp\left[\frac{\beta F}{RT}(E - E_f^0)\right] \quad (1)$$

$$k_{red} = k_0 \exp\left[-\frac{\alpha F}{RT}(E - E_f^0)\right] \quad (2)$$

The MH theory describes nonadiabatic electron transfer between a donor (D) and acceptor (A) species in terms of Gibbs energy (ΔG^0) and reorganization energy (λ) (eq 3).[70] This theory considers the reorganization of reacting species (D and A), and solvent molecules (e.g., changes in the structure of the reacting species and solvent molecules, etc.), represented by the term λ. The driving force for electron transfer is represented by ΔG^0. The term V reflects the distance dependence of electron transfer between D and A and is expressed in eq 4. Here, β is a constant that reflects the electron transfer properties between D and A, while r is the distance between D and A. V^0 represents electronic coupling at the nearest distance r^0, and R, T, k_B, $\hbar$ have their usual meanings.

$$k = \frac{2\pi}{\hbar} V^2 \sqrt{4\pi\lambda k_B T}\, \exp[-(\Delta G^0 + \lambda^2)/4\lambda k_B T] \quad (3)$$

$$V = V^0 \exp[-\beta(r - r^0)] \quad (4)$$

The electron transfer, therefore, depends on λ, ΔG^0, and r between the participating species D and A (one of them is the electrode in the case of electrochemical biosensors). In the context of electrochemical biosensors, redox enzymes are extensively used as biorecognition elements, and the electron transfer between the electrode and the enzyme is crucial for efficient signal transduction. The complete mechanistic explanation of the electrochemical biosensors on the basis of these equations is, however, difficult because of the complex nature of the biological system.[70] Although DET between the enzyme and the electrode is desirable, it is not always possible, as, in many cases, the active site is shielded by the enzyme shell. Therefore, to facilitate the electron transfer, redox mediators either in freely diffusible form or in bound form such as, by wiring them to the enzyme or as electrode immobilized redox polymers (MET) are used.[24,14]

To study the electron transfer mechanism and kinetics of enzyme-modified electrodes, different electroanalytical techniques, namely, protein film voltammetry, classical voltammetric techniques, and chronoamperometry, are widely used. As discussed earlier, many electroanalytical methods are possible using the three main signal sources. The following section will briefly discuss common electroanalytical approaches.

2.2.2. Common Electroanalytical Techniques Used in Biosensors. *2.2.2.1. Voltammetry.* Voltammetry is the study of current as a function of applied potential; it requires a 3-electrode system where the potential of the working electrode

https://doi.org/10.1021/acsmeasuresciau.3c00034
ACS Meas. Sci. Au 2023, 3, 404−433

(WE), immersed in an electroactive solution is swept linearly across a potential window. As stated earlier, the electron transfer rate constant and hence the magnitude of the current depends on the applied potential according to the BV model.[71] There are varieties of voltammetry techniques, such as linear sweep voltammetry (LSV), cyclic voltammetry (CV), differential pulse voltammetry (DPV), and square wave voltammetry (SWV), to name a few that are commonly used for biosensor study. In CV, the potential of the WE is cycled at a fixed rate on either side of the equilibrium potential, E^0, and the resulting current is monitored. When the applied potential is more positive than E^0, the species become oxidized and an anodic current is obtained. When a more negative potential is applied to the WE, a cathodic current is obtained, resulting from the reduction of the species. Considering the negative sweeping of applied potential at a rate of v, the potential at time t is given by eq 5:

$$E(t) = E_i - vt \tag{5}$$

where E_i is the initial potential.[71] The shape of a voltammogram gets influenced by the electrode geometry; however, the basic shape can be understood by rearranging the Nernst equation (eqs 6 and 7),[71]

$$(E_i - vt - E^0) = \frac{RT}{nF} \ln\left(\frac{[O]_s(t)}{[R]_s(t)}\right) \tag{6}$$

By rearranging, we get

$$\frac{[O]_s(t)}{[R]_s(t)} = \exp\left[\frac{nF}{RT}((E_i - vt - E^0))\right] \tag{7}$$

Considering the reduction of species O to R at the electrode surface, when the electrode potential is held at a sufficiently positive value compared to E_0, no electron transfer will take place. As the applied potential approaches toward E_0, the reduction of O starts and the corresponding reduction current increases making changes in the surface concentrations of R and O, $[R]_s$ and $[O]_s$, larger and smaller, respectively. However, after a certain applied negative potential, the reduction current approaches a limiting value, and a peak is observed in the so-called potential−current curve, the voltammogram. The peak current, I_p reflects the concentration of the species, and is related to the v, concentration (C), and diffusional coefficient (D) of the electroactive species according to the Randles−Sevcik equation (eq 8), where the other parameters bear usual meaning.[72]

$$I_p = 0.4463nFAC\left(vD_0\frac{nF}{RT}\right)^{1/2} \tag{8}$$

Apart from concentration measurements,[73] CV has also been used for electrochemical deposition during bioelectrode fabrication,[74] and is commonly used for studying reaction mechanism.[66] Similar to CV, LSV is another technique in which the sweeping is done only in one direction. Pulse voltammetric techniques such as DPV or SWV are more sensitive compared to CV due to their ability to reduce the nonfaradaic current and are widely used in biosensing.[75,76] In DPV, pulses of fixed magnitude superimposed on the linear sweep are applied on the WE, whereas in SWV, a square waveform is superimposed on a staircase base potential.[66]

2.2.2.2. Chronoamperometry. Chronoamperometry is a constant potential technique where the WE is stepped to a value (typically in a region of limiting current) where the redox reaction of interest takes place and is held for a specific amount of time.[66] The resulting limiting current is related to the concentration of the analyte and can be expressed through the Cottrell equation as follows: C, I_{lim}, and D represent bulk analyte concentration, limiting current, and diffusion constant of the analyte, respectively, whereas other terms bear their usual meanings (eq 9)[63]

$$I_{lim} = nFAC\sqrt{\frac{D}{\pi t}} \tag{9}$$

Chronoamperometry is another commonly used technique for measuring an analyte concentration in biosensing applications.[77,78]

2.2.2.3. Electrochemical Impedance Spectroscopy (EIS). EIS measurements are carried out by applying a small amplitude sinusoidal perturbing voltage to an electrochemical system following the measurement of the resulting current response.[71] It does not involve the interaction of electromagnetic radiation with the sample; rather, the current response is measured in a range of frequencies, and hence it is termed "spectroscopy". Impedance is represented by Z and is expressed as the ratio between the voltage and time phasor. It is a complex quantity and can be divided into two parts real, Z_{real}, and imaginary, Z_{imag}, ($Z = Z_{real} + iZ_{imag}$, $i = \sqrt{-1}$), with a graph between these two called a Nyquist plot being commonly used to represent impedance.

There are two types of EIS used for electrode/electrolyte interfacial study, faradaic and nonfaradaic, based upon the use of a redox label during measurements.[79] A study using faradaic EIS requires the presence of a redox label that gets oxidized/reduced at the electrode to result in current, whereas nonfaradaic EIS is based on the charging and discharging of the electrical double layer capacitance. To evaluate different components, such as resistance and capacitance, the EIS data can be modeled to an equivalent circuit. Both faradaic and nonfaradaic EIS have been studied for biosensor application.[80,60,81]

2.2.2.4. Coulometry. Here the charge corresponding to the redox event is measured instead of current. Although not so common, a few coulometry-based biosensors have been reported for the detection of D-fructose, H_2O_2, L-lactate, cholesterol, and glucose.[82−84]

2.2.2.5. Potentiometry. Here, the potential difference established between the transducer and reference electrodes is measured. The potential is related to the analyte concentration by the Nernst equation. It is a well-established method and has been used for the analysis of a variety of ions, a well-known example is the pH meter.[85,86] Based on the concept of potentiometry, origami paper-based biosensor has also been reported.[87] Field effect transistor (FET)-based biosensors have recently gained much attention owing to their suitability to use as a point-of-diagnostics device; one of the most commonly used FET is the ion selective FET (ISFET).[88] When a biological layer is placed on top of the ISFET gate surface for biorecognition, then it is termed a BioFET, the biologically modified FET.[89] The working principle of BioFET is similar to that of ISFET. Interestingly, these FET-based potentiometric devices also utilize the current (called drain current) as the response signal for the target of interest. The use of FET-based devices for biosensing has been reviewed recently.[88]

https://doi.org/10.1021/acsmeasuresciau.3c00034
ACS Meas. Sci. Au 2023, 3, 404−433

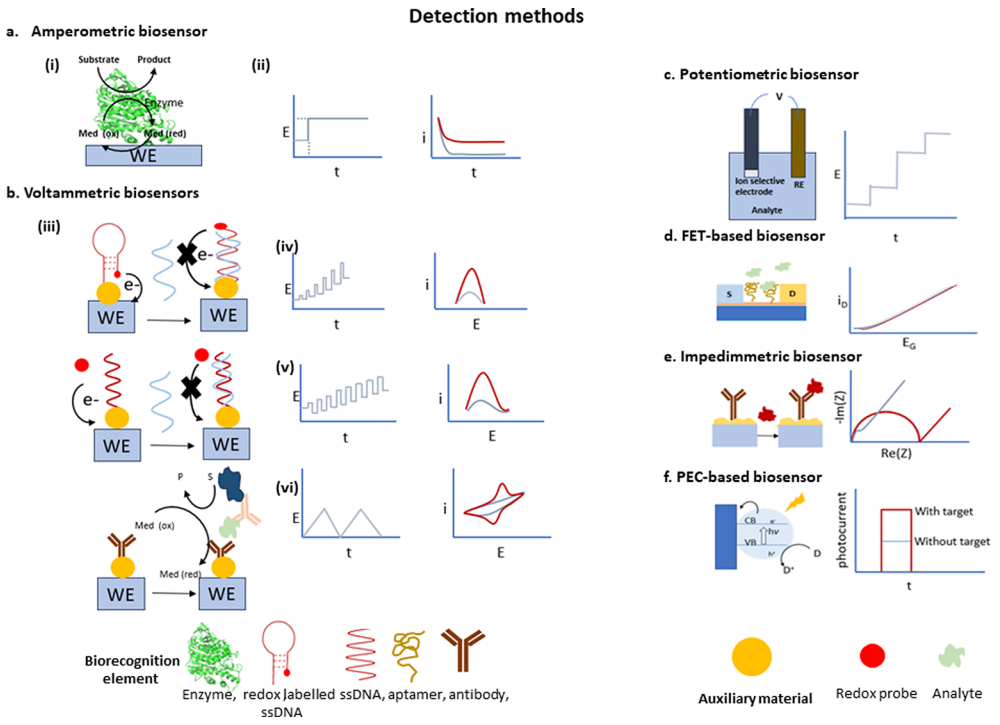

Figure 4. Schematic representation of electrochemical biosensors. (a) (i) Amperometric biosensor, based on a redox enzyme, (ii) chronoamperometry waveform and response curve; (b) voltammetric biosensors, (iii) commonly used detection strategies; (iv), (v), (vi) waveform of DPV, SWV, and, CV, and their response curves, respectively); (c) potentiometric biosensor; (d) aptamer-based FET biosensor; (e) impedimetric biosensor using antibody as a biorecognition element; (f) photoelectrochemical biosensor.

2.2.2.6. Conductometry. Unlike voltammetry and amperometry, the use of conductometry for biosensing is limited. It involves the measurement of changes in the conductance of the samples. Most of the enzymatic reactions are associated with the production or consumption of ions, which changes the ionic conductance of the sample.[90] Therefore, the change in conductance is a reflection of the analyte concentration. For example, the detection of arginine using arginase and urease is reported, where the catalytic activity of the two enzymes immobilized on the electrode surface changed the bulk ion concentration that was proportional to the arginine concentration.[91]

2.2.2.7. Other Techniques. The use of photoelectrochemical (PEC) biosensors in the field of bioanalysis is relatively new but highly promising.[92] Unlike other electrochemical biosensors, PEC biosensors require photoactive materials, apart from the immobilized biorecognition elements on the electrode surface. Interaction of the analyte with the biorecognition element causes a change in the generated photocurrent, which is related to the analyte concentration. Another very promising technique is electrochemiluminescence (ECL). In fact, more than 150 ECL-based assay is currently available.[93] ECL involves the generation of reactive species on the electrode surface that undergo fast electron transfer to form light-emitting excited states that, in turn, emit light, and the intensity of the emitted light is linearly dependent on the reactant concentration. The use of ECL analysis has been reviewed recently.[94]

Recently, a novel detection strategy has been reported that demonstrated the possibility of combining two transduction principles for single analyte detection. Here *P. falciparum* lactate dehydrogenase was detected simultaneously using EIS and an optical method.[95] Although very limited work has been done in this line, such a detection strategy is attractive as it corroborates each other's results and is, therefore, more reliable. A schematic representation of various electrochemical biosensors is presented in Figure 4.

3. MATERIALS FOR BIOELECTRODE FABRICATION

Bioelectrode fabrication involves the coupling of the biorecognition element to the electrode surface. During the process of fabrication, different auxiliary materials (common examples: inorganic and organic nanostructures, composite materials, and polymeric materials) are often included in the interface of the bioelectrode. The main purposes of using these materials are to improve the electron/charge transfer efficiency, increase the active surface area of the electrode, and serve as an immobilization matrix to provide better stability and reusability of the biorecognition element. Various bio/polymers such as, polysaccharides, proteins, and their composites are widely used as the immobilization matrix.[96−99] Synthetic polymers such as redox polymers and conducting polymers have also been explored for this purpose.[100,101] Many redox polymers, used as electron transfer mediators and enzyme immobilizing matrices, offered improved bioelectrode performance.[100,102] Conducting polymers have often been used for improving signal transduction and amplifications and to serve as an immobilization matrix.[101,103,104] Polyelectrolytes, which have ionic properties, help to incorporate various species with sensing/mediating/transducing properties and serve as a matrix for immobilizing the biorecognition elements.[105−107] The role of polyelectrolytes in the development of the sensing systems and the architectures of the sensing layers have been reviewed.[108] Organic frameworks, such as metal−organic frameworks (MOFs) and covalent organic frameworks (COFs), have also been explored for biosensor applications.

https://doi.org/10.1021/acsmeasuresciau.3c00034
ACS Meas. Sci. Au 2023, 3, 404−433

Table 1. Representative Materials Commonly Used in Electrochemical Biosensor Fabrications[a]

	Material and Its Composites	Use/function
Conducting polymer	PEDOT nanofiber,[127] Polypyrrole[104]	Matrix for GOx entrapment, reduces microelectrode impedance,[127] entrapments[104]
	Composites: Polypyrrole-polythionine hydrogel[128]	Enhances conductivity, surface area, signal amplification[128]
Redox polymer	Ferrocene based,[100] osmium based[102]	Immobilization, mediator[100,102]
Biopolymer	Chitosan,[78] alginate[129]	Improves processability of enzyme.[78] a component of the fabricated transducer[129]
Polyelectrolytes	PDDA, PAS[107]	ChOx immobilization[107]
	Composites: Pt-graphene-PDDA hybrid[105]	Dispersion and stabilization of graphene, attracts $PtCl_6^{2-}$ for in situ formation of Pt nanoparticles[105]
MOF	ZIF,[109] Cu-MOF[110]	Matrix for coimmobilizing GDH and methylene green,[109] served as a matrix for tyrosinase, pre enriches the substrate BPA on the electrode surface[110]
COF	$COF_{DHNDA-BTH}$[113]	Covalently immobilizes AChE and improves catalytic activity[113]
CNT	VACNT,[130] SACNT[119]	For streptavidin functionalization,[130] utilized for enzyme immobilization[119] enhanced sensitivity, detection range, lowered detection limit and response time[119]
	Composite: HAp-CNT[120]	CNT enhances electrical communication, HAp was used for immobilizing HRP[120]
Graphene	Composite: Graphene hybrid,[131] Graphene/PVP/PANI[132]	For immobilizing ChOx, enhancing sensitivity, faster response time,[131] graphene enhances electron transfer kinetics,[132] PVP improves graphene dispersion[132]
Metal particles	AuNP[133]	For anchoring antibody[133]
	Composites: PEDOT-AuNP[134]	PEDOT increases surface area, AuNP for biorecognition element immobilization[134]
Metal oxide nanoparticles	Composite: Fe_3O_4 -ZnO[135]	ZnO for enzyme immobilization, Fe_3O_4 for reducing anionic interferents[135]
Metal sulfide nanoparticles	Composite: AuNP-MoS_2[122,136]	MoS_2 was used for structuring AuNP,[122] AuNP-MoS_2 was used for covalent immobilization of antibody[136]
Metal nanoclusters	DF/AgNC[121]	AgNC and generated Ag^+ from AgNC used in dual mode detection[121]
MXenes	Ti_3C_2[137]	Immobilizing tyrosinase[137]
	Composite:T DN- Ti_3C_2[138]	Ti_3C_2 provides space for TDN adsorption, TDN facilitates molecular recognition[138]
Quantum dots	AMQD,[126] MPA-ZnS QD[125]	For enhancing surface area and immobilizing catalase,[126] reduces charge transfer resistance, act as an immobilization matrix and provides high sp. surface area[125]

[a]Abbreviations: PEDOT: poly(3,4-ethylenedioxythiophene), GOx: glucose oxidase, PDDA: polydimethyldiallyl ammonium chloride, PAS: sodium poly(anethol sulfonate), ChOx: cholesterol oxidase, ZIF: zeolitic imidazolate framework, Cu-MOF: copper-centered metal−organic framework, GDH: glucose dehydrogenase, BPA: bisphenol A, $COF_{DHNDA-BTH}$: covalent organic framework synthesized from 2,6-dialdehyde-1,5-dihydroxynaphthalene (DHNDA) and 1,3,5-phenyltriformylhydrazine (BTH), AChE: acetyl choline esterase, VACNT: vertically aligned carbon nanotube, SACNT: super aligned CNT, HAp-CNT: hydroxyapatite-CNT, PVP: polyvinylpyrrolidone, PANI: polyaniline, AuNP: gold nanoparticle, DF/AgNC: three-dimensional DNA flowers-templated Ag nanoclusters composite, AMQD: antimonene quantum dots, TDN: tetrahedral DNA nanostructures, MPA: mercaptopropionic acid.

MOFs have emerged as an immobilization matrix for protecting enzymes. For instance, the zeolite imidazolate framework 90 (ZIF-90), a MOF subclass, embeds catalase to prevent its leaching.[109] The MOFs for enzyme immobilization,[110] signal amplification,[111] immobilization of nanoparticles and as a redox probe[111] have also been reported. The application of MOFs in different biosensor designs has been reviewed.[112] Covalent immobilization of enzymes into the pores of COF demonstrated enhanced activity of the enzyme because of the presence of confined holes of the COF.[113] Enzyme loaded COF microcapsules were also synthesized utilizing ZIF-8 as a sacrificial material.[114] The COF shell in such a microcapsule protects the enzymes from harsh external environments. Carbon-based materials[115,116] and nanomaterials such as graphene and its derivatives,[117,118] carbon nanotubes[119,120] are also widely used as a platform for immobilizing the biorecognition element and for improving the biosensor performance. Similarly, noble metal nanoparticles (NPs), such as gold, silver, palladium and platinum NPs, metal nanoclusters, metal oxides and sulfides have been extensively used for the fabrication of bioelectrode interfaces.[6,121,77,122] MXenes are relatively a new class of material and possesses properties like large surface area, high electrical conductivity, hydrophilicity, biocompatibility and ease of functionalization which make these materials suitable for biosensor electrode fabrication.[123] Use of quantum dots for attaching biorecognition elements to its surfaces, and for improving the signal transduction and amplification have also been reported.[124−126] Few of the representative examples of these commonly used materials and their roles during the fabrication have been listed in Table 1.

4. FABRICATION OF BIOELECTRODES

The electrode in electrochemical biosensors transduces biochemical signals into electrical ones, such as current, voltage, and impedance. Immobilization of the biorecognition element without losing its recognition ability is crucial for bioelectrode performance. Along with the biorecognition element, various other materials are also introduced on the electrode surface to improve the biosensor performance. A plethora of techniques are available for bioelectrode fabrication and are often used in combination to get the desired structure and functions.[80,139,140] Fabrication of the bioelectrode is one of the key components for a successful biosensor design (Figure 5). Often, nanomaterials, inorganic, organic, and polymeric materials and their composites are introduced during the fabrication. This may lead to enhanced surface area, electrical conductivity, signal transduction, selectivity, and stability of the bioelectrode.[141] Different coating and deposition methods have evolved for the construction of the base electrode's matrix, where the biorecognition elements may be simultaneously or subsequently attached.

Based on the type of biorecognition elements, different methods can be adopted to attach them to the electrode

https://doi.org/10.1021/acsmeasuresciau.3c00034
ACS Meas. Sci. Au 2023, 3, 404−433

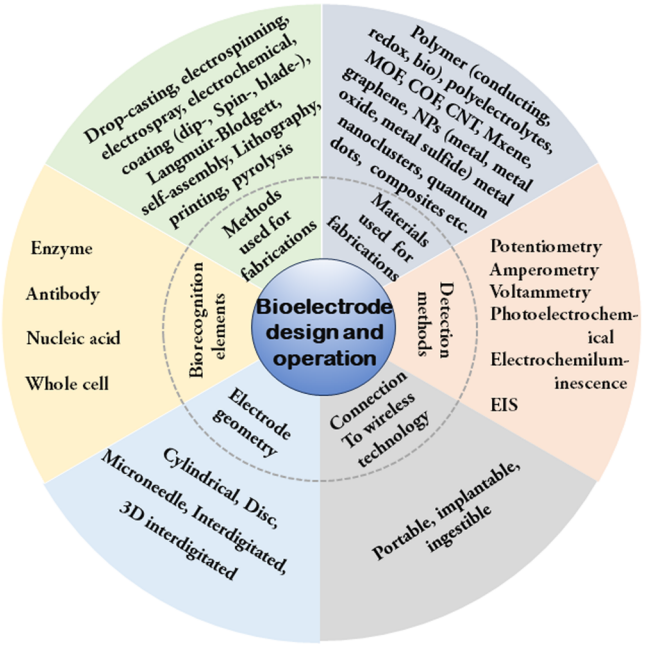

Figure 5. Key components for biosensor electrode design.

surface; commonly used methods are based on adsorption, covalent attachment, entrapment, cross-linking, and affinity.[142] For example, the immobilization of an enzyme using a layer-by-layer technique and onto an already-formed Langmuir–Blodgett film is based on the adsorption principle. Primarily, three types of forces are involved during the adsorption process: van der Waals force, electrostatic interaction, and hydrophobic interaction.[142] In the covalent attachment, the biorecognition element is attached to the electrode through functional groups such as −COOH (e.g., −COOH of carboxylated CNTs) on the electrode surface. Immobilization of certain polymers on the electrode surface also furnishes functional groups such as −COOH, −OH, NH_2 to the electrode surface.[96,143] Functional groups in the biorecognition elements can also be used for immobilization on the electrode surface if those groups are not essential for detection activity. Various multifunctional reagents such as glutaraldehyde and EDC (1-ethyl-3-(3-(dimethylamino)propyl) carbodiimide) carbodiimide) are used to couple the biorecognition element to the electrode surface. For example, the $-NH_2$ groups present on the electrode surface can be attached to the −COOH groups of the enzymes using this EDC-NHS (*N*-hydroxysuccinimide) coupling. Glutaraldehyde is used for coupling between the -NH_2 groups of the electrode and enzyme molecules. Thiol-containing biorecognition elements (e.g., thiol-modified aptamers) can directly be attached to Au electrodes via a Au–S bond utilizing the chemisorption property. Additionally, short thiol-containing linker molecules (e.g., 3-mercaptopropionic acid,[144] Lomant's reagent,[145] aromatic thiols,[146] cystamine[147]) are also used for linking nonthiolated aptamers (e.g., amine-functionalized aptamers). These molecules form self-assembled monolayers (SAM) on the gold electrode surface through the thiol group, whereas their other end is utilized for aptamer immobilization. In the entrapment method, enzymes are generally incorporated inside three-dimensional matrices, created by techniques such as electropolymerization, photopolymerization, polysaccharide-based gel, and carbon paste-derived gel.[142] In the cross-linking method, the bifunctional linker molecules like glutaraldehyde are used to cross-link the enzymes or cells with each other[148] or with a functionally inactive protein.[149] It enhances the loading efficiency of the enzymes on the electrode. The strong streptavidin–biotin affinity interaction ($K_d \sim 10^{-14}$ M)[150] is frequently reported for immobilizing different biorecognition elements, e.g., peptides,[151] antibodies,[152] nucleic acids.[153]

Conventionally, GC (glassy carbon), ITO (indium tin oxide), FTO (fluorine doped tin oxide), Au, and Pt are widely used as base electrodes. However, this trend is gradually shifting to composite forms of electrodes for the preparation of miniaturized electrodes. Advanced techniques such as lithography and additive manufacturing processes are mainly used for making such miniaturized electrodes. In the following sections, different fabrication methods are discussed with recent examples.

4.1. Fabrication Techniques for Macroscale Electrodes

4.1.1. Drop-Casting. It is typically a manual deposition method used for the fabrication of thin films on smaller electrode surfaces. Nanomaterials, in combination with binders, are widely used for such fabrication. A homogeneous dispersion is prepared by mixing nanomaterial (often with binder) in a solvent which is then drop-casted onto the bare electrode surface and subsequently dried. Various nanomaterials such as metallic, carbonaceous, and their hybrids, composites were used for the casting method.[154] In a study, carbon-based nanocomposite and nanohybrid materials were investigated to improve glucose biosensor performances where 3-mercaptophenyl boronic acid functionalized gold nanoparticles (AuNPs) and bamboo-like MWCNT were explored.[155] The process involved drop-casting of bMWCNT dispersed in polyethylene imine onto a GCE. The functionalized AuNPs were then adsorbed onto the platform, followed by the immobilization of GOx. Here, the boronic acid residue on the AuNPs surface provides easy immobilization of the enzyme, whereas the MWCNT is involved in electrochemical signal transduction. Structuring of conductive nanoparticles on the electrode surfaces offers better electrochemical properties. Drop-casting method can be utilized for effectively depositing such structured material on the electrode surface.[122]

Although it is a simple and rapid technique, "coffee-ring-effect" on the surface is observed due to the nonuniform distribution of nonvolatile components used in the casting material.[156] Strategies such as using Marangoni effect, anisotropic particles or surfactants can help in reducing the coffee-ring effect.[156]

4.1.2. Dip-Coating. Here, the substrate is immersed into a coating solution for a certain amount of time and withdrawn vertically at a fixed speed, following solvent evaporation. The withdrawal speed and the evaporation condition play an important role in the film formation process.[157] Nanomaterials can be deposited using the dip-coating method on the electrode surface.[135,158] Mikani et al. investigated the performance of a urea biosensor on an F-doped SnO_2 electrode using a nanocomposite of ZnO and Fe_3O_4.[135] This nanocomposite was dip-coated onto the electrode that serves as the attachment of urease (the biocatalyst) via electrostatic attraction at pH 7.4. Fe_3O_4 is negatively charged at this pH that therefore served as a repulsion layer for the anionic interferents from approaching the electrode surface. Apart from the commonly used electrodes such as ITO and GCE, paper is also used in the dip coating method. A paper-based immunosensor for

https://doi.org/10.1021/acsmeasuresciau.3c00034
ACS Meas. Sci. Au 2023, 3, 404–433

carcinoembryonic antigen (CEA) detection utilizing a nanocomposite of metal oxide, Fe_3O_4, and conducting polymer, PEDOT:PSS was reported.[77] The dispersion of Fe_3O_4 and PEDOT:PSS was deposited on paper by dip-coating. When the electrode platform was further dipped into DMSO solution, the conductivity of the electrode was increased further. The ejection of the insulating PSS ions by the DMSO treatment was attributed to this enhanced current. Antibody against the CEA was then immobilized onto this fabricated electrode via the drop-casting method and then detection was performed using chronoamperometry. This procedure was superior to another one where reduced graphene oxide and ethylene glycol was used in place of Fe_3O_4, and DMSO, respectively, to treat the electrode.[159]

Dip-coating requires a considerable volume of the coating solution for immersion. This is a critical issue for cases: (a) when the solution is not stable enough over time; (b) when the handling of a large volume of the solution is risky and the solution is harmful, or (c) when it is expensive or can only be synthesized only in small quantities.[157]

4.1.3. Spin-Coating. It is also used for thin film fabrication. The process involves casting a solution of interest onto the substrate, which is then spread across the substrate by spinning it. During the spinning step, some amount of solution may be expelled from the surface. The solution remaining on the substrate surface forms the shape of a thin film once solvent evaporation completes. The thickness of the thin film can be controlled by altering the spin speed and concentration of the solution used for casting. Besides, multilayer films may also be deposited by repeating the above steps. Polymers are extensively used for spin coating due to their good film-forming characteristics and ability to allow functional modification in them.[160] It is another commonly used technique for nanomaterial deposition during bioelectrode fabrication.[161,162] For example, three different morphologies of ZnS nanomaterials (nanoparticle, nanoflake, and urchin-like structure) were deposited onto an ITO-coated glass electrode and their performances were evaluated toward uric acid biosensing.[161] Here, ZnS allowed physical adsorption of the uricase enzyme, and the urchin-like structure showed the highest sensitivity. In another study, a nanocomposite of AuNP and reduced graphene oxide was spin-coated, which provided a platform for covalent immobilization of the uricase enzyme.[162]

Spin coating is often used during the fabrication of microelectrodes through photolithography. Before performing photolithography, a photoresist is deposited on the electrode surface, usually by the spin-coating method.[139,163,164] The spin coating method is adapted for fabricating thick, multilayer uniform films.

4.1.4. Doctor-Blade-Coating. It is another low-cost and easy-to-perform method for electrode fabrication. Here, a well-mixed slurry is placed on the substrate beyond the blade and is spread using the constant relative motion between the substrate and the blade. Because of its ability to create flat and uniform films on a large area, this method has been extensively used in different industries (namely, printing, paper, textile, solar cells, batteries etc.). Use of this method to fabricate biosensor electrodes was also reported. For example, during the fabrication of a urea biosensor (urease/nanoporous $ZnO/TiO_2/FTO$), TiO_2 was coated onto the FTO-coated glass.[80] The coated surface was then covered with PVA in a parallel pattern, which was followed by sputtering of ZnO. PVA acted as an omissible polymer and its removal in the final step resulted in the nanoporous $ZnO/TiO_2/FTO$ electrode. The roles of TiO_2 here are to improve the electron transfer between ZnO and TiO_2, reduce the anionic interferents by electrostatic repulsion, and increase the sensor performance by forming a heterojunction with nanoporous ZnO.

4.1.5. Electrochemical Deposition. This thin film deposition technique utilizes a three-electrode system (WE, RE, and CE), which is dipped into a solution containing the components to be deposited. The deposition (on the WE surface) can be done following various methods. It is mostly done by applying a constant potential at the WE or by sweeping the potential for multiple cycles using CV. Other methods, such as constant current techniques, are also explored for the depositions.[165] In this method, the morphologies of the deposited particles are controlled by the applied current density.[166] In a comparative analysis, LSV was found to be superior to chronoamperometric electrochemical deposition for a nanostructured gold electrodes.[74] Gold electrode surface generated using LSV showed better surface homogeneity, higher surface-to-volume ratio, and better redox activity. The electrochemical deposition method is a simple, cost-effective, and time-saving method, but it needs a conductive surface.

A method for the detection of human IgG using an electrochemically deposited film of PEDOT and AuNPs on a GCE described.[134] This method utilized a Y-shaped peptide, one branch of which recognizes the target and the other branch reduces the electrode fouling event. This Y-shaped peptide was attached to the AuNPs via a Au−S bond. To achieve PEDOT and AuNP fabricated GCE, electrodeposition of PEDOT was first carried out onto the GCE using a constant potential of 1.1 V (vs SCE) for 200 s. AuNP was then electrodeposited on the PEDOT surface using 4 sweeps of CV in a solution of $HAuCl_4$ and KNO_3 between the potential range −1.5−0.5 V. The resulting electrode was further modified with the Y-shaped peptide and subsequent IgG detection was carried out. In another report, gold-deposited carbon paper (Au/CP) with GOx as the biocatalyst was used as bioelectrode for glucose biosensing.[148] For the fabrication, gold was electrochemically deposited onto the surface of a CP by applying −4 V on the CP electrode in a solution containing $HAuCl_4$ in H_2SO_4. This Au/CP electrode was then chemically coupled to GOx. Laser-scribed graphene (LSG) electrodes, which may be fabricated on a commercial polymer film using a laser,[167] are regarded as sensitive transducers for biosensor applications. Its performance can further be enhanced by introducing nanomaterial onto the LSG electrode. For example, electrochemically deposited Au nanostructures on LSG were explored for aptasensing of human epidermal growth factor receptor-2 (HER-2).[168] Here, the Au nanostructure incorporated into the LSG electrode, prepared on a polyimide substrate, exhibited increased electron transfer.

4.1.6. Electrospray Deposition (ESD). Here, a small capillary is used through which the solution of interest flows. The capillary is separated by a few millimeters away from the counter electrode and held at a high voltage of a few kV that results in the generation of charged molecules. At the tip of the capillary, a typical cone-like shape, known as a "Taylor cone", forms where the repulsion of these charged molecules is counterbalanced by the liquid's surface tension. Once a critical point is achieved where the liquid's surface tension cannot hold the charged molecules further, a coulomb explosion takes place that results in a fine jet of charged droplets issuing from the

https://doi.org/10.1021/acsmeasuresciau.3c00034
ACS Meas. Sci. Au 2023, 3, 404−433

apex of the cone. The size of these charged droplets reduces further due to solvent evaporation and finally, gas of molecular ions forms, moving toward the counter electrode.[169] This technique has even been used to develop a prototype for paper-based cholesterol biosensor where a nanocomposite prepared from graphene, polyvinylpyrrolidone (PVP), and polyaniline (PANI) was deposited on a paper using electrospraying.[117] Cholesterol oxidase (ChOx) was then immobilized onto the nanocomposite via physical adsorption. Oxidation of cholesterol by ChOx produces H_2O_2, which was quantitatively detected amperometrically at 0.6 V by using the electrode. ESD could also be used for the immobilization of enzyme onto the electrode surface as demonstrated in,[140] where laccase was immobilized on a carbon black (CB) modified screen-printed electrode (CB-SPE), prepared by drop-casting CB on the SPE. This electrode was then subjected to amperometric detection of catechol at −0.16 V (vs Ag/AgCl) that offered a limit of detection (LoD) 2.0 μM and the linear range of 5−50 μM. This biosensor showed reproducibility for 25 consecutive measurements and stability for 90 days at room temperature. Further, the measurement could be increased to 63 times by replacing the CB-SPE with a commercially available carbon screen-printed electrode (C-SPE).[169] This also widened the linear range from 2 to 100 μM with an LoD of 1.7 μM and the reason has been ascribed to the greater uniformity of the C-SPE than that of the CB-modified SPE. When the working stability of this SPE prepared via electrospraying was compared with that of an SPE prepared via drop casting of laccase, the previous one was found to be much superior. The SPE produced via drop casting lost almost 78% of its activity after 20 times washing. The main concern associated with this deposition technique is ink stability. Therefore, nanomaterial deposition is not widely used using this technique.

4.1.7. Electrospinning Deposition. The process of electrospinning is analogous to electrospraying. This process has four main components: a reservoir that contains the dispersion solution, a high-voltage power source for an alternating or direct current supply, a spinneret, and a grounded collector. Here the solution is pushed using an external pump, and a pendant droplet is formed at the spinneret. Upon application of voltage, the shape of the droplet changes to a "Taylor cone". In the presence of the electric field, a charged jet ejects in the form of a straight line, which becomes thinner and whips in the air medium, which leads to the continuous formation of the fiber. As the jet becomes thinner, it solidifies, which is ultimately deposited on the grounded collector. Electrospun fiber formation and control of their diameters are mainly dependent on the voltage applied, the liquid flow rate, and the spinneret tip-to-collector distance.[170] When a solution of higher concentration is used, the jet coming from the tip of the Taylor cone elongates by whipping, whereas droplets are formed for a solution of lower concentration and get electrosprayed.

Electrospinning can be used to produce nanofibers that can serve as a platform for biomolecule immobilization. For example, bisphenol A (BPA) can be detected by using tyrosinase immobilized electrospun nanofiber.[171] A solution of Polyamide 6 (PA6) and poly(allylamine hydrochloride) (PAH), prepared in formic acid, was used, and the produced nanofibers were collected on a FTO electrode. This was then modified with AuNPs and subsequently, tyrosinase was immobilized utilizing EDC-NHS coupling. Tyrosinase oxidizes BPA to *O*-quinone, which could be detected amperometrically at a low potential (0.1 V) with the modified electrode. The use of a 3D open porous structure is a good choice for transducing application. Such a porous structure can be produced using the electrospinning method if the choice of the formulation is made smartly so that it produces continuous fiber without clogging the spinneret. A method for Zika virus detection using a 3D porous structure has been described.[129] This 3D structure was prepared from a blend of PVA and alginate by using electrospinning. The resulting electrospun nanofiber mat (ENM) was then treated with a glutaraldehyde solution. This treatment bridges the carboxylic and hydroxyl groups of the alginate and the PVA, respectively, which improved the physicochemical property and stability of the ENM. This was followed by the treatment of the ENM with PANI, which changes the organization of the ENM from thin, separate fibers to thick, assembled fibers. Subsequently, a polyclonal antibody against the Zika virus was immobilized on the PANI-modified ENM and detection was performed.

The cost of electrospinning is less and the setup for electrospinning is commercially available for industrial production. Besides, almost all the main types of materials can be electrospun either directly or indirectly. However, the fabrication of nanofibers with smaller diameters is challenging.

4.1.8. Vapor Deposition. Fabrication of biosensors using conventional methods is easy and is used widely. But one of the main issues is its reproducibility, especially when scaled up from the laboratory to the industrial level.[172] In the case of nanomaterial deposition which is often used for biosensor fabrication, this reproducibility issue greatly affects the performance.[173] Vapor deposition is an emerging deposition method that is widely used for thin film preparation. Based on the principle of deposition, it can be divided into physical vapor deposition (PVD) and chemical vapor deposition (CVD).[174] In PVD, the source material is evaporated to gas and then again condensed onto a solid substrate. The most commonly used PVD methods are evaporation and sputtering. PVD was used for fabricating a biosensor electrode for *Salmonella* DNA detection.[175] Here, AuNPs were deposited onto the ITO substrate by thermal evaporation from a pure Au granule. Before performing the PVD, the chamber was pumped down to 9×10^{-6} mbar, and the Au granule was melted to evaporate and deposit. The probe ssDNA sequences were then attached to the resulting AuNP/ITO electrode. The hybridization event between the target and probe DNA was then monitored using DPV in the presence of a redox probe. The DPV peak intensity decreases with increasing target concentration since the electron transfer between the redox probe and the electrode gets hindered. Another method of PVD is sputtering, where the source is connected to the cathode and the high-energy ions are used to knock out atoms from the source.[174] A RF magnetron sputtering method for depositing nanostructured NiO on F-doped SnO_2 conducting glass (FTO) was described.[176] These nanostructured NiO was then utilized for GOx immobilization, and subsequently, glucose sensing was performed. The PVD method is also used for miniaturized electrode fabrication.[139,177,164]

In CVD, the vapor is generated by chemically reacting the volatile precursor(s) and is deposited on the substrate. Usually, CVD offers a higher rate of deposition compared to PVD.[178] CVD-derived graphene is superior to chemically derived graphene in terms of quality and production of monolayer graphene in larger areas. Singh et al. used CVD-derived

https://doi.org/10.1021/acsmeasuresciau.3c00034
ACS Meas. Sci. Au 2023, 3, 404−433

graphene during the fabrication of an impedimetric biosensor for carcinoembryonic antigen (CEA).[172] Here graphene was deposited on a Cu foil substrate using hexane as a precursor. To do so, the Cu foil was loaded inside a quartz furnace tube and the temperature of the furnace was raised to 980 °C and stabilized there for 30 min. Thereafter hexane vapor was directed to the furnace for 5 min and then it was cooled to room temperature under H_2 environment. The resulting deposited graphene layer was then surface modified with 1-pyrenebutanoic acid succinimidyl ester (PBSE) by utilizing $\pi-\pi$ stacking. These PBSE molecules act as a linker for binding anti-CEA. Similarly, Yuan et al. also reported a glucose biosensor that utilized CVD in combination with a sputtering method during electrode fabrication.[179] Here graphene was deposited onto a Cu foil using the CVD method. After that, AuNPs were deposited on the graphene-deposited Cu film by using a sputtering method. Cu film from the AuNP/graphene/Cu was subsequently etched using 0.2 M $(NH_4)_2S_2O_8$, which resulted in Au/graphene film. This film was then attached to the surface of a GCE. The AuNP/graphene/GCE was further modified with linker molecules to immobilize GOx. 6-(ferrocenyl)hexanethiol acts as a redox mediator for the detection.

Among the different CVD methods, atomic layer deposition (ALD) is commonly used for bioelectrode fabrication.[180] Here two gas precursors are used, and their self-limiting reactions of precursors result in thin film deposition. At first, a precursor is introduced to the reaction chamber and allowed to react with the substrate. Thereafter non reacting gas is removed by purging an inert gas into the chamber. Subsequently, the other gas is introduced and allowed to react, and unreacted gas and byproducts are removed by purging an inert gas. This cycle is continued to achieve the desired layer thickness. The ALD method for fabricating a miRNA biosensor was reported.[181] Here MoS_2 films were formed in situ in the ALD chamber. To produce MoS_2, $MoCl_5$ and H_2S were used as precursors and N_2 was used as the inert gas. Both precursor gases were kept at two different conditions and allowed to enter the reaction chamber alternatively. AuNP was then electrodeposited onto this deposited MoS_2 film and further modified with a probe ssDNA. In the presence of the target miRNA, the probe ssDNA hybridizes with the target. This event was electrochemically studied by using DPV.

4.1.9. Langmuir–Blodgett (LB). LB films are known for their ability to provide well-organized molecular architecture.[182,183] There are two main steps involved in the formation of an LB film; the first step is the formation of a floating monolayer film in the air–water interface, and the second step is the deposition of that film onto a solid substrate. Classically, amphiphilic molecules (e.g., lipids and fatty acids) are used during the preparation of LB films. Initially, a dilute solution is prepared by dissolving the amphiphilic molecules in a volatile solvent. This solution is then spread out on top of the water surface. After the spreading, the solvent evaporates, and a very thin layer of amphiphilic molecules remains on the interface, the hydrophilic part of which is immersed in water, leaving the hydrophobic tail on the air phase. After that, a densely packed layer is formed by compressing the liquid barriers, which are then transferred to a surface by dipping either vertically (called LB technique) or horizontally (called Langmuir–Schaefer (LS) technique).[184] Apart from amphiphilic molecules, other molecules have also been reported to be employed in the LB techniques. For example, Solanki et al. reported the deposition of LB film of AuNP decorated MoS_2 on an ITO electrode.[136] The composite of MoS_2–AuNP was prepared by heating $AuCl_3$ with a chemically exfoliated MoS_2 nanosheet at 80 °C which was followed by the addition of citrate and heated again at 60 °C. Preparation of the LB film was achieved through the dispersion of the composite in $CHCl_3$ and its subsequent spreading onto the water subphase. During the spreading process, evaporation of $CHCl_3$ occurs and results in a spread monolayer at the water–air interface, which can be compressed to a dense LB film. Here also, the dense LB film was prepared by compressing the monolayer at an optimized pressure, and then the resulting layer was transferred onto an ITO substrate through its vertical dipping. Polyclonal antibody NS1 was then immobilized to the resulting ITO/MoS_2–AuNP electrode to detect NS1 (a biomarker for dengue-infected people) using EIS. Here decoration of MoS_2 by AuNP acts as a spacer between the MoS_2 sheets that prevents the restacking of them. It also reduces the charge transfer resistance of the ITO/MoS_2–AuNP electrode compared to ITO/MoS_2, and therefore could improve the performance of the sensor. The LoD and the linear range for the detection could further be enhanced by replacing ITO/MoS_2 with reduced graphene oxide (RGO).[118]

4.1.10. Self-Assembly Technique. A self-assembled monolayer (SAM) forms at the solid–liquid interface. In principle, two limiting routes are there for self-assembly: substrate coupled and substrate decoupled.[185] In the substrate coupled method, the SAM is formed using the self-assembly of molecules on the solid substrate by chemisorption. It is a substrate-dependent process, and the crystalline structure plays an important role. Here, the headgroup of the SAM forming molecules directly binds to the specific site of the substrate, and the substrate structure dictates the monolayer organization. Typically used molecules are alkanethiols and thiophenols and they possess three characteristic parts; a headgroup that binds to the solid surface strongly, an alkyl chain or an aromatic structure that provides stability, and a terminal group that is used to couple biomolecules to the monolayer.[186] One classical example of a solid surface that is utilized is the gold surface, where a strong Au–S bond formation takes place. In the substrate decoupled process, the organization of the molecules to form SAM depends on the interaction among the SAM forming molecules, and the intermolecular packing dictates the molecular organization. The classical example is the formation of a SAM of alkyltrichlorosilane on a hydrated silicon substrate. The formation of a good quality SAM of alkyltrichlorosilane requires careful control of the water quantity. In the absence of water, incomplete monolayer forms, whereas in the presence of excess water polysiloxane forms due to facile polymerization and deposit on the substrate.[187] The proposed mechanism of organosilane SAM formation involves the formation of assembly of the $RSi(OH)_3$ intermediate on the water-adsorbed surface, which is 2–3 monolayers thick. This intermediate layer self-assembles due to intermolecular interaction. Subsequently, cross-linking of the silanol groups occurs. Apart from silicon substrate, other substrates like aluminum oxide, glass, zinc oxide, germanium oxide, indium oxide, mica, etc. can also be used.[187] A prototype for the detection of epithelial growth factor receptor (EGFR), based on the formation of SAM was proposed.[74] Here mercaptoundecanoic acid (MUA) was used to construct the monolayer. The –SH group of MUA binds to the Au surface via a Au–S bond, and the exposed

https://doi.org/10.1021/acsmeasuresciau.3c00034
ACS Meas. Sci. Au 2023, 3, 404–433

terminal −COOH group was used for EDC-NHS coupling for immobilization of the EGFR antibody. This study showed that changing the surface morphology of gold electrodes from plain to hyperbranched nanostructure enhances the immobilization efficiency tremendously, 28.4% to 94% for BSA. Besides, the time for the formation of SAM reduces from 12 h to 45 min.

Although thiol-modified hydrocarbons are widely used for preparing the SAM layer on gold electrodes, incorporation of oligonucleotide containing the −SH group may enhance the performance of the biosensor during impedimetric measurements. The performance of an impedimetric biosensor chip toward cardiac troponin I detection using different thiol-containing molecules was investigated.[188] During such measurements, attention should be given to minimizing the binding of nonspecific proteins. Here HSA was used as the model protein for studying the nonspecific binding. In this context, various thiolated hydrocarbons and thiolated oligonucleotides were used for SAM preparation onto a gold substrate. Hydrocarbon chains with longer chain lengths were effective in reducing the nonspecific protein adsorption but increased the impermeability and hence hindered the charge transfer required during the EIS study. Aromatic thiols, on the other hand, increased the permeability but were not effective in reducing nonspecific protein adsorption compared to the thiolated hydrocarbon chain. Thiolated oligonucleotides were shown effective in terms of charge transfer permeability and in reducing nonspecific adsorption. Thus, thiolated DNA-based SAM was found to be more promising compared with the thiolated hydrocarbons.

4.1.11. Layer-by-Layer (LbL) Technique. It is another technique for developing a thin film. Conventionally, LbL films are prepared by the alternate adsorption of oppositely charged molecules sequentially on a solid surface. For this purpose, a SAM is formed at the solid surface onto which further layers of molecules (e.g., polyelectrolytes) are deposited, which ultimately leads to a structurally well-defined material of molecular thickness. Although the multilayer LbL film growth is primarily based on the Coulombic interaction between the substrate and the polyelectrolytes, other interactions, namely, hydrogen bonding, van der Waals interactions, dipole−dipole interactions, etc. also influence the LbL film stability.[189,190] The LbL method is simple and inexpensive and often results in a robust film. Further, incorporation of metal nanoparticles and carbon-based nanomaterials is also possible which can enhance the biosensor's performance.[190] The method was exploited to fabricate the biosensor electrode for immunosensing of PSA.[133] At first, an SAM was prepared onto a gold electrode, which was further subjected to LbL film construction. This SAM-modified electrode was then immersed in a solution of cationic polymer poly(ethylenimine) (PEI), subsequently in an anionic solution of poly(vinylsulfonic acid, sodium salt) (PVS), and again in PEI. This outer PEI leaves positively charged groups on the surface that was utilized for immobilization of AuNP conjugated PSA antigen. In comparison to the conventional sandwich-assay-based PSA detection, this proposed sensing method took less analysis time and did not require secondary antibodies. Conducting polymers were also explored for constructing the LbL film. For example, David et al. reported an amperometric glucose biosensor that utilized electropolymerized PEDOT:PSS, on which LbL films were formed.[191] This electropolymerized surface possesses negatively charged SO_3^- groups that can be utilized for the deposition of a positively charged layer. Based on this understanding, a positively charged chitosan layer was deposited on the PEDOT:PSS surface. Here, along with the chitosan, N-doped graphene (NG) and GOx were incorporated, by making a solution of these three components in acetic acid. A layer of chit$^+$(NG + GOx) was then deposited on the surface of the electropolymerized PEDOT:PSS by immersing it in the above-mentioned solution. This modified electrode was further immersed in a solution of PSS and, subsequently, another layer of chit$^+$(NG + GOx) was deposited. This bilayer electrode was used for glucose detection by posing the electrode at −0.2 V vs Ag/AgCl.

4.1.12. Printing and 3D Printing. There are different printing methods available for patterning conductive patches, among which screen printing is widely used for patterning macroscale electrodes. It is achieved by squeezing a conductive ink onto a substrate through a screen mask containing mesh, followed by curing of the printed electrode. Customized designs are made on the mask, which act as a negative for the image to be printed on the substrate.[192] It is extensively used to pattern conductive patches on a paper substrate. For example, an immunosensor for detecting avian influenza virus using a paper-based screen-printed electrode was reported.[193] Similar to screen printing, stencil printing is another method where the ink is applied to the hole of the stencil and comes directly in contact with the substrate. Then it is smoothened with the help of a squeeze. A stencil-printed carbon electrode was reported for the detection of bacteria.[194]

Additive manufacturing, also known as 3D printing, is a technology that relies on the layer-by-layer addition of the desired material in a digitally controlled process that ultimately results in a 3D object.[195] Although there are different 3D printing methods available, the most commonly used methods in the context of biosensor fabrication are based on extrusion, photopolymerization, and powder bed diffusion.[195,196] Recently, 3D printing has been explored as an alternative method for electrode fabrication.[196−198] For example, fused deposition modeling (FDM) and powder bed diffusion were used for fabricating electrodes toward H_2O_2[199] and DNA[198] sensing, respectively. FDM, also known as fused filament fabrication (FFF), is an extrusion-based technique where a thermoplastic polymeric material is extruded from a heated nozzle onto a surface to construct the desired structure. Commonly used polymeric materials are acrylonitrile butadiene styrene, polycarbonate (PC), and polylactic acid (PLA). FDM allows the incorporation of many conductive materials (e.g., graphene, pyrolytic graphite, metal nanoparticles, etc.,) into the thermoplastic matrix, which enables FDM to print circuits and electrodes.[195] FDM has been used for fabricating macroelectrodes.[197,200,201] For example, a H_2O_2 biosensor that used FDM for printing graphene/PLA 3D electrodes has been reported.[199] PLA is an insulator but helps in binding the graphene sheets and improves the mechanical property, whereas the presence of graphene provides conductivity to the filament. The 3D-printed graphene/PLA electrode was then subjected to chemical and electrochemical treatment, which enhanced the electrochemical response toward H_2O_2 sensing. It was then incubated in AuNP solution, which was followed by incubation in HRP solution. The incorporation of AuNP in this graphene/PLA 3D electrode further enhanced the electrochemical response toward H_2O_2.

Powder bed diffusion is another 3D printing technique by which particles of powdered materials (e.g., metals, ceramics etc.) can be deposited to form solid electrodes.[195] Selective

https://doi.org/10.1021/acsmeasuresciau.3c00034
ACS Meas. Sci. Au 2023, 3, 404−433

laser melting (SLM) is a powder bed diffusion method, where the powdered material is heated using a laser source that results in the melting of the material, forming a solid layer. Subsequently, another layer is added, and the process is repeated in a layer-by-layer fashion. Use of SLM to construct helical-shaped stainless-steel electrodes for DNA biosensing was reported. Once prepared, gold was deposited onto this steel electrode, and a thiol-modified capture probe was attached via Au−S bond. Although this process can produce printed metal electrodes, the process is costly compared to other 3D printing methods.[198]

4.2. Fabrication of Miniaturized Electrodes

Miniaturized electrodes, e.g., microelectrodes and nanoelectrodes, offer several advantages over conventional electrodes.[209,63] The primary reason for using such electrodes is the benefit obtained from the enhancement in mass transport. The current obtained due to certain analytes consists of two parts; faradaic and nonfaradaic. Enhancement of mass transport makes the faradaic component greater. Besides, the nonfaradaic part is small in such miniaturized electrodes due to the smaller area. This ratio of faradaic to nonfaradaic components is related to the sensitivity of the electrode. Therefore, the use of micro- and nanoelectrodes enhances the sensitivity of the measurement. Unlike macroelectrodes, where the rate of the redox reaction is limited by mass transport, the rate of the reaction in such electrodes is limited by electron transfer. Also, double-layer capacitance is reduced, which results in a small RC (resistive-capacitive) time constant. It allows measuring voltammetry at a faster speed in the microsecond time scale, which helps to study the kinetics. Apart from that, the use of miniaturized electrodes requires less sample volume and makes the system more portable due to the smaller electrode size.

Biosensing systems that use miniaturized electrodes are investigated under three popular types: micro and nanopatterned biosensors, microfluidic biosensor, and microelectromechanical (MEMs) based biosensor.[210] Lithographic and printing techniques are mainly used to fabricate such systems, often in combination with conventional macroelectrode fabrication techniques. The following sections discuss different fabrication techniques with recent examples.

4.2.1. Lithography and Related Techniques. Lithographic techniques are widely used for micro- and nanofabrications, among which photolithography and a few soft lithographic techniques have mostly been explored to fabricate biosensor electrodes. They require multiple steps. For example, in photolithography, although the sequences vary, common steps involved are deposition of conducting material, coating and patterning of photoresist, and finally pattern revealing by performing etching or lift-off. It is widely used to prepare metal interdigitated electrodes (IDEs). They involve the deposition of thin metal layer/s on the target substrate, followed by the coating of a photoresist layer, onto which the sensor design is produced using a mask by exposing under the UV-light.[139,211] The IDE is then revealed by using etching. Alternatively, the substrate can first be coated with a photoresist, and subsequently, the sensor pattern is produced using a mask by exposing to UV-light.[212] Thereafter, the deposition of a thin metallic layer is completed, and the IDE pattern can be revealed by performing the lift-off process.

Etching and lift-off are two important steps performed during microfabrication which can selectively remove previously deposited layers, and/or substrate of a sample.[139,213] Such a selective removal can reveal structures of μm or sub μm dimensions. During etching, the material is chemically and/or physically attacked, which results in its erosion. Etching is often divided into wet etching and plasma etching; where the etching reactions utilize liquid etchants and gaseous etchants, respectively.[214] The terms plasma etching and reactive ion etching are also interchangeably used. Lift-off is an alternative technique to etching, and is easier to pattern noble metals e.g., Pt and Au, which are not easily etched away.[215] Here, a sacrificial layer is first spin coated and patterned, and then the target metal is deposited on the substrate. Removal of the sacrificial layer with a solvent revealed the metal patterns on the substrate.

4.2.1.1. Photolithography. It is the most dominant and mature method used in the semiconductor industry for micro- and nanofabrication. There are basically two types of photolithography techniques: (a) contact and proximity photolithography, and (b) projection photolithography.[205] In contact photolithography, the photomask is in direct contact with the photoresist layer, whereas in proximity photolithography, the photomask is in close proximity to the photoresist layer. In the first type, a desired pattern is designed on the photomask, and UV light is passed through this. This creates the desired pattern on the target substrate coated with photoresist. Here, both the photomask and the photoresist-coated substrate are the same size. In the second type, i.e., projection photolithography, a pattern is formed on the photoresist-coated substrate with the help of a photomask and a sophisticated optical image projection system. UV light source is utilized for this purpose which passes through the photomask and the projection system. The pattern formed on the photoresist is typically smaller than that of the photomask. The projection system contains a projection lens by which this reduction in magnification is achieved.

A Si-based substrate is often used while fabricating biosensor electrodes through photolithography. For example, the detection of ssDNA (for monitoring *E. coli* O157:H7) was performed using an interdigitated gold electrode (Au IDE), fabricated on a Si-substrate.[139] At first, it is thermally oxidized to prepare a 1 μm thick SiO_2 layer on the Si-substrate, followed by the deposition of a gold layer using sputtering. The gold-deposited surface was then coated with a positive photoresist by employing spin-coating. Thereafter the IDE mask having the desired pattern was aligned with the surface and subjected to UV-light exposure. Subsequently, the unexposed photoresist was removed, and hard baking was done. Finally, the Au IDE was obtained after one step of etching. The resulting Au IDE was then attached to the capture probes using APTES (3-aminopropyl)triethoxysilane), which bonds with the SiO_2 layer using a self-assembly mechanism, and further allows immobilization of the capture probe via the formation of amide bonds. In the presence of the target ssDNA, hybridization between the target and the capture probes occurred, which changed the resistivity of the APTES layer according to the target concentration. This was reflected by the recorded $I-V$ curve, which showed a linear range from 1 fM to 10 μM target concentration. Similarly, an Au IDE electrode fabricated using contact mode photolithography on Si-based substrate was used for HLA-B*15:02 genotyping.[212]

Photolithography is possible with substrates other than silicon-based substrates, as well. For example, PDMS, PET, and PEN are a few of the substrates that are commonly used to pattern microelectrodes.[216−218] In ref 216, photocurable

https://doi.org/10.1021/acsmeasuresciau.3c00034
ACS Meas. Sci. Au 2023, 3, 404−433

PDMS was mixed with an initiator and then spin-coated on a glass slide and allowed to cross-link by exposing UV light. This resulted in a thin PDMS film. After that, a photoreactive conducting ink was prepared by mixing silk-sericin photoresist, PEDOT:PSS, and an initiator was then cast on the PDMS film. Micropatterning of the conducting ink was then achieved using photolithography. Subsequently, it was soaked in water, which resulted in a flexible micropatterned PDMS.

4.2.1.2. Soft Lithography and Related Techniques. Soft lithography refers a set of techniques used to generate micro- and nanostructures using an elastomeric stamp having a patterned relief structures.[219] The stamp is generally constructed by casting a prepolymer against an initial master, which itself is produced using photolithography or electron beam lithography, however, other methods have also emerged.[219] There are several established soft-lithographic methods available and they are essentially based on printing, molding, and embossing with an elastomeric stamp.[219] For example, microcontact printing (μCP), which is based on printing, can generate microstructured patterns on the target substrate and is commonly used to form SAM. In μCP, the stamp is inked with the material of interest and then transferred to the substrate's surface by applying mild pressure. The pattern is determined by the relief structure of the stamp. Commonly used molding-based soft lithography techniques are microtransfer molding (μTM) and replica molding. In μTM, a liquid prepolymer is first applied on the surface of the patterned stamp, and after removal of the excess liquid, it is subsequently brought in contact with the target substrate. The molded prepolymer is then set to solidify using light or heat and subsequently lifted off.[206] In the replica molding, a replica of the initial master is formed by coating a prepolymer on the master, which is then cured by heat or light treatment.[206] Removal of the stamp thus leads to a negative of the initial master, which can be used as a stamp for other methods, e.g., in μCP or μTM.

Soft lithography was used to fabricate microelectrodes. For example, a biosensor for the detection of IL-10 cytokine reported the use of replica molding and the μCP to fabricate Au microelectrodes.[220] Here, a PDMS-based elastomeric stamp was fabricated by using the replica molding method. Using this stamp, a SAM of octadecanethiol was patterned on a gold deposited polyimide substrate using the μCP method, which was followed by wet etching. The patterned SAM layer acted as a mask to protect gold during the wet etching step. After the Ag/AgCl was fabricated as the RE, the WE was attached to the antibody against IL-10, and tested against IL-10 using EIS. Fabrication of microchannels can also be achieved using soft lithography. For example, a prototype of a microfluidic biosensor for cholesterol detection demonstrated where the PDMS microchannels were prepared using the photolithography and the replica molding method.[221] The constructed microchannel was subsequently bonded to the biosensor chip containing the patterned WE and the CE. Here, ChOx was used as the biorecognition element and immobilized onto the WE using physical adsorption. Finally, cholesterol measurement was performed using chronoamperometry by inserting a Ag/AgCl RE in the outlet of the microchannel.

Another two methods that are conceptually related to soft lithography are hot embossing and nanoimprint lithography. Unlike soft lithography, a hard master is used in hot embossing to transfer the stamp's pattern directly onto a polymeric material. It requires high pressure and temperature during the patterning, and hence, limited materials can be used. Generation of nano- and microhemisphere arrays on polycarbonate and PET, respectively, were reported using this method. The resulting nano and the microstructures were then subjected to sputtering to coat a thin gold film on it and subsequently attached with biorecognition element following standard protocol.[222,223]

Nanoimprint lithography is another lithography method that is conceptually similar to replica molding. It also uses a hard material as a stamp/mask/mold. Here the stamp is pressed into an imprint fluid that covers the substrate. A thin residual layer is intentionally created under the mask, which prevents the mask from direct impact and, therefore, protects the relief structure of the mask. Thereafter it is cured using heat or UV light and the stamp is removed subsequently.[208] The pattern achieved using nanoimprint lithography is 1:1 between the mask and the polymeric material. Use of UV nanoimprint lithography to fabricate a glucose biosensor platform was reported.[224] The fabrication process involved spin-coating a photoresist on a glass substrate, followed by baking and subsequent engraving of the electrode array using UV lithography. This step was followed by the deposition of a 100 nm thick Pt layer by using electron beam evaporation. It acted as a WE on which a pillar-patterned pyrrole-based electrode was fabricated using nanoimprint lithography. This was achieved through spin-coating of a UV-curable pyrrole layer and subsequent nanoimprinting using a pillar-patterned stamp. Finally, lift-off was performed using acetone, and passivation of the needleless parts was done. Unlike UV-based nanolithography, thermal nanoimprint lithography (TNIL) uses heat during the curing process. Use of TNIL was reported to fabricate a nanoelectrode array (NEA) for detecting gliadin.[225] The fabrication of the NEA involved the spin-coating of polycarbonate on a boron-doped diamond electrode. This spin-coated polycarbonate was then annealed, and subsequently, the nanopattern of the master was replicated on the polycarbonate by applying a pressure of 10 MPa for 10 min at 180 °C. Further, the residual layer was removed using reactive ion etching, and the resulting NEA electrode was functionalized with the antigen gliadin. The binding event of gliadin was then quantified using the gliadin-specific antibody coupled with an HRP-attached secondary antibody.

4.2.1.3. Other Lithographic Techniques. Other lithography techniques are also available but are less studied in the context of biosensor electrode fabrication compared to that of photo- and soft lithography. For example, electron beam lithography (EBL) is capable of resulting in feature sizes lower than conventional photolithography but is not suitable for mass production.[207] EBL was used to fabricate nanowires for biosensor uses. For example, nanowire FET, fabricated using EBL, was reported for detecting prostate specific antigen,[226] γ-aminobutyric acid,[227] and nanowire electrode for detecting glucose.[228] Besides, EBL was used to fabricate nanoelectrode arrays on boron-doped diamond macroelectrode.[229] Recently, an inkjet printing base lithography technique was developed, termed inkjet maskless lithography, for graphene patterning and was utilized for detecting organophosphates.[230,231] Another method, nanosphere lithography, was used for detecting *Staphylococcus aureus* 16S rRNA hybridization, where AuNP arrays were patterned on ITO electrodes using nanosphere lithography.

https://doi.org/10.1021/acsmeasuresciau.3c00034
ACS Meas. Sci. Au 2023, 3, 404−433

4.2.2. Additive Manufacturing (AM) or 3D Printing. Additive manufacturing or 3D printing creates 3D structures in a layer-by-layer fashion using computer-aided design (CAD). Some of the AM techniques have been explored to fabricate miniaturized biosensor electrodes. The following section discusses the use of 3D printing for fabricating miniaturized electrodes for biosensing applications.

4.2.2.1. Extrusion-Based 3D Printing Methods. *4.2.2.1.1. Inkjet Printing (IJP) and 3D IJP.* It is based on the generation of sequences of droplets, achieved either by continuous inkjet or by drop-on-demand (DoD) inkjet. The DoD is the most commonly used method and the steps involved are drop ejection, drop flight, drop impact, drop spreading, and drop solidification, followed by a sintering step for creating a continuous conducting path.[232] The IJP is a versatile, scalable, cost-effective technique and can print highly intricate patterns on multiple substrates.[230] Like other conventional printing techniques, the resolution achieved through IJP is lower compared to that of the lithographic techniques, but patterning in microscale resolution is possible. Nauran et al. demonstrated the ability of IJP to print microgap electrodes with an interelectrode gap down to 1 μm.[233] The printed electrode was then used to detect HIV-related ss-DNA using peptide nucleic acid as the biorecognition element. An extension of the classical IJP is 3D IJP, which allows patterning in the vertical direction also and therefore can result in a 3D pattern. Recently, fabrication of a 3D microelectrode array using IJP was demonstrated and used to monitor the extracellular activity of cardiomyocyte-like cells (HL-1).[234] Apart from electrode printing, IJP could successfully pattern enzyme and aptamers.[78,235] Bihar et al. reported a paper-based glucose biosensor that demonstrated the ability of IJP to print all the components of the sensor.[78]

4.2.2.1.2. Direct Ink Writing (DIW). DIW is another extrusion-based AM technique. Unlike FDM, it can print inherently conductive polymer without needing a secondary polymer and provides higher resolution compared to that of the FDM technique.[196] This simple and low-cost method is capable of rapidly producing patterns with microscale resolution. For example, electrodes as small as 35 μm resolution could be printed for glutamate biosensing using the DIW method.[236] The resolution of the printed pattern is dependent on the printing speed and dispensing pressure. Besides, the DIW method was found more advantageous in terms of sensitivity, specificity, and reduction in material consumption compared to the screen printing method.[237]

4.2.2.1.3. Aerosol Jet Printing (AJP). AJP is another technique capable of printing microstructures. Here the active ink for printing is generated by ultrasonic atomization in the form of droplets. The resulting droplets are then carried to the deposition head using a carrier gas (also termed aerosol gas), and the aerosol stream is then met with a stream of sheath gas for collimating the beam. The flowing droplets beam is then directed toward the substrate for printing.[238] AJP can produce spatial patterns with a microscale resolution. For example, Parate et al. reported printing of graphene IDE electrodes with 40 μm width and 100 μm spacing using AJP. The graphene ink was first ultrasonically atomized, and carried using N_2 toward the deposition nozzle, where another N_2 stream was introduced before printing. Once fabricated, the IDE electrodes were attached with antibovine interferon gamma (IFN-γ) or interleukin 10 (IL-10) antibody for sensing the respective antigens (IFN-γ or IL-10).[239] Fabrication of sophisticated structures using AJP is also possible. For example, microelectrode arrays with 3D needle-like electrode tips using PEDOT:PSS-MWCNT composite ink were printed using AJP, and were used to record extracellular signals from cardiomyocyte-like HL-1 cells.[240]

4.2.2.2. Photopolymerization-Based Printing. Photopolymerization-based printing is based on the cross-linking of photocurable monomer in the presence of a photoinitiator, which promotes the generation of reactive species and chain growth. Two commonly used methods are vat photopolymerization and photopolymer jetting.[195] Stereolithography (SLA) and digital image processing (DLP) are the two commonly used vat polymerization techniques for fabricating microstructures. In SLA, each layer is printed by projecting the light source in a 2D layer-by-layer fashion. Once this fabrication is completed, a liquid resin is allowed to cover the previous layer and the mixture is subsequently cured. This process ultimately results in the formation of a 3D structure. On the other hand, unlike SLA, where light-driven point-by-point curing is used, DLP uses single light exposure to construct the whole layer shape in one shot. Therefore, DLP takes less time than SLA to form the 3D structure. A photopolymerizable conducting ink for fabricating bioelectrodes for human electrocardiography (ECG) and electromyography (EMG) was developed.[241] The ink contains dispersed PEDOT:PSS in poly(ethylene glycol) diacrylate (PEGDA), ethylene glycol (EG), and a photoinitiator. PEGDA increases the dispersion of PEDOT:PSS and the ink conductivity. However, ethylene glycol also enhanced the conductivity 3-fold. This ink could be processed using the DLP method by placing it into a vat of the 3D printer and by exposing it to UV light. It was observed that the chain length of PEGDA affects the printing resolution. Fabrication of the ECG and EMG electrodes was done on a Kapton sheet covered with a thin layer of Ti (10 nm) and Au (100 nm). This sheet was then laser cut according to the required shape and size and subsequently used for printing. The other method, photopolymer jetting, uses a moving printhead from which photocurable resin extrudes layer-by-layer. Once the printing is done, the printed layer is photocured by using UV light. This method has been used during the fabrication of a microfluidic device for monitoring neurochemicals, glutamate, glucose, and lactate.[242]

4.2.3. Pyrolysis. In the context of micro- and nanofabrication, carbon MEMS and NEMS have recently received attention toward biosensing applications. For the fabrication of these devices, photolithographic methods and SU-8 photoresist are widely used.[243] SU-8 is a highly sensitive photoresist, patternable to a high aspect ratio and 3D structure. During the fabrication process, the micro- and nanopatterned photoresist are converted to photoresist-derived glassy carbon using pyrolysis. This converts the photoresist patterns to conductive carbon patterns while retaining the shape. During the pyrolysis step, the photoresist coating is heated at a high temperature in an inert atmosphere. This step is critical as it defines the important physicochemical properties (microstructure, shrinkage, electrical and thermal conductivity, mechanical stiffness, and chemical reactivity) of the C-MEMS/C-NEMS. Various structures, e.g., 2D and 3D C-MEMS, flexible C-MEMS, suspended C-MEMS, C-MEMS nanogap have already been developed.[243] Fabrication of 2D and 3D C-MEMS starts with photopatterning of a base layer. A second layer is then patterned on top of the first layer. This developed structure is

https://doi.org/10.1021/acsmeasuresciau.3c00034
ACS Meas. Sci. Au 2023, 3, 404−433

Table 2. General Advantages and Disadvantages of Different Fabrication Methods Used for Electrochemical Biosensor Fabrication

Fabrication method	Advantages	Disadvantages	References
Drop-casting	Extensively used method, simple, low waste of materials	Controlling the thickness, porosity, and uniformity is difficult. Binder is often needed which increases resistance, blocks catalytic active sites, and affects electrolyte diffusion.	154
Dip-coating	Simple, provides better control compared to drop-casting in terms of layer uniformity, suitable for larger area fabrication	Not suitable for single face coating, require significant volume of precursor, flat and curved surfaces can be fabricated, not all substrate shape can be fabricated	157
Spin-coating	Better choice compared to drop/dip coating in consideration to uniformity, wastage of depositing material is lesser compared to dip-coating	Planar surface is required, not effective for larger area fabrication	160
Blade-coating	Low-cost, scalable, simple, large area fabrication possible, less solution wastage compared to dip-coating and spin-coating	Not suitable for fabricating thin films, difficult to control micrometric level precision, not precise as spin-coating	154
Electrochemical deposition	Time saving, thin film coating possible, provides better control in terms of uniformity, thickness, nanostructure morphology	Nonconducting surface such as paper cannot be used	148, 134
Electrospray deposition	Nanostructures can be deposited on any surface, metallic or nonmetallic, less time-consuming, higher surface area structure such as 3D droplet-like structure can be fabricated	Lots of parameters need to be optimized	140, 169, 117
Electrospinning	Low cost, less time-consuming, can generate wide range of morphologies	Low yield, requires high voltage which is not suitable for electric sensitive molecule	170
Vapor deposition	Provides excellent reproducibility, high quality film with controlled thickness	Vacuum and high temperature required, CVD coating produces volatile precursors, residual gas that have certain toxicity. ALD provides better film uniformity but requires high temperature, also a slow technique	178, 180
Langmuir–Blodgett	Sophisticated method for producing homogeneous monolayer of organic compounds	Use of aqueous subphase has limitation, not suitable for aggregative materials on water at room temperature	202
SAM	Provides good stability to the immobilized biomolecules, relatively easy to control thickness, helps in oriented and controlled immobilization	Vulnerable to various environmental factors	186, 203
Layer-by-layer	Results in high molecular order, multilayer film with tailored property	Time consuming, labor intensive	204
Photolithography	Projection: High resolution, line width is down to nm	Capital investment and running cost is high	205
	Proximity: Relatively inexpensive, patterning on larger area is possible	Resolution is limited, line width is above 1 μm	
Soft lithography	Can be applied to pattern large area, wide range of materials can be used, convenient and inexpensive, suitable for rigid as well as flexible surfaces, mass production is possible, tunable surface coating	Defect level is higher than photolithography, a master is needed to generate the stamp, also new master is needed while feature design is changed	206, 207
Nano imprint lithography	Pattern replication over a large area with <10 nm feature is possible	Not high throughput, new mold is required while design is changed	208
Scanning and electron Beam lithography	High resolution, mold is not required, can result in <10 nm feature	Mass production not suitable	207
Screen printing	Large area printing possible, low cost, many types of ink can be used	Low resolution, thick film gets printed	192
Inkjet printing	Inexpensive fabrication, well-known technique	Low resolution, nozzle blocking	196
FDM	Fast printing, portability, running cost is lower, cheap material	Limited resolution, limited to polymers	196
DIW	Can print inherently conducting polymer unlike FDM, resolution is high	Limited to nanosized particles	196
Aerosol printing	High viscosity material and large particle size can be used; high resolution with complex geometry can be generated	Expensive	196
Photopolymerization	Higher resolution than FDM, SLM; processing time is fast	Limited to UV curable materials, expensive printer than FDM, inkjet	196
SLM	Can be used to fabricate ceramics, polymers, metallic structures; lower production time	Expensive machine cost than other AM techniques	196

https://doi.org/10.1021/acsmeasuresciau.3c00034
ACS Meas. Sci. Au 2023, 3, 404–433

then pyrolyzed under an inert atmosphere. For the 2D C-MEMS, the fabrication of the second layer of patterning is not needed.

For the application in electrochemical biosensors, the C-MEMS/C-NEMS surfaces need to attach with appropriate biorecognition elements, e.g., enzymes,[244] antibodies,[245] and aptamers.[246] It, therefore, requires functionalization and activation of the C-MEMS surface. Four main techniques are available for carboxyl functionalization of the C-MEMS surface; vacuum ultraviolet, electrochemical activation, UV/O_3, and reactive ion etching.[243] Similarly, direct amination and diazonium grafting are two ways to achieve amino functionalization. Utilizing these surface-exposed functional groups, biorecognition elements can be attached to their surface through covalent immobilization.

4.2.4. Other Techniques. Principles involved in some of the commonly used fabrication techniques have already been discussed in the context of conventional electrode fabrication techniques. These techniques are also used to fabricate miniaturized biosensor electrodes, mainly to deposit nanomaterials and to attach biorecognition elements on their surfaces. There are plenty of examples in the literature. For example, drop-casting to deposit metal oxide nanofibers,[247] dip-coating for depositing cellulose acetate to prevent the dissolution of the active layer of tyrosinase,[248] spin-coating during photolithography,[139] electrodeposition of Prussian blue on carbon fiber electrodes,[249] and to directionally immobilize enzyme together with redox mediator,[250] electrospinning to deposit polymer nanofibers,[247,127] plasma-enhanced CVD for growing vertically aligned carbon nanofibers,[251] PVD for depositing metal layers,[252] SAM technique for patterning alkanethiol,[220] and layer-by-layer technique for depositing biorecognition elements[253] are few representative examples where these techniques are used for fabricating different miniaturized electrodes.

4.3. Fabrication of Paper-Based Miniaturized Electrochemical Biosensors

Paper has become an attractive substrate for microfluidic systems. Herein, the liquid samples are passively pumped through the paper substrate by lateral flow. For its use in detection purposes, it requires the creation of the reaction and the detection zone, which can mainly be achieved in two ways; (a) by cutting the paper to define physical boundaries,[116] or (b) by creating nonconducting patterns, using photolithography or printing.[254] Such nonconducting patterning creates defined hydrophobic and hydrophilic zones on the paper substrate. Compared to photolithography, printing is a cost-effective and easy-to-use technique. It can be divided into template-based (e.g., screen printing) and nontemplate methods (e.g., wax printing).[254]

For patterning conductive tracks, there are different techniques available, including: printing techniques, namely, screen-printing, inkjet printing, and stencil printing. Biosensors based on screen-printed electrodes are many, reported with various targets, mostly belonging to clinical interest. For instance, a glucose biosensor was developed,[255] where the microfluidic channel was created using screen printing ink on a chromatographic paper substrate. Screen printing in combination with wax-printed paper is widely used for creating electrochemical microfluidic systems.[256−258] Generally, wax printing is done to draw the nonconducting pattern, as can be seen in an electrochemical aptasensor developed for the detection of 17β-Estradiol.[257] Here, the microfluidic channel was patterned using wax-printing, and then, electrodes were screen printed. The WE was modified by drop-casting a nanocomposite containing rGO, streptavidin-conjugated AuNP, thionine, and chitosan. Onto this, the biotinylated aptamers that are specific to the targets were attached and performed the detection. Origami paper platforms have also been developed for electrochemical biosensor application.[258] An origami platform using a combination of wax printing and screen printing methods for detecting microRNA was developed.[256] Here, on the microfluidic platform, AuNPs were grown in situ to immobilize the capture probes via Au−S bonds. Thiol-modified hairpin structures were used as capture probes for the target microRNA. The miRNA-induced open hairpin structure was further attached to a bioconjugate containing GOx and CeO_2. Attachment of these bioconjugates was possible only when miRNA binds to the hairpin structure and function for enhancing electrochemical signal and colorimetric detection. This particular platform could, therefore able to produce both electrochemical and optical signals. The paper-based screen printing protocol could further be adapted to different dimensional configurations.[259] Here, for the detection of phosphate ions, a 1D construction was used, and for the detection of a nerve agent, a 2D construction was used. Phosphate ions, in the presence of molybdate ions in acidic media, form a phosphate-molybdate complex, which can be reduced at the WE. For detecting organophosphorus compounds, an enzyme inhibition-based principle was used.

General advantages and disadvantages of commonly used fabrication methods used for electrochemical biosensor fabrication are highlighted in Table 2.

4.4. Miniaturized Electrochemical Biosensor for Detection of Multiple Analytes

In the field of clinical diagnosis, the detection of multiple analytes is often required for conclusive and meaningful information that encourages the introduction of multiplexed biosensor. Integration of electrochemical biosensors with microfluidic chips is a suitable method for designing small-scale multiplexed electrochemical biosensor. Various analytes such as DNA,[260] proteins,[261,262] and small molecules, e.g., glucose,[116] were detected using multiplexed electrochemical biosensors. Three different sepsis biomarkers could be detected simultaneously using a multiplexed electrochemical biosensor,[261] where the biosensor platform was fabricated on a glass wafer onto which gold electrodes were prepared using the photolithography method. Paper-based microfluidic platforms were also explored for multiplexed detection. For example, multiplexed detection of four cancer biomarkers using a paper-based microfluidic platform demonstrated by Wu et al.[263] Recent advances on this topic can be found in the review articles by Liao et al. and Adam et al.[264,265]

5. EFFECT OF ELECTRODE GEOMETRY AND GEOMETRICAL PARAMETERS ON BIOSENSOR PERFORMANCE

In addition to the surface structure and electrode material, the electrode geometry also greatly influences the electrochemical biosensor performance. Early works used traditional macroelectrodes for biosensing. The advent of advanced fabrication methods and materials has made it possible to design miniaturized electrodes with different geometries. Currently, interdigitated and microneedle electrodes are widely used,

https://doi.org/10.1021/acsmeasuresciau.3c00034
ACS Meas. Sci. Au 2023, 3, 404−433

while electrodes of different geometries have also been explored.[130,266−270] For example, cylindrical and disc electrodes have been studied and inferred that disc geometry electrodes offer better sensitivity.[269,270] Signal-to-noise ratio (SNR) for circular shaped electrode geometry with various modifications has also been reported.[271] Different types of microneedles (MN), namely, hollow MN, coated MN, planar MN, and bulk MN have also been reported for biosensing applications.[272] MNs are receiving growing attention because of their ability for minimal skin invasion and their low pain penetration nature. A recent review discussed mechanical and geometrical electrode designs for developing effective biosensors for detecting target analytes in interstitial fluid. Advanced material for their fabrication, opportunities and challenges have also been reviewed.[273] IDEs are generally reported while discussing geometrical effects on the sensor performance. The SNR of an IDE depends on various design parameters such as width, height, length, electrode material, and spacing between the electrodes.[274] With potassium ferro/ferricyanide, the electrode finger with smaller width offered better SNR. Electrode height also plays a significant role in the SNR. It has also been noticed that the role played by the number of electrodes is not significant on the SNR.[274] Increase in sensitivity, as well as noise, is observed with decreasing interelectrode gap in IDEs.[212,275] In a study, the glucose biosensing performance was examined on 3D IDE by varying the space between the electrodes and observed that the optimum gap between the electrode is necessary to trade-off between the noise and detection limit.[275] Another study claims 50% enhancement in the sensitivity of a cardiac troponin I immunosensor when the gaps between the electrodes were reduced from 75 to 5 μm.[266] Further, to enhance the signal by changing the IDE from coplanar to comb structure, about 3-fold increase in signal could be achieved.[276] An immunosensor designed to detect *E. coli* and *S. typhimurium* showed that IDE having features comparable to that of the size of the target analyte provides better sensitivity.[211]

The current density and electric field distribution surrounding the IDE may be analyzed by using simulation study.[276,267] Such studies help to predict the electrode performance by virtually varying different parameters such as height, width, and gap. A recent study showed that the gap between the electrodes is a more important parameter in determining electric field distribution and current density than other parameters, namely, the electrode width and height.[267] After carrying out the preliminary studies using simulation, the electrodes were fabricated and their sensitivity was studied toward the detection of anti-tissue transglutaminase antibodies. Further, it was observed that the incorporation of Au nanoparticles enhanced the sensitivity by over 350%.

Deposition of vertically aligned CNT (VACNT) on the IDE can result in a 3D structure. Such a pattern had been studied toward impedimetric biosensing, and a positive impact of VACNT on the biosensor performance was observed.[130] Additionally, a comparative study was also carried out between an electrode having serpentine geometry and an interdigitated electrode. The latter one performed well compared to the previous one. 3D interdigitated electrodes can also be constructed by placing parallel interdigitated electrodes in close proximity. Signal amplification using such a 3D electrode was reported and subsequent detection of mouse IgG was demonstrated.[277] The amplified signal was found to be sensitive to the interelectrode distance and spacing between the bottoms and ceiling interdigitated electrode. A study focusing on the detection of H1N1 AIV DNA compared the performance of two geometries of interdigitated electrodes, which showed better sensitivity and lower SNR with the rolled-up than planner geometry.[268] Calculation of electric field distribution in the two geometries showed that the rolled-up geometry is efficient in deploying an enriched electric field inside the tube, which enhanced the electron hopping/tunnelling along the DNA chain and thus affected the biosensor performance. A recent study on three commercially available interdigitated electrodes having three unique designs: microarray, concentric circle, and capacitor array design showed that the interdigitated electrode having the concentric circle design is more susceptible to biosensing among the three.[278]

6. COUPLING ELECTROCHEMICAL BIOSENSORS WITH WIRELESS TECHNOLOGY

The research on wireless sensor technology is gaining momentum primarily in the medical, sports, and environmental sectors to achieve fast data exchange and analyses, remote sensing, and onsite applications. Internet of Things (IoT) has greatly boosted the research. Advances in material science led to the development of various materials with highly improved properties suitable for biosensor fabrications on the body and in body applications.[279] On the other hand, advanced printing and lithographic techniques enabled the fabrication of miniaturized electrodes for biosensor applications. All such developments, in turn, led to the construction of miniaturized electrochemical biosensors that are highly promising for portable, wearable, and even implantable and ingestible applications. However, to fully harvest its potential, it requires integration with modern communication technologies, which allows signal processing and wireless data transmission between the sensor and the user interface, the successful accomplishment of which will be very effective in health management and telemedicine as it paves the way for continuous and noninvasive/minimal invasive monitoring.

Among the available wireless technologies, Bluetooth, radiofrequency identification (RFID), and near-field communication (NFC) are widey reported for biosensor device interfacing. Bluetooth is attractive for wireless applications because of its ability to transmit and receive information over long distances and at a higher rate. However, it usually leads to a higher power consumption. In this consideration, NFC and RFID are good choices, but their read ranges are short.[280] Various types of wireless biosensor devices have been reported using these widely used communication systems. Interestingly, many of them use the electrochemical transduction principle.

Many of the electrochemical biosensors are based on wearable platforms such as tattoo platforms, mouthguards, and eyeglasses, which allows minimally invasive and noninvasive monitoring. Noninvasive glucose monitoring using extra body fluids such as sweat, tears, and saliva is highly desired due to its painless approach, free from infection susceptibility, and scope for continuous monitoring.

The human oral cavity has a space that can accommodate a sensor. In this line, a mouthguard attached biosensor for glucose detection in saliva was demonstrated that could perform wireless communication via Bluetooth.[281] To reduce the effects of interferents often present in saliva, namely, ascorbic acid and uric acid, a cellulose acetate membrane was coated on the electrode. García-Carmona et al. demonstrated a

https://doi.org/10.1021/acsmeasuresciau.3c00034
ACS Meas. Sci. Au 2023, 3, 404−433

pacifier-based device coupled with a Bluetooth system to wirelessly detect salivary glucose in infants.[282] This device was specially designed for infants where the mouth movement of the infant on the pacifier results in the effective flow of saliva through the electrochemical chamber attached next to the saliva inlet chamber. The glucose present in the saliva could be detected using a GOx-based-electrode.

An accurate monitoring of sweat-based glucose requires the integration of other sensors, namely, pH, temperature, humidity sensors, etc. A recent study shows that more reliable results can be obtained in epidermal glucose biosensor patches if the effect of glucose level with the real-time fluctuation in pH and temperature are taken into account.[283] A wearable system that incorporated pH, temperature, and humidity sensors along with the glucose biosensor and, integrated to a feedback transdermal drug delivery module, was reported which could communicate wirelessly with a mobile phone via Bluetooth.[284] Martín et al. reported an amperometric wearable wireless sensing platform for the detection of glucose and lactate in sweat[213] (Figure 6). This sensor was also based on a screen-

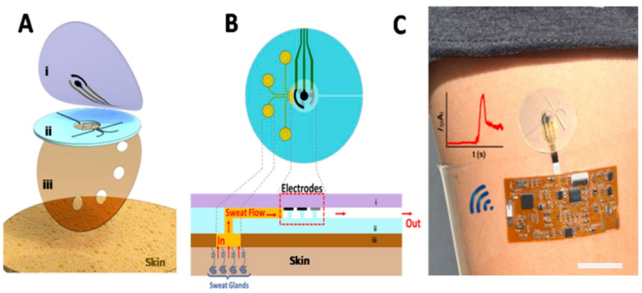

Figure 6. Epidermal microfluidic electrochemical detection. (A) Schematic representation of layered microfluidic device configuration on skin. (B) Schematic representation of sweat collection and operation on skin in top-down and cross-sectional views. (C) Microfluidic device integrated with wireless electronics integrated device. Reprinted with permission from ref 213. Copyright 2017 American Chemical Society.

printed electrode on a polydimethylsiloxane substrate. The microfluidic sampling part and the electrode were fabricated using lithographic and screen-printing technology. The "lab-on-a-chip" system was then integrated with an electronic circuit for the wireless transmission of data via Bluetooth.

In another effort, eyeglasses were used for wireless glucose monitoring of tear drops and the data were transmitted to a laptop via Bluetooth communication[285] (Figure 7B). For this purpose, a microfluidic electrochemical detection platform was placed on the nose-bridge pad of the eyeglasses. Unlike the contact-lens-based systems, this design avoids direct contact of the device with the eye. Apart from the tear glucose, this prototype could detect tear alcohol and tear vitamins.

A contact-lens-based wearable platform has been introduced for tear fluid-based glucose monitoring.[286] A wearable contact lens that could measure glucose in tear solution as well as intraocular pressure was also reported[287] (Figure 7A). Sufficiently transparent electrodes made from a hybrid material consisting of graphene and Ag nanowire were patterned on a stretchable and transparent platform. By integrating these components into a resistance, inductance, and capacitance circuit, real-time monitoring of glucose and intraocular pressure were demonstrated in live rabbit and bovine eyeball, respectively. In this context, a smart contact lens for wireless continuous glucose monitoring and treating diabetic retinopathy was also reported.[286] The designed platform consists of 5 principal parts, the EC biosensor, a flexible on-demand drug delivery system (f-DDS), a wireless energy transfer system, an application specific integrated circuit (ASIC), and a RF communication system. From the f-DDS, drugs can be released in a self-regulating way using RF communication. The feasibility of this device was validated in a diabetic rabbit model.

Besides glucose, many other analytes have also been successfully detected. A prototype of a tattoo-based wireless electrochemical biosensor for noninvasive alcohol monitoring in blood was reported.[288] The wearable sensing platform allows the transdermal delivery of pilocarpine drugs to induce sweat through iontophoresis followed by amperometric detection of ethanol in sweat using the alcohol-oxidase enzyme and the Prussian blue electrode transducer. The data obtained were wirelessly transferred through an electronic circuit in real time via Bluetooth communication. Gao et al. demonstrated a multiplexed point-of-care wound monitoring platform to assay tumor necrosis factor-α (TNF-α), interleukin-6 (IL-6) and IL-8, transforming growth factor-β1 (TGF-β1), *Staphylococcus aureus*, temperature, and pH.[289] Electrochemical measurements were performed by interfacing the multiplexed platform with a portable electrochemical analyzer, and the data were transferred wirelessly using Bluetooth low energy (BLE).

To make the wireless wearable biosensing more sustainable, renewable and sustainable energy sources have been explored.[290,291] For example, Yu et al. demonstrated a BFC-powered electronic skin that allowed multiplexed and continuous monitoring of glucose, urea, NH_4^+, pH and skin temperature.[290] The BFC exploited lactate present in sweat for its operation and enabled wireless data transmission from the electronic skin via a Bluetooth low energy. Zhao et al. reported sweat glucose monitoring smartwatch that used photovoltaic cells for energy harvesting and conversion and, Zn-MnO_2 rechargeable batteries.[292] Besides these, the use of near field communication (NFC) is also an effective strategy in this context.[291,293] For example, Bandodkar et al. reported an NFC-based device that could perform sweat analysis by monitoring chloride, lactate, and glucose, simultaneously with pH, sweat rate, and sweat loss.[291] Interestingly, the device could allow embedding of a colorimetric reagent, which made both the electrochemical and colorimetric analyses possible. Xiong et al. reported a wireless battery-free wound-healing monitoring system based on selective degradation of a DNA hydrogel interfaced with the wound, which gets selectively degraded by deoxyribonucleases secreted by the opportunistic pathogens from the wound.[293] This event modulated the capacitance, and the signal could be wirelessly read using NFC.

Compared to wearable electrochemical biosensors, reports on implantable and ingestible electrochemical biosensors are limited, and successful development of such systems is challenging as they need immense consideration of in vivo biocompatibility. Recently, De la Paz et al. reported a biofuel cell-based self-powered ingestible wireless biosensing system for monitoring glucose dynamics in small intestine.[294] The system utilized a magnetic human body communication scheme for receiving the transmitted signal. Although reports on implantable and ingestible wireless electrochemical biosensing are limited, few reports that utilize other sensing platforms. For example, Kalantar-Zadeh et al. reported a Bluetooth-based wireless sensing system that combined

https://doi.org/10.1021/acsmeasuresciau.3c00034
ACS Meas. Sci. Au 2023, 3, 404−433

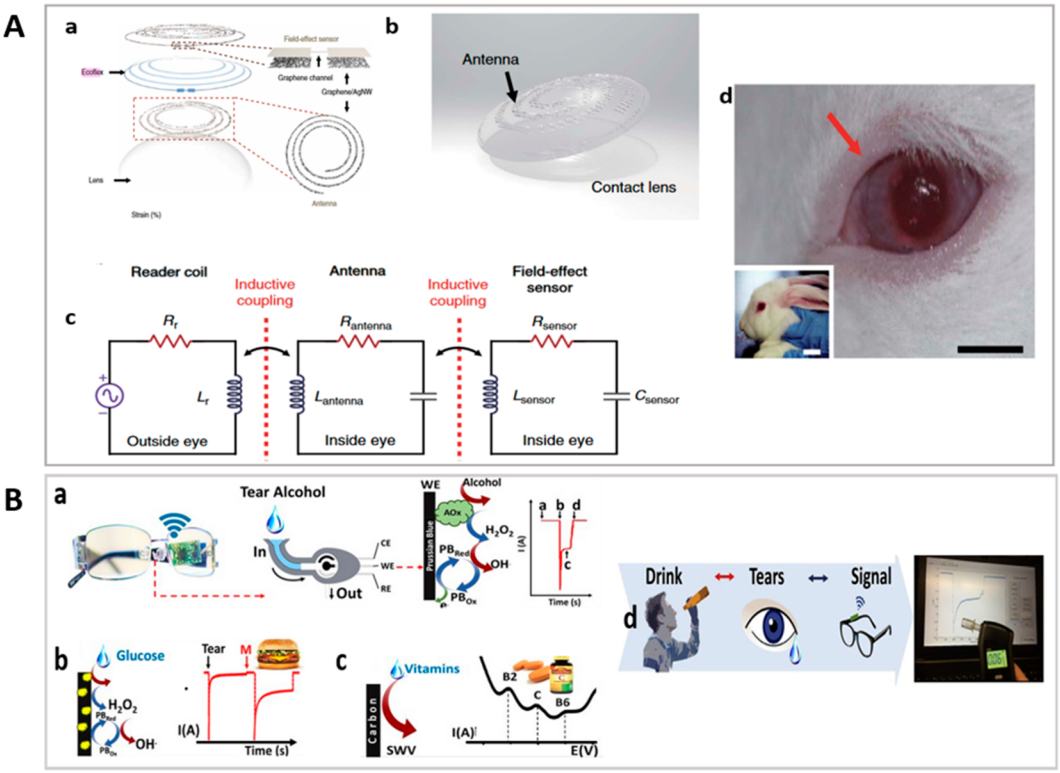

Figure 7. Wearable sensing platforms. (A) Wireless contact lens for glucose and intraocular pressure monitoring: (a) schematic of the wearable contact lens containing both the glucose sensor and intraocular pressure sensor, (b) transparent glucose sensor on contact lens, (c) circuit representation for wireless glucose sensing, and (d) sensor integration to a rabbit eye. Reprinted with permission under a Creative Commons CC BY License from ref 287 with permission. Copyright 2017 Springer Nature. (B) Representation of eyeglass-based tear monitoring system. Sensor platform attached to the nose-bridge of the eyeglass for monitoring (a) alcohol, (b) glucose, and (c) vitamins; (d) steps involved in the tear detection. Reprinted with permission from ref 285. Copyright 2019 Elsevier.

thermal conductivity and semiconducting sensors for selective and sensitive sensing of temperature profile, hydrogen, oxygen, and carbon dioxide in the human gut.[295] Xu et al. reported an implantable device for peritoneal glucose monitoring in rat. The device used platinum tree as a catalyst on the working electrode and, NFC for data transmission and power supply.[296]

7. CONCLUSION

The demand for a simple and portable analytical device that detects analytes sensitively and rapidly in diverse application fields has led to a surge in research on electrochemical biosensors due to their high potential to meet these requirements. The progress made in the development of bioelectrodes, the kingpin of electrochemical biosensors, is impressive, as revealed by the plethora of experimental papers published over the past decade. A continuous strive to gain robust biorecognition elements to function well in complex environments prompted the search for nucleic-acid-based systems achieving significant success with examples of aptamers and CRISPR-based sensors. Similarly, promising results are also gathered for stabilizing the traditional protein-based recognition elements on the electrode surface, leveraging the effect of various emerging biocompatible substances, including polymers and nanocomposite materials. However, the bioelectrochemical signal efficiency is also subjective to the electrode fabrication strategies embraced by a suitable signal-generating principle, immobilization mode of the biorecognition elements, substrate diffusion, reaction kinetics, and signal stability. The demand for device miniaturization for production cost reductions, portable operations, and other advantages prompted the search for newer bioelectrode and biosensor platform fabrication strategies that introduced microscale engineering techniques such as lithography, microfluidics, and various printing methods. Efforts are also underway to develop self-powered biosensors with minimum operational intervention and energy input to meet the growing needs in various fields, including sports, healthcare, and other biomedical applications. Integrating such devices with body parts (implantable and skin worn) will significantly boost health monitoring systems and, thus, bear enormous prospects to improve the human lifestyle. Coupling bioelectrode functions with microelectronic chips and mobile communicating devices such as a smartphone allows remote control and access to sensor data, enabling real-time monitoring and automated operation. While all of these developments are in place, the rational design of the bioelectrode for optimum sensor performance is yet to be adequately realized to adopt as a simple general strategy. The diversity of the biorecognition systems and linked bioelectrochemical signals poses a significant challenge to evolving the rational design. With the vast data gathered so far and their accumulation in the coming days, the application of emerging computational tools such as machine learning may facilitate the convergence of the concepts of electrode fabrication and design strategies to a more coherent knowledge platform for developing electrochemical biosensors for diverse applications.

https://doi.org/10.1021/acsmeasuresciau.3c00034
ACS Meas. Sci. Au 2023, 3, 404−433

AUTHOR INFORMATION

Corresponding Authors

Shelley D. Minteer − *Department of Chemistry, University of Utah, Salt Lake City, Utah 84112, United States; Kummer Institute Center for Resource Sustainability, Missouri University of Science and Technology, Rolla, Missouri 65409, United States;* orcid.org/0000-0002-5788-2249; Email: minteer@chem.utah.edu, shelley.minteer@mst.edu

Pranab Goswami − *Department of Biosciences and Bioengineering, Indian Institute of Technology Guwahati, Guwahati, Assam 781039, India*; Email: pgoswami@iitg.ac.in

Authors

Nabajyoti Kalita − *Department of Biosciences and Bioengineering, Indian Institute of Technology Guwahati, Guwahati, Assam 781039, India*

Sudarshan Gogoi − *Department of Chemistry, Sadiya College, Chapakhowa, Assam 786157, India*

Complete contact information is available at: https://pubs.acs.org/10.1021/acsmeasuresciau.3c00034

Author Contributions

¶N.K. and S.G.: Equal contributions. CRediT: **Nabajyoti Kalita** visualization, writing-original draft, writing-review & editing; **Sudarshan Gogoi** writing-original draft, writing-review & editing; **Shelley D. Minteer** supervision, writing-review & editing; **Pranab Goswami** conceptualization, supervision, writing-review & editing.

Notes

The authors declare no competing financial interest.

ACKNOWLEDGMENTS

We acknowledge the financial assistance (Grant No. BT/PR41449/NER/95/1687/2020) of DBT, India, for carrying out this work.

REFERENCES

(1) Song, M.; Lin, X.; Peng, Z.; Xu, S.; Jin, L.; Zheng, X.; Luo, H. Materials and Methods of Biosensor Interfaces With Stability. *Front. Mater.* **2021**, *7*, 1−11.

(2) Kuri, P. R.; Das, P.; Goswami, P. Fundamentals of Biosensors. In *Advanced Materials and Techniques for Biosensors and Bioanalytical Applications*; Pranab, G., Ed.; CRC Press: Boca Raton, FL, 2020; pp 1−28.

(3) Das, P.; Das, M.; Chinnadayyala, S. R.; Singha, I. M.; Goswami, P. Recent Advances on Developing 3rd Generation Enzyme Electrode for Biosensor Applications. *Biosens. Bioelectron.* **2016**, *79*, 386−397.

(4) Singh, A.; Sharma, A.; Ahmed, A.; Sundramoorthy, A. K.; Furukawa, H.; Arya, S.; Khosla, A. Recent Advances in Electrochemical Biosensors: Applications, Challenges, and Future Scope. *Biosensors* **2021**, *11* (9), 336.

(5) Sanati, A.; Jalali, M.; Raeissi, K.; Karimzadeh, F.; Kharaziha, M.; Mahshid, S. S.; Mahshid, S. A Review on Recent Advancements in Electrochemical Biosensing Using Carbonaceous Nanomaterials. *Microchim. Acta* **2019**, *186* (12), 773.

(6) Kucherenko, I. S.; Soldatkin, O. O.; Kucherenko, D. Y.; Soldatkina, O. V.; Dzyadevych, S. V. Advances in Nanomaterial Application in Enzyme-Based Electrochemical Biosensors: A Review. *Nanoscale Adv.* **2019**, *1* (12), 4560−4577.

(7) Morales, M. A.; Halpern, J. M. Guide to Selecting a Biorecognition Element for Biosensors. *Bioconjugate Chem.* **2018**, *29* (10), 3231−3239.

(8) Bazin, I.; Tria, S. A.; Hayat, A.; Marty, J. L. New Biorecognition Molecules in Biosensors for the Detection of Toxins. *Biosens. Bioelectron.* **2017**, *87*, 285−298.

(9) Kjær, T.; Hauer Larsen, L.; Revsbech, N. P. Sensitivity Control of Ion-Selective Biosensors by Electrophoretically Mediated Analyte Transport. *Anal. Chim. Acta* **1999**, *391* (1), 57−63.

(10) Grattieri, M.; Minteer, S. D. Self-Powered Biosensors. *ACS Sensors* **2018**, *3* (1), 44−53.

(11) Nguyen, H. H.; Lee, S. H.; Lee, U. J.; Fermin, C. D.; Kim, M. Immobilized Enzymes in Biosensor Applications. *Materials (Basel).* **2019**, *12* (1), 121.

(12) Juska, V. B.; Pemble, M. E. A Critical Review of Electrochemical Glucose Sensing: Evolution of Biosensor Platforms Based on Advanced Nanosystems. *Sensors (Switzerland)* **2020**, *20* (21), 6013.

(13) Das, J.; Jo, K.; Lee, J. W.; Yang, H. Electrochemical Immunosensor Using P-Aminophenol Redox Cycling by Hydrazine Combined with a Low Background Current. *Anal. Chem.* **2007**, *79* (7), 2790−2796.

(14) Hatada, M.; Loew, N.; Inose-Takahashi, Y.; Okuda-Shimazaki, J.; Tsugawa, W.; Mulchandani, A.; Sode, K. Development of a Glucose Sensor Employing Quick and Easy Modification Method with Mediator for Altering Electron Acceptor Preference. *Bioelectrochemistry* **2018**, *121*, 185−190.

(15) Fang, Y.; Umasankar, Y.; Ramasamy, R. P. A Novel Bi-Enzyme Electrochemical Biosensor for Selective and Sensitive Determination of Methyl Salicylate. *Biosens. Bioelectron.* **2016**, *81*, 39−45.

(16) Chinnadayyala, S. R.; Kakoti, A.; Santhosh, M.; Goswami, P. A Novel Amperometric Alcohol Biosensor Developed in a 3rd Generation Bioelectrode Platform Using Peroxidase Coupled Ferrocene Activated Alcohol Oxidase as Biorecognition System. *Biosens. Bioelectron.* **2014**, *55*, 120−126.

(17) Schachinger, F.; Chang, H.; Scheiblbrandner, S.; Ludwig, R. Amperometric Biosensors Based on Direct Electron Transfer Enzymes. *Molecules* **2021**, *26* (15), 4525.

(18) Milton, R. D.; Minteer, S. D. Direct Enzymatic Bioelectrocatalysis: Differentiating between Myth and Reality. *J. R. Soc. Interface* **2017**, *14* (131), 20170253.

(19) Bartlett, P. N.; Al-Lolage, F. A. There Is No Evidence to Support Literature Claims of Direct Electron Transfer (DET) for Native Glucose Oxidase (GOx) at Carbon Nanotubes or Graphene. *J. Electroanal. Chem.* **2018**, *819*, 26−37.

(20) Tasca, F.; Zafar, M. N.; Harreither, W.; Nöll, G.; Ludwig, R.; Gorton, L. A Third Generation Glucose Biosensor Based on Cellobiose Dehydrogenase from Corynascus Thermophilus and Single-Walled Carbon Nanotubes. *Analyst* **2011**, *136* (10), 2033−2036.

(21) Bollella, P.; Hibino, Y.; Kano, K.; Gorton, L.; Antiochia, R. Highly Sensitive Membraneless Fructose Biosensor Based on Fructose Dehydrogenase Immobilized onto Aryl Thiol Modified Highly Porous Gold Electrode: Characterization and Application in Food Samples. *Anal. Chem.* **2018**, *90* (20), 12131−12136.

(22) Saengdee, P.; Promptmas, C.; Zeng, T.; Leimkühler, S.; Wollenberger, U. Third-Generation Sulfite Biosensor Based on Sulfite Oxidase Immobilized on Aminopropyltriethoxysilane Modified Indium Tin Oxide. *Electroanalysis* **2016**, *29* (1), 110−115.

(23) Hiraka, K.; Tsugawa, W.; Asano, R.; Yokus, M. A.; Ikebukuro, K.; Daniele, M. A.; Sode, K. Rational Design of Direct Electron Transfer Type L-Lactate Dehydrogenase for the Development of Multiplexed Biosensor. *Biosens. Bioelectron.* **2021**, *176*, 112933.

(24) Bollella, P.; Katz, E. Enzyme-Based Biosensors: Tackling Electron Transfer Issues. *Sensors (Switzerland)* **2020**, *20* (12), 3517.

(25) Kim, J.; Park, M. Recent Progress in Electrochemical Immunosensors. *Biosensors.* **2021**, *11*, 360.

(26) Yu, X.; Munge, B.; Patel, V.; Jensen, G.; Bhirde, A.; Gong, J. D.; Kim, S. N.; Gillespie, J.; Gutkind, J. S.; Papadimitrakopoulos, F.; Rusling, J. F. Carbon Nanotube Amplification Strategies for Highly Sensitive Immunodetection of Cancer Biomarkers. *J. Am. Chem. Soc.* **2006**, *128* (34), 11199−11205.

(27) Feng, J.; Li, Y.; Li, M.; Li, F.; Han, J.; Dong, Y.; Chen, Z.; Wang, P.; Liu, H.; Wei, Q. A Novel Sandwich-Type Electrochemical Immunosensor for PSA Detection Based on PtCu Bimetallic Hybrid (2D/2D) RGO/g-C3N4. *Biosens. Bioelectron.* **2017**, *91*, 441−448.
(28) Cheng, S.; Hotani, K.; Hideshima, S.; Kuroiwa, S.; Nakanishi, T.; Hashimoto, M.; Mori, Y.; Osaka, T. Field Effect Transistor Biosensor Using Antigen Binding Fragment for Detecting Tumor Marker in Human Serum. *Materials (Basel).* **2014**, *7* (4), 2490−2500.
(29) Brogan, K. L.; Wolfe, K. N.; Jones, P. A.; Schoenfisch, M. H. Direct Oriented Immobilization of F(Ab′) Antibody Fragments on Gold. *Anal. Chim. Acta* **2003**, *496*, 73−80.
(30) Crivianu-Gaita, V.; Thompson, M. Immobilization of Fab' Fragments onto Substrate Surfaces: A Survey of Methods and Applications. *Biosens. Bioelectron.* **2015**, *70*, 167−180.
(31) Grewal, Y. S.; Shiddiky, M. J.; Spadafora, L. J.; Cangelosi, G. A.; Trau, M. Nano-yeast−scFv probes on screen-printed gold electrodes for detection of *Entamoeba histolytica* antigens in a biological matrix. *Biosens. Bioelectron.* **2014**, *55*, 417−422.
(32) Crivianu-Gaita, V.; Thompson, M. Aptamers, Antibody ScFv, and Antibody Fab' Fragments: An Overview and Comparison of Three of the Most Versatile Biosensor Biorecognition Elements. *Biosens. Bioelectron.* **2016**, *85*, 32−45.
(33) Lagarde, F.; Jaffrezic-Renault, N. Cell-Based Electrochemical Biosensors for Water Quality Assessment. *Anal. Bioanal. Chem.* **2011**, *400* (4), 947−964.
(34) Gui, Q.; Lawson, T.; Shan, S.; Yan, L.; Liu, Y. The Application of Whole Cell-Based Biosensors for Use in Environmental Analysis and in Medical Diagnostics. *Sensors (Switzerland)* **2017**, *17* (7), 1623.
(35) Sevda, S.; Garlapati, V. K.; Naha, S.; Sharma, M.; Ray, S. G.; Sreekrishnan, T. R.; Goswami, P. Biosensing Capabilities of Bioelectrochemical Systems towards Sustainable Water Streams: Technological Implications and Future Prospects. *J. Biosci. Bioeng.* **2020**, *129* (6), 647−656.
(36) Tucci, M.; Grattieri, M.; Schievano, A.; Cristiani, P.; Minteer, S. D. Electrochimica Acta Microbial Amperometric Biosensor for Online Herbicide Detection : Photocurrent Inhibition of Anabaena Variabilis. *Electrochim. Acta* **2019**, *302* (2019), 102−108.
(37) Ben-Yoav, H.; Biran, A.; Pedahzur, R.; Belkin, S.; Buchinger, S.; Reifferscheid, G.; Shacham-Diamand, Y. A Whole Cell Electrochemical Biosensor for Water Genotoxicity Bio-Detection. *Electrochim. Acta* **2009**, *54* (25), 6113−6118.
(38) Sciuto, E. L.; Petralia, S.; van der Meer, J. R.; Conoci, S. Miniaturized Electrochemical Biosensor Based on Whole-Cell for Heavy Metal Ions Detection in Water. *Biotechnol. Bioeng.* **2021**, *118* (4), 1456−1465.
(39) Yang, Y.; Fang, Z.; Yu, Y. Y.; Wang, Y. Z.; Naraginti, S.; Yong, Y. C. A Mediator-Free Whole-Cell Electrochemical Biosensing System for Sensitive Assessment of Heavy Metal Toxicity in Water. *Water Sci. Technol.* **2019**, *79* (6), 1071−1080.
(40) Sánchez, S.; McDonald, M.; Silver, D. M.; de Bonnault, S.; Chen, C.; LeBlanc, K.; Hicks, E. C.; Mayall, R. M. The Integration of Whole-Cell Biosensors for the Field-Ready Electrochemical Detection of Arsenic. *J. Electrochem. Soc.* **2021**, *168* (6), 067508.
(41) Fan, C.; Plaxco, K. W.; Heeger, A. J. Electrochemical Interrogation of Conformational Changes as a Reagentless Method for the Sequence-Specific Detection of DNA. *Proc. Natl. Acad. Sci. U. S. A.* **2003**, *100* (16), 9134−9137.
(42) Otero, F.; Shortall, K.; Salaj-Kosla, U.; Tofail, S. A. M.; Magner, E. Electrochemical Biosensor for the Detection of a Sequence of the TP53 Gene Using a Methylene Blue Labelled DNA Probe. *Electrochim. Acta* **2021**, *388*, 138642.
(43) Mirzapoor, A.; Turner, A. P. F.; Tiwari, A.; Ranjbar, B. Electrochemical Detection of DNA Mismatches Using a Branch-Shaped Hierarchical SWNT-DNA Nano-Hybrid Bioelectrode. *Mater. Sci. Eng., C* **2019**, *104* (June), 109886.
(44) Farjami, E.; Clima, L.; Gothelf, K.; Ferapontova, E. E. off-On" Electrochemical Hairpin-DNA-Based Genosensor for Cancer Diagnostics. *Anal. Chem.* **2011**, *83*, 1594−1602.
(45) Alzate, D.; Lopez-Osorio, M. C.; Cortés-Mancera, F.; Navas, M. C.; Orozco, J. Detection of Hepatitis E Virus Genotype 3 in Wastewater by an Electrochemical Genosensor. *Anal. Chim. Acta* **2022**, *1221*, 340121.
(46) Cajigas, S.; Alzate, D.; Fernández, M.; Muskus, C.; Orozco, J. Electrochemical Genosensor for the Specific Detection of SARS-CoV-2. *Talanta* **2022**, *245*, 123482.
(47) Ferapontova, E. E. DNA Electrochemistry and Electrochemical Sensors for Nucleic Acids. *Annu. Rev. Anal. Chem.* **2018**, *11*, 197−218.
(48) Zavvar, T. S.; Khoshbin, Z.; Ramezani, M.; Alibolandi, M.; Abnous, K.; Taghdisi, S. M. CRISPR/Cas-Engineered Technology: Innovative Approach for Biosensor Development. *Biosens. Bioelectron.* **2022**, *214*, 114501.
(49) Priya Swetha, P. D.; Sonia, J.; Sapna, K.; Prasad, K. S. Towards CRISPR Powered Electrochemical Sensing for Smart Diagnostics. *Curr. Opin. Electrochem.* **2021**, *30*, 100829.
(50) Bruch, R.; Johnston, M.; Kling, A.; Mattmüller, T.; Baaske, J.; Partel, S.; Madlener, S.; Weber, W.; Urban, G. A.; Dincer, C. CRISPR-Powered Electrochemical Microfluidic Multiplexed Biosensor for Target Amplification-Free MiRNA Diagnostics. *Biosens. Bioelectron.* **2021**, *177*, 112887.
(51) Bruch, R.; Baaske, J.; Chatelle, C.; Meirich, M.; Madlener, S.; Weber, W.; Dincer, C.; Urban, G. A. CRISPR/Cas13a-Powered Electrochemical Microfluidic Biosensor for Nucleic Acid Amplification-Free MiRNA Diagnostics. *Adv. Mater.* **2019**, *31* (51), 1905311.
(52) Abnous, K.; Abdolabadi, A. K.; Ramezani, M.; Alibolandi, M.; Nameghi, M. A.; Zavvar, T. S.; Khoshbin, Z.; Lavaee, P.; Taghdisi, S. M.; Danesh, N. M. A Highly Sensitive Electrochemical Aptasensor for Cocaine Detection Based on CRISPR-Cas12a and Terminal Deoxynucleotidyl Transferase as Signal Amplifiers. *Talanta* **2022**, *241*, 123276.
(53) Zhang, Z.; Sen, P.; Adhikari, B. R.; Li, Y.; Soleymani, L. Development of Nucleic-Acid-Based Electrochemical Biosensors for Clinical Applications. *Angewandte Chemie - International Edition.* **2022**, DOI: 10.1002/anie.202212496.
(54) Kakoti, A. Aptamer: An Emerging Biorecognition System. In *Advanced Materials and Techniques for Biosensors and Bioanalytical Applications*; Goswami, P., Ed.; CRC Press: Boca Raton, FL, 2020; pp 69−89.
(55) Rozenblum, G. T.; Pollitzer, I. G.; Radrizzani, M. Challenges in Electrochemical Aptasensors and Current Sensing Architectures Using Flat Gold Surfaces. *Chemosensors* **2019**, *7* (4), 57.
(56) Xiao, Y.; Lubin, A. A.; Heeger, A. J.; Plaxco, K. W. Label-Free Electronic Detection of Thrombin in Blood Serum by Using an Aptamer-Based Sensor. *Angew. Chemie - Int. Ed.* **2005**, *44* (34), 5456−5459.
(57) Xiao, Y.; Piorek, B. D.; Plaxco, K. W.; Heegert, A. J. A Reagentless Signal-on Architecture for Electronic, Aptamer-Based Sensors via Target-Induced Strand Displacement. *J. Am. Chem. Soc.* **2005**, *127* (51), 17990−17991.
(58) Nakatsuka, N.; Yang, K. A.; Abendroth, J. M.; Cheung, K. M.; Xu, X.; Yang, H.; Zhao, C.; Zhu, B.; Rim, Y. S.; Yang, Y.; Weiss, P. S.; Stojanović, M. N.; Andrews, A. M. Aptamer-Field-Effect Transistors Overcome Debye Length Limitations for Small-Molecule Sensing. *Science (80-.).* **2018**, *362* (6412), 319−324.
(59) So, H. M.; Won, K.; Kim, Y. H.; Kim, B. K.; Ryu, B. H.; Na, P. S.; Kim, H.; Lee, J. O. Single-Walled Carbon Nanotube Biosensors Using Aptamers as Molecular Recognition Elements. *J. Am. Chem. Soc.* **2005**, *127* (34), 11906−11907.
(60) Singh, N. K.; Arya, S. K.; Estrela, P.; Goswami, P. Capacitive Malaria Aptasensor Using Plasmodium Falciparum Glutamate Dehydrogenase as Target Antigen in Undiluted Human Serum. *Biosens. Bioelectron.* **2018**, *117* (June), 246−252.
(61) Downs, A. M.; Plaxco, K. W. Real-Time, in Vivo Molecular Monitoring Using Electrochemical Aptamer Based Sensors: Opportunities and Challenges. *ACS Sensors* **2022**, *7* (10), 2823−2832.
(62) Arroyo-Currás, N.; Somerson, J.; Vieira, P. A.; Ploense, K. L.; Kippin, T. E.; Plaxco, K. W. Real-Time Measurement of Small

Molecules Directly in Awake, Ambulatory Animals. *Proc. Natl. Acad. Sci. U. S. A.* **2017**, *114* (4), 645−650.
(63) Wang, J. *Analytical Electrochemistry*, Second ed.; Wiley-VCH, 2000.
(64) Hanrahan, G.; Patil, D. G.; Wang, J. Electrochemical Sensors for Environmental Monitoring: Design, Development and Applications. *J. Environ. Monit.* **2004**, *6* (8), 657−664.
(65) Fernández Abedul, M. T. Dynamic Electroanalysis: An Overview. *Lab. Methods Dyn. Electroanal.* **2020**, No. 1959, 1−10.
(66) Sandford, C.; Edwards, M. A.; Klunder, K. J.; Hickey, D. P.; Li, M.; Barman, K.; Sigman, M. S.; White, H. S.; Minteer, S. D. A Synthetic Chemist's Guide to Electroanalytical Tools for Studying Reaction Mechanisms. *Chem. Sci.* **2019**, *10* (26), 6404−6422.
(67) Laborda, E.; Henstridge, M. C.; Molina, A.; Martínez-Ortiz, F.; Compton, R. G. A Comparison of Marcus-Hush vs. Butler-Volmer Electrode Kinetics Using Potential Pulse Voltammetric Techniques. *J. Electroanal. Chem.* **2011**, *660* (1), 169−177.
(68) Laborda, E.; Henstridge, M. C.; Batchelor-Mc Auley, C.; Compton, R. G. Asymmetric Marcus-Hush Theory for Voltammetry. *Chem. Soc. Rev.* **2013**, *42* (12), 4894−4905.
(69) Zeng, Y.; Smith, R. B.; Bai, P.; Bazant, M. Z. Simple Formula for Marcus-Hush-Chidsey Kinetics. *J. Electroanal. Chem.* **2014**, *735*, 77−83.
(70) Borgmann, S.; Hartwich, G.; Schulte, A.; Schuhmann, W. Amperometric Enzyme Sensors Based on Direct and Mediated Electron Transfer. *Perspect. Bioanal.* **2005**, *1* (C), 599−655.
(71) Ronald Pethig, S. S. *Introductory Bioelectronics for Engineers and Physical Scientists*; Wiley-Blackwell, 2012.
(72) González-Meza, O. A.; Larios-Durán, E. R.; Gutiérrez-Becerra, A.; Casillas, N.; Escalante, J. I.; Bárcena-Soto, M. Development of a Randles-Ševčík-like Equation to Predict the Peak. *J. Solid State Electrochem.* **2019**, *23*, 3123−3133.
(73) Saxena, U.; Chakraborty, M.; Goswami, P. Covalent Immobilization of Cholesterol Oxidase on Self-Assembled Gold Nanoparticles for Highly Sensitive Amperometric Detection of Cholesterol in Real Samples. *Biosens. Bioelectron.* **2011**, *26* (6), 3037−3043.
(74) Bakshi, S.; Mehta, S.; Kumeria, T.; Shiddiky, M. J. A.; Popat, A.; Choudhury, S.; Bose, S.; Nayak, R. Rapid Fabrication of Homogeneously Distributed Hyper-Branched Gold Nanostructured Electrode Based Electrochemical Immunosensor for Detection of Protein Biomarkers. *Sensors Actuators, B Chem.* **2021**, *326*, 128803.
(75) Prado, T. M. D.; Foguel, M. V.; Gonçalves, L. M.; Sotomayor, M. D. P. T. *β*-Lactamase-Based Biosensor for the Electrochemical Determination of Benzylpenicillin in Milk. *Sensors and Actuators, B: Chemical.* **2015**, *210*, 254−258.
(76) Goyal, R. N.; Gupta, V. K.; Chatterjee, S. Voltammetric Biosensors for the Determination of Paracetamol at Carbon Nanotube Modified Pyrolytic Graphite Electrode. *Sensors Actuators, B Chem.* **2010**, *149* (1), 252−258.
(77) Kumar, S.; Umar, M.; Saifi, A.; Kumar, S.; Augustine, S.; Srivastava, S.; Malhotra, B. D. Electrochemical Paper Based Cancer Biosensor Using Iron Oxide Nanoparticles Decorated PEDOT:PSS. *Anal. Chim. Acta* **2019**, *1056*, 135−145.
(78) Bihar, E.; Wustoni, S.; Pappa, A. M.; Salama, K. N.; Baran, D.; Inal, S. A Fully Inkjet-Printed Disposable Glucose Sensor on Paper. *npj Flex. Electron.* **2018**, *2* (1), 1−8.
(79) Dorledo de Faria, R. A.; Dias Heneine, L. G.; Matencio, T.; Messaddeq, Y. Faradaic and Non-Faradaic Electrochemical Impedance Spectroscopy as Transduction Techniques for Sensing Applications. *Int. J. Biosens. Bioelectron.* **2019**, *5* (1), 29−31.
(80) Rahmanian, R.; Mozaffari, S. A.; Amoli, H. S.; Abedi, M. Development of Sensitive Impedimetric Urea Biosensor Using DC Sputtered Nano-ZnO on TiO2 Thin Film as a Novel Hierarchical Nanostructure Transducer. *Sensors Actuators, B Chem.* **2018**, *256*, 760−774.
(81) Tanak, A. S.; Jagannath, B.; Tamrakar, Y.; Muthukumar, S.; Prasad, S. Non-Faradaic Electrochemical Impedimetric Profiling of Procalcitonin and C-Reactive Protein as a Dual Marker Biosensor for Early Sepsis Detection. *Anal. Chim. Acta X* **2019**, *3*, 100029.
(82) Tsujimura, S.; Nishina, A.; Kamitaka, Y.; Kano, K. Coulometric D-Fructose Biosensor Based on Direct Electron Transfer Using D-Fructose Dehydrogenase. *Anal. Chem.* **2009**, *81* (22), 9383−9387.
(83) Vianello, F.; Zennaro, L.; Rigo, A. Coulometric Biosensor to Determine Hydrogen Peroxide Using a Monomolecular Layer of Horseradish Peroxidase Immobilized on a Glass Surface. *Biosens. Bioelectron.* **2007**, *22*, 2694−2699.
(84) Cao, Q.; Liang, B.; Yu, C.; Fang, L.; Tu, T.; Wei, J.; Ye, X. High Accuracy Determination of Multi Metabolite by an Origami-Based Coulometric Electrochemical Biosensor. *J. Electroanal. Chem.* **2020**, *873*, 114358.
(85) Matzeu, G.; O'Quigley, C.; McNamara, E.; Zuliani, C.; Fay, C.; Glennon, T.; Diamond, D. An Integrated Sensing and Wireless Communications Platform for Sensing Sodium in Sweat. *Anal. Methods* **2016**, *8* (1), 64−71.
(86) Hu, J.; Stein, A.; Bühlmann, P. A Disposable Planar Paper-Based Potentiometric Ion-Sensing Platform. *Angew. Chemie - Int. Ed.* **2016**, *55* (26), 7544−7547.
(87) Ding, J.; Li, B.; Chen, L.; Qin, W. A Three-Dimensional Origami Paper-Based Device for Potentiometric Biosensing. *Angew. Chemie - Int. Ed.* **2016**, *55* (42), 13033−13037.
(88) Sadighbayan, D.; Hasanzadeh, M.; Ghafar-Zadeh, E. Biosensing Based on Field-Effect Transistors (FET): Recent Progress and Challenges. *TrAC - Trends in Analytical Chemistry* **2020**, 116067.
(89) Dutta, J. C. FET-Based Biosensors (BioFETs) Principle, Methods of Fabrication, Characteristics, and Applications. In *Advanced Materials and Techniques for Biosensors and Bioanalytical Applications*; Pranab, G., Ed.; CRC Press: Boca Raton, FL, 2020; pp 283−296.
(90) Jaffrezic-Renault, N.; Dzyadevych, S. V. Conductometric Microbiosensors for Environmental Monitoring. *Sensors.* **2008**, *8*, 2569−2588.
(91) Soldatkina, O. V.; Soldatkin, O. O.; Velychko, T. P.; Prilipko, V. O.; Kuibida, M. A.; Dzyadevych, S. V. Conductometric Biosensor for Arginine Determination in Pharmaceutics. *Bioelectrochemistry* **2018**, *124*, 40−46.
(92) Ge, L.; Liu, Q.; Hao, N.; Kun, W. Recent Developments of Photoelectrochemical Biosensors for Food Analysis. *Journal of Materials Chemistry B* **2019**, 7283−7300.
(93) Hu, L.; Xu, G. Applications and Trends in Electrochemiluminescence. *Chem. Soc. Rev.* **2010**, *39* (8), 3275−3304.
(94) Li, L.; Chen, Y.; Zhu, J. *Recent Advances in Electrochemiluminescence Analysis.* **2017**, *89*, 358.
(95) Lenyk, B.; Figueroa-miranda, G.; Pavlushko, I.; Lo, Y.; et al. Dual-Transducer Malaria Aptasensor Combining Electrochemical Impedance and Surface Plasmon Polariton Detection on Gold Nanohole Arrays. *ChemElectroChem* **2020**, *7*, 4594−4600.
(96) Suginta, W.; Khunkaewla, P.; Schulte, A. Electrochemical Biosensor Applications of Polysaccharides Chitin and Chitosan. *Chem. Rev.* **2013**, *113* (7), 5458−5479.
(97) Kamel, S.; Khattab, T. Recent Advances in Cellulose-Based Biosensors for Medical Diagnosis. *Biosensors* **2020**, *10*, 67.
(98) Borah, H.; Gogoi, S.; Kalita, S.; Puzari, P. A Broad Spectrum Amperometric Pesticide Biosensor Based on Glutathione S-Transferase Immobilized on Graphene Oxide-Gelatin Matrix. *J. Electroanal. Chem.* **2018**, *828* (May), 116−123.
(99) Kaushik, S.; Thungon, P. D.; Goswami, P. Silk Fibroin: An Emerging Biocompatible Material for Application of Enzymes and Whole Cells in Bioelectronics and Bioanalytical Sciences. *ACS Biomaterials Science and Engineering.* **2020**, *6*, 4337−4355.
(100) Hickey, D. P.; Reid, R. C.; Milton, R. D.; Minteer, S. D. A Self-Powered Amperometric Lactate Biosensor Based on Lactate Oxidase Immobilized in Dimethylferrocene-Modified LPEI. *Biosens. Bioelectron.* **2016**, *77*, 26−31.
(101) Ghorbani Zamani, F.; Moulahoum, H.; Ak, M.; Odaci Demirkol, D.; Timur, S. Current Trends in the Development of

https://doi.org/10.1021/acsmeasuresciau.3c00034
ACS Meas. Sci. Au 2023, 3, 404−433

Conducting Polymers-Based Biosensors. *TrAC - Trends Anal. Chem.* **2019**, *118*, 264−276.
(102) Wijayanti, S. D.; Schachinger, F.; Ludwig, R.; Haltrich, D. Electrochemical and Biosensing Properties of an FAD-Dependent Glucose Dehydrogenase from Trichoderma Virens. *Bioelectrochemistry* **2023**, *153* (March), 108480.
(103) Yoon, W.; Lee, S. H.; Kwon, O. S.; Song, H. S.; Oh, E. H.; Park, T. H.; Jang, J. Polypyrrole Nanotubes Conjugated with Human Olfactory Receptors: High-Performance Transducers for FET-Type Bioelectronic Noses. *Angew. Chemie - Int. Ed.* **2009**, *48* (15), 2755−2758.
(104) Soares, J. C.; Brisolari, A.; Rodrigues, V. D. C.; Sanches, E. A.; Gonçalves, D. Amperometric Urea Biosensors Based on the Entrapment of Urease in Polypyrrole Films. *React. Funct. Polym.* **2012**, *72* (2), 148−152.
(105) Wang, T.; Liu, J.; Ren, J.; Wang, J.; Wang, E. Mimetic Biomembrane-AuNPs-Graphene Hybrid as Matrix for Enzyme Immobilization and Bioelectrocatalysis Study. *Talanta* **2015**, *143*, 438−441.
(106) Wang, Z.; Xia, J.; Guo, X.; Xia, Y.; Yao, S.; Zhang, F.; Li, Y.; Xia, L. Platinum/Graphene Functionalized by PDDA as a Novel Enzyme Carrier for Hydrogen Peroxide Biosensor. *Anal. Methods* **2013**, *5* (2), 483−488.
(107) Dontsova, E. A.; Zeifman, Y. S.; Budashov, I. A.; Eremenko, A. V.; Kalnov, S. L.; Kurochkin, I. N. Screen-Printed Carbon Electrode for Choline Based on MnO2 Nanoparticles and Choline Oxidase/Polyelectrolyte Layers. *Sensors Actuators, B Chem.* **2011**, *159* (1), 261−270.
(108) Rončević, I. Š.; Krivić, D.; Buljac, M.; Vladislavić, N.; Buzuk, M. Polyelectrolytes Assembly: A Powerful Tool for Electrochemical Sensing Application. *Sensors (Basel)* **2020**, *20*, 3211.
(109) Ma, W.; Jiang, Q.; Yu, P.; Yang, L.; Mao, L. Zeolitic Imidazolate Framework-Based Electrochemical Biosensor for in Vivo Electrochemical Measurements. *Anal. Chem.* **2013**, *85* (15), 7550−7557.
(110) Wang, X.; Lu, X.; Wu, L.; Chen, J. 3D Metal-Organic Framework as Highly Efficient Biosensing Platform for Ultrasensitive and Rapid Detection of Bisphenol A. *Biosens. Bioelectron.* **2015**, *65*, 295−301.
(111) Yan, T.; Zhu, L.; Ju, H.; Lei, J. DNA-Walker-Induced Allosteric Switch for Tandem Signal Amplification with Palladium Nanoparticles/Metal-Organic Framework Tags in Electrochemical Biosensing. *Anal. Chem.* **2018**, *90* (24), 14493−14499.
(112) Kempahanumakkagari, S.; Kumar, V.; Samaddar, P.; Kumar, P.; Ramakrishnappa, T.; Kim, K. H. Biomolecule-Embedded Metal-Organic Frameworks as an Innovative Sensing Platform. *Biotechnol. Adv.* **2018**, *36* (2), 467−481.
(113) Xiao, Y.; Wu, N.; Wang, L.; Chen, L. A Novel Paper-Based Electrochemical Biosensor Based on N,O-Rich Covalent Organic Frameworks for Carbaryl Detection. *Biosensors* **2022**, *12* (10), 899.
(114) Liang, H.; Wang, L.; Yang, Y.; Song, Y.; Wang, L. A Novel Biosensor Based on Multienzyme Microcapsules Constructed from Covalent-Organic Framework. *Biosens. Bioelectron.* **2021**, *193*, 113553.
(115) Torrinha, C.; Amorim, C. G.; Montenegro, M. C. B. S. M.; Araújo, A. N. Biosensing Based on Pencil Graphite Electrodes. *Talanta* **2018**, *190* (July), 235−247.
(116) Fava, E. L.; Silva, T. A.; Prado, T. M. do; Moraes, F. C. de; Faria, R. C.; Fatibello-Filho, O. Electrochemical Paper-Based Microfluidic Device for High Throughput Multiplexed Analysis. *Talanta* **2019**, *203* (May), 280−286.
(117) Ruecha, N.; Rangkupan, R.; Rodthongkum, N.; Chailapakul, O. Novel Paper-Based Cholesterol Biosensor Using Graphene/Polyvinylpyrrolidone/Polyaniline Nanocomposite. *Biosens. Bioelectron.* **2014**, *52*, 13−19.
(118) Solanki, S.; Soni, A.; Agrawal, V. V.; Pandey, M. K.; Sumana, G. Ultrasensitive Immunosensor Based on Langmuir-Blodgett Deposited Ordered Graphene Assemblies for Dengue Detection. *Langmuir* **2021**, *37* (29), 8705−8713.
(119) Yang, M.; Wang, H.; Liu, P.; Cheng, J. A 3D Electrochemical Biosensor Based on Super-Aligned Carbon NanoTube Array for Point-of-Care Uric Acid Monitoring. *Biosens. Bioelectron.* **2021**, *179*, 113082.
(120) Alvarez-Paguay, J.; Fernández, L.; Bolaños-Méndez, D.; González, G.; Espinoza-Montero, P. J. Evaluation of an Electrochemical Biosensor Based on Carbon Nanotubes, Hydroxyapatite and Horseradish Peroxidase for the Detection of Hydrogen Peroxide. *Sens. Bio-Sensing Res.* **2022**, *37*, 100514.
(121) Qiao, Z.; Yan, Y.; Bi, S. Three-Dimensional DNA Structures in Situ Decorated with Metal Nanoclusters for Dual-Mode Biosensing of Glucose. *Sensors Actuators B Chem.* **2022**, *352* (P2), 131073.
(122) Parlak, O.; İncel, A.; Uzun, L.; Turner, A. P. F.; Tiwari, A. Structuring Au Nanoparticles on Two-Dimensional MoS2 Nanosheets for Electrochemical Glucose Biosensors. *Biosens. Bioelectron.* **2017**, *89*, 545−550.
(123) Khan, R.; Andreescu, S. Mxenes-Based Bioanalytical Sensors: Design, Characterization, and Applications. *Sensors (Switzerland)* **2020**, *20* (18), 5434.
(124) Ye, W.; Guo, J.; Bao, X.; Chen, T.; Weng, W.; Chen, S.; Yang, M. Rapid and Sensitive Detection of Bacteria Response to Antibiotics Using Nanoporous Membrane and Graphene Quantum Dot (GQDs)-Based Electrochemical Biosensors. *Materials (Basel).* **2017**, *10* (6), 603.
(125) Safitri, E.; Heng, L. Y.; Ahmad, M.; Tan, L. L.; Nazaruddin, N.; Suhud, K.; Chiang, C. P.; Iqhrammullah, M. Electrochemical DNA Biosensor Based on Mercaptopropionic Acid-Capped ZnS Quantum Dots for Determination of the Gender of Arowana Fish. *Biosensors* **2022**, *12* (8), 650.
(126) Fatima, B.; Hussain, D.; Bashir, S.; Hussain, H. T.; Aslam, R.; Nawaz, R.; Rashid, H. N.; Bashir, N.; Majeed, S.; Ashiq, M. N.; Najam-ul-Haq, M. Catalase Immobilized Antimonene Quantum Dots Used as an Electrochemical Biosensor for Quantitative Determination of H2O2 from CA-125 Diagnosed Ovarian Cancer Samples. *Mater. Sci. Eng., C* **2020**, *117*, 111296.
(127) Yang, G.; Kampstra, K. L.; Abidian, M. R. High-Performance Conducting Polymer Nanofiber Biosensors for Detection of Biomolecules. *Adv. Mater.* **2014**, *26* (29), 4954−4960.
(128) Wang, H.; Ma, Z. A Cascade Reaction Signal-Amplified Amperometric Immunosensor Platform for Ultrasensitive Detection of Tumour Marker. *Sensors Actuators, B Chem.* **2018**, *254*, 642−647.
(129) Frias, I. A. M.; Vega Gonzales Gil, L. H.; Cordeiro, M. T.; Oliveira, M. D. L.; Andrade, C. A. S. Self-Enriching Electrospun Biosensors for Impedimetric Sensing of Zika Virus. *ACS Appl. Mater. Interfaces* **2022**, *14* (1), 41−48.
(130) Brownlee, B. J.; Claussen, J. C.; Iverson, B. D. 3D Interdigitated Vertically Aligned Carbon Nanotube Electrodes for Electrochemical Impedimetric Biosensing. *ACS Appl. Nano Mater.* **2020**, *3* (10), 10166−10175.
(131) Parlak, O.; Tiwari, A.; Turner, A. P. F.; Tiwari, A. Template-Directed Hierarchical Self-Assembly of Graphene Based Hybrid Structure for Electrochemical Biosensing. *Biosens. Bioelectron.* **2013**, *49*, 53−62.
(132) Ruecha, N.; Rangkupan, R.; Rodthongkum, N.; Chailapakul, O. Novel Paper-Based Cholesterol Biosensor Using Graphene/Polyvinylpyrrolidone/Polyaniline Nanocomposite. *Biosens. Bioelectron.* **2014**, *52*, 13−19.
(133) Camilo, D. E.; Miyazaki, C. M.; Shimizu, F. M.; Ferreira, M. Improving Direct Immunoassay Response by Layer-by-Layer Films of Gold Nanoparticles - Antibody Conjugate towards Label-Free Detection. *Mater. Sci. Eng., C* **2019**, *102*, 315−323.
(134) Chen, M.; Song, Z.; Han, R.; Li, Y.; Luo, X. Low Fouling Electrochemical Biosensors Based on Designed Y-Shaped Peptides with Antifouling and Recognizing Branches for the Detection of IgG in Human Serum. *Biosens. Bioelectron.* **2021**, *178*, 113016.
(135) Mikani, M.; Talaei, S.; Rahmanian, R.; Ahmadi, P.; Mahmoudi, A. Sensitive Electrochemical Sensor for Urea Determination Based on F-Doped SnO 2 Electrode Modified with ZnO-Fe 3

O 4 Nanoparticles Transducer: Application in Biological Fluids. *J. Electroanal. Chem.* **2019**, *840* (March), 285−294.
(136) Solanki, S.; Soni, A.; Pandey, M. K.; Biradar, A.; Sumana, G. Langmuir-Blodgett Nanoassemblies of the MoS2-Au Composite at the Air-Water Interface for Dengue Detection. *ACS Appl. Mater. Interfaces* **2018**, *10* (3), 3020−3028.
(137) Wu, L.; Lu, X.; Dhanjai; Dong, Y.; Wang, X.; Zheng, S.; Chen, J. 2D Transition Metal Carbide MXene as a Robust Biosensing Platform for Enzyme Immobilization and Ultrasensitive Detection of Phenol. *Biosens. Bioelectron.* **2018**, *107*, 69−75.
(138) Wang, H.; Li, H.; Huang, Y.; Xiong, M.; Wang, F.; Li, C. A Label-Free Electrochemical Biosensor for Highly Sensitive Detection of Gliotoxin Based on DNA Nanostructure/MXene Nanocomplexes. *Biosens. Bioelectron.* **2019**, *142* (May), 111531.
(139) Rajapaksha, R. D.; Hashim, U.; Uda, M. N.; Fernando, C. A. N.; Silva, S. N. T. Target SsDNA Detection of E. Coli O157 : H7 through Electrical Based DNA Biosensor. *Microsyst. Technol.* **2017**, *23* (12), 5771−5780.
(140) Castrovilli, M. C.; Bolognesi, P.; Chiarinelli, J.; Avaldi, L.; Cartoni, A.; Calandra, P.; Tempesta, E.; Giardi, M. T.; Antonacci, A.; Arduini, F.; Scognamiglio, V. Electrospray Deposition as a Smart Technique for Laccase Immobilisation on Carbon Black-Nano-modified Screen-Printed Electrodes. *Biosens. Bioelectron.* **2020**, *163*, 112299.
(141) Welch, E. C.; Powell, J. M.; Clevinger, T. B.; Fairman, A. E.; Shukla, A. Advances in Biosensors and Diagnostic Technologies Using Nanostructures and Nanomaterials. *Adv. Funct. Mater.* **2021**, *31* (44), 1−38.
(142) Sassolas, A.; Blum, L. J.; Leca-Bouvier, B. D. Immobilization Strategies to Develop Enzymatic Biosensors. *Biotechnol. Adv.* **2012**, *30* (3), 489−511.
(143) Xu, Z.; Chen, X.; Dong, S. Electrochemical Biosensors Based on Advanced Bioimmobilization Matrices. *TrAC - Trends Anal. Chem.* **2006**, *25* (9), 899−908.
(144) Ying, G. Q.; Wang, M. J.; Yi, Y.; Chen, J. S.; Mei, J. F.; Zhang, Y. L.; Chen, S. Q. Construction and Application of an Electrochemical Biosensor Based on an Endotoxin Aptamer. *Biotechnol. Appl. Biochem.* **2018**, *65* (3), 323−327.
(145) Chakma, B.; Jain, P.; Singh, N. K.; Goswami, P. Development of Electrochemical Impedance Spectroscopy Based Malaria Aptasensor Using HRP-II as Target Biomarker. *Electroanalysis* **2018**, *30* (8), 1847.
(146) Miranda-Castro, R.; Sánchez-Salcedo, R.; Suárez-Álvarez, B.; de-los-Santos-Álvarez, N.; Miranda-Ordieres, A. J.; Jesús Lobo-Castañón, M. Thioaromatic DNA Monolayers for Target-Amplification-Free Electrochemical Sensing of Environmental Pathogenic Bacteria. *Biosens. Bioelectron.* **2017**, *92*, 162−170.
(147) Malvano, F.; Albanese, D.; Pilloton, R.; Di Matteo, M. A New Label-Free Impedimetric Aptasensor for Gluten Detection. *Food Control* **2017**, *79*, 200−206.
(148) Yan, L.; Ma, P.; Liu, Y.; Ma, X.; Chen, F.; Li, M. 3D Coral-like Gold/Carbon Paper Electrode Modified with Covalent and Cross-Linked Enzyme Aggregates for Electrochemical Sensing of Glucose. *Microchem. J.* **2020**, *159* (July), 105347.
(149) Berezhetskyy, A. L.; Sosovska, O. F.; Durrieu, C.; Chovelon, J. Alkaline Phosphatase Conductometric Biosensor for Heavy-Metal Ions Determination. *IRBM* **2008**, *29*, 136−140.
(150) Dundas, C. M.; Demonte, D.; Park, S. Streptavidin-Biotin Technology: Improvements and Innovations in Chemical and Biological Applications. *Appl. Microbiol. Biotechnol.* **2013**, *97* (21), 9343−9353.
(151) Chang, Y.; Ma, X.; Sun, T.; Liu, L.; Hao, Y. Electrochemical Detection of Kinase by Converting Homogeneous Analysis into Heterogeneous Assay through Avidin-Biotin Interaction. *Talanta* **2021**, *234* (June), 122649.
(152) Barton, A. C.; Collyer, S. D.; Davis, F.; Garifallou, G. Z.; Tsekenis, G.; Tully, E.; ÓKennedy, R.; Gibson, T.; Millner, P. A.; Higson, S. P. Labeless AC Impedimetric Antibody-Based Sensors with Pg Ml-1 Sensitivities for Point-of-Care Biomedical Applications. *Biosens. Bioelectron.* **2009**, *24*, 1090−1095.
(153) Chung, D. J.; Kim, K. C.; Choi, S. H. Electrochemical DNA Biosensor Based on Avidin-Biotin Conjugation for Influenza Virus (Type A) Detection. *Appl. Surf. Sci.* **2011**, *257* (22), 9390−9396.
(154) Ahmad, R.; Wolfbeis, O. S.; Hahn, Y. B.; Alshareef, H. N.; Torsi, L.; Salama, K. N. Deposition of Nanomaterials: A Crucial Step in Biosensor Fabrication. *Mater. Today Commun.* **2018**, *17* (July), 289−321.
(155) Eguílaz, M.; Villalonga, R.; Pingarrón, J. M.; Ferreyra, N. F.; Rivas, G. A. Functionalization of Bamboo-like Carbon Nanotubes with 3-Mercaptophenylboronic Acid-Modified Gold Nanoparticles for the Development of a Hybrid Glucose Enzyme Electrochemical Biosensor. *Sensors Actuators, B Chem.* **2015**, *216*, 629−637.
(156) Kaliyaraj Selva Kumar, A.; Zhang, Y.; Li, D.; Compton, R. G. A Mini-Review: How Reliable Is the Drop Casting Technique? *Electrochem. commun.* **2020**, *121*, 106867.
(157) Ceratti, D. R.; Louis, B.; Paquez, X.; Faustini, M.; Grosso, D. A New Dip Coating Method to Obtain Large-Surface Coatings with a Minimum of Solution. *Adv. Mater.* **2015**, *27* (34), 4958−4962.
(158) Jain, S.; Verma, S.; Singh, S. P.; Sharma, S. N. An Electrochemical Biosensor Based on Novel Butylamine Capped CZTS Nanoparticles Immobilized by Uricase for Uric Acid Detection. *Biosens. Bioelectron.* **2019**, *127*, 135−141.
(159) Kumar, S.; Kumar, S.; Srivastava, S.; Yadav, B. K.; Lee, S. H.; Sharma, J. G.; Doval, D. C.; Malhotra, B. D. Reduced Graphene Oxide Modified Smart Conducting Paper for Cancer Biosensor. *Biosens. Bioelectron.* **2015**, *73*, 114−122.
(160) Guan, W.; Zhou, W.; Lu, J.; Lu, C. Luminescent Films for Chemo- and Biosensing. *Chem. Soc. Rev.* **2015**, *44* (19), 6981−7001.
(161) Zhao, Y.; Wei, X.; Peng, N.; Wang, J.; Jiang, Z. Study of ZnS Nanostructures Based Electrochemical and Photoelectrochemical Biosensors for Uric Acid Detection†. *Sensors (Switzerland)* **2017**, *17* (6), 1235.
(162) Verma, S.; Choudhary, J.; Singh, K. P.; Chandra, P.; Singh, S. P. Uricase Grafted Nanoconducting Matrix Based Electrochemical Biosensor for Ultrafast Uric Acid Detection in Human Serum Samples. *Int. J. Biol. Macromol.* **2019**, *130*, 333−341.
(163) Dastider, S. G.; Abdullah, A.; Jasim, I.; Yuksek, N. S.; Dweik, M.; Almasri, M. Low Concentration E. Coli O157:H7 Bacteria Sensing Using Microfluidic MEMS Biosensor. *Rev. Sci. Instrum.* **2018**, *89* (12), 125009.
(164) Chen, Y.; Lu, S.; Zhang, S.; Li, Y.; Qu, Z.; Chen, Y.; Lu, B.; Wang, X.; Feng, X. Skin-like Biosensor System via Electrochemical Channels for Noninvasive Blood Glucose Monitoring. *Sci. Adv.* **2017**, *3* (12), 1−8.
(165) Stine, K. J. Biosensor Applications of Electrodeposited Nanostructures. *Appl. Sci.* **2019**, *9* (4), 797.
(166) Zhang, K.; Wei, J.; Zhu, H.; Ma, F.; Wang, S. Electrodeposition of Gold Nanoparticle Arrays on ITO Glass as Electrode with High Electrocatalytic Activity. *Mater. Res. Bull.* **2013**, *48* (3), 1338−1341.
(167) Lin, J.; Peng, Z.; Liu, Y.; Ruiz-Zepeda, F.; Ye, R.; Samuel, E. L. G.; Yacaman, M. J.; Yakobson, B. I.; Tour, J. M. Laser-Induced Porous Graphene Films from Commercial Polymers. *Nat. Commun.* **2014**, *5*, 5−12.
(168) Rauf, S.; Lahcen, A. A.; Aljedaibi, A.; Beduk, T.; Ilton de Oliveira Filho, J.; Salama, K. N. Gold Nanostructured Laser-Scribed Graphene: A New Electrochemical Biosensing Platform for Potential Point-of-Care Testing of Disease Biomarkers. *Biosens. Bioelectron.* **2021**, *180*, 113116.
(169) Castrovilli, M. C.; Tempesta, E.; Cartoni, A.; Plescia, P.; Bolognesi, P.; Chiarinelli, J.; Calandra, P.; Cicco, N.; Verrastro, M. F.; Centonze, D.; Gullo, L.; Del Giudice, A.; Galantini, L.; Avaldi, L. Fabrication of a New, Low-Cost, and Environment-Friendly Laccase-Based Biosensor by Electrospray Immobilization with Unprecedented Reuse and Storage Performances. *ACS Sustain. Chem. Eng.* **2022**, *10* (5), 1888−1898.

https://doi.org/10.1021/acsmeasuresciau.3c00034
ACS Meas. Sci. Au 2023, 3, 404−433

(170) Xue, J.; Wu, T.; Dai, Y.; Xia, Y. Electrospinning and Electrospun Nanofibers: Methods, Materials, and Applications. *Chem. Rev.* **2019**, *119* (8), 5298−5415.
(171) Mercante, L. A.; Iwaki, L. E. O.; Scagion, V. P.; Oliveira, O. N.; Mattoso, L. H. C.; Correa, D. S. Electrochemical Detection of Bisphenol a by Tyrosinase Immobilized on Electrospun Nanofibers Decorated with Gold Nanoparticles. *Denki Kagaku* **2021**, *2* (1), 41−49.
(172) Singh, V. K.; Kumar, S.; Pandey, S. K.; Srivastava, S.; Mishra, M.; Gupta, G.; Malhotra, B. D.; Tiwari, R. S.; Srivastava, A. Fabrication of Sensitive Bioelectrode Based on Atomically Thin CVD Grown Graphene for Cancer Biomarker Detection. *Biosens. Bioelectron.* **2018**, *105*, 173−181.
(173) Manawi, Y. M.; Ihsanullah; Samara, A.; Al-Ansari, T.; Atieh, M. A. A Review of Carbon Nanomaterials' Synthesis via the Chemical Vapor Deposition (CVD) Method. *Materials (Basel).* **2018**, *11* (5), 822.
(174) Mubarak, a; Hamzah, E.; Toff, M. R. M. Review of Physical Vapour Deposition (PVD) Techniques for Hard Coating. *J. Mek.* **2005**, *20* (20), 42−51.
(175) Azizi, S.; Gholivand, M. B.; Amiri, M.; Manouchehri, I. DNA Biosensor Based on Surface Modification of ITO by Physical Vapor Deposition of Gold and Carbon Quantum Dots Modified with Neutral Red as an Electrochemical Redox Probe. *Microchem. J.* **2020**, *159* (June), 105523.
(176) Naderi Asrami, P.; Saber Tehrani, M.; Aberoomand Azar, P.; Mozaffari, S. A. Impedimetric Glucose Biosensor Based on Nanostructure Nickel Oxide Transducer Fabricated by Reactive RF Magnetron Sputtering System. *J. Electroanal. Chem.* **2017**, *801* (July), 258−266.
(177) Madianos, L.; Tsekenis, G.; Skotadis, E.; Patsiouras, L.; Tsoukalas, D. A Highly Sensitive Impedimetric Aptasensor for the Selective Detection of Acetamiprid and Atrazine Based on Microwires Formed by Platinum Nanoparticles. *Biosens. Bioelectron.* **2018**, *101*, 268−274.
(178) Deng, Y.; Chen, W.; Li, B.; Wang, C.; Kuang, T.; Li, Y. Physical Vapor Deposition Technology for Coated Cutting Tools: A Review. *Ceram. Int.* **2020**, *46* (11), 18373−18390.
(179) Yuan, Y.; Wang, Y.; Wang, H.; Hou, S. Gold Nanoparticles Decorated on Single Layer Graphene Applied for Electrochemical Ultrasensitive Glucose Biosensor. *J. Electroanal. Chem.* **2019**, *855*, 113495.
(180) Graniel, O.; Weber, M.; Balme, S.; Miele, P.; Bechelany, M. Atomic Layer Deposition for Biosensing Applications. *Biosens. Bioelectron.* **2018**, *122* (July), 147−159.
(181) Liu, L.; Zhu, S.; Wei, Y.; Liu, X. L.; Jiao, S.; Yang, J. Ultrasensitive Detection of MiRNA-155 Based on Controlled Fabrication of AuNPs@MoS2 Nanostructures by Atomic Layer Deposition. *Biosens. Bioelectron.* **2019**, *144* (May), 111660.
(182) Yin, F.; Shin, H. K.; Kwon, Y. S. Direct Electrochemistry of Hemoglobin Immobilized on Gold Electrode by Langmuir-Blodgett Technique. *Biosens. Bioelectron.* **2005**, *21* (1), 21−29.
(183) Cabaj, J.; Sołoducho, J.; Nowakowska-Oleksy, A. Langmuir-Blodgett Film Based Biosensor for Estimation of Phenol Derivatives. *Sensors Actuators, B Chem.* **2010**, *143* (2), 508−515.
(184) Iost, R. M.; Madurro, J. M.; Brito-Madurro, A. G.; Nantes, I. L.; Caseli, L.; Crespilho, F. N. Strategies of Nano-Manipulation for Application in Electrochemical Biosensors. *Int. J. Electrochem. Sci.* **2011**, *6* (7), 2965−2997.
(185) Allara, D. L. Critical Issues in Applications of Self-Assembled Monolayers. *Biosens. Bioelectron.* **1995**, *10* (9−10), 771−783.
(186) Arya, S. K.; Solanki, P. R.; Datta, M.; Malhotra, B. D. Recent Advances in Self-Assembled Monolayers Based Biomolecular Electronic Devices. *Biosens. Bioelectron.* **2009**, *24* (9), 2810−2817.
(187) Ulman, A. Formation and Structure of Self-Assembled Monolayers. *Chem. Rev.* **1996**, *96*, 1533−1554.
(188) Alsabbagh, K.; Hornung, T.; Voigt, A.; Sadir, S.; Rajabi, T.; Länge, K. Microfluidic Impedance Biosensor Chips Using Sensing Layers Based on Dna-Based Self-Assembled Monolayers for Label-Free Detection of Proteins. *Biosensors* **2021**, *11* (3), 80.
(189) Iost, R. M.; Crespilho, F. N. Layer-by-Layer Self-Assembly and Electrochemistry: Applications in Biosensing and Bioelectronics. *Biosens. Bioelectron.* **2012**, *31* (1), 1−10.
(190) Barsan, M. M.; Brett, C. M. A. Recent Advances in Layer-by-Layer Strategies for Biosensors Incorporating Metal Nanoparticles. *TrAC - Trends Anal. Chem.* **2016**, *79*, 286−296.
(191) David, M.; Barsan, M. M.; Brett, C. M. A.; Florescu, M. Improved Glucose Label-Free Biosensor with Layer-by-Layer Architecture and Conducting Polymer Poly(3,4-Ethylenedioxythiophene). *Sensors Actuators, B Chem.* **2018**, *255*, 3227−3234.
(192) Ahmed, M. U.; Hossain, M. M.; Safavieh, M.; Wong, Y. L.; Rahman, I. A.; Zourob, M.; Tamiya, E. Toward the Development of Smart and Low Cost Point-of-Care Biosensors Based on Screen Printed Electrodes. *Crit. Rev. Biotechnol.* **2016**, *36* (3), 495−505.
(193) Lee, D.; Bhardwaj, J.; Jang, J. Paper-Based Electrochemical Immunosensor for Label-Free Detection of Multiple Avian Influenza Virus Antigens Using Flexible Screen-Printed Carbon Nanotube-Polydimethylsiloxane Electrodes. *Sci. Rep.* **2022**, *12*, 2311.
(194) Adkins, J. A.; Boehle, K.; Friend, C.; Chamberlain, B.; Bisha, B.; Henry, C. S. Colorimetric and Electrochemical Bacteria Detection Using Printed Paper- and Transparency-Based Analytic Devices. *Anal. Chem.* **2017**, *89* (6), 3613−3621.
(195) Muñoz, J.; Pumera, M. 3D-Printed Biosensors for Electrochemical and Optical Applications. *TrAC - Trends Anal. Chem.* **2020**, *128*, 115933.
(196) Elbadawi, M.; Ong, J. J.; Pollard, T. D.; Gaisford, S.; Basit, A. W. Additive Manufacturable Materials for Electrochemical Biosensor Electrodes. *Adv. Funct. Mater.* **2021**, *31* (10), 1−26.
(197) Stefano, J. S.; Guterres e Silva, L. R.; Rocha, R. G.; Brazaca, L. C.; Richter, E. M.; Abarza Muñoz, R. A.; Janegitz, B. C. New Conductive Filament Ready-to-Use for 3D-Printing Electrochemical (Bio)Sensors: Towards the Detection of SARS-CoV-2. *Anal. Chim. Acta* **2022**, *1191*, 339372.
(198) Loo, A. H.; Chua, C. K.; Pumera, M. DNA Biosensing with 3D Printing Technology. *Analyst* **2017**, *142* (2), 279−283.
(199) López Marzo, A. M.; Mayorga-Martinez, C. C.; Pumera, M. 3D-Printed Graphene Direct Electron Transfer Enzyme Biosensors. *Biosens. Bioelectron.* **2020**, *151*, 111980.
(200) Manzanares-Palenzuela, C. L.; Hermanova, S.; Sofer, Z.; Pumera, M. Proteinase-Sculptured 3D-Printed Graphene/Polylactic Acid Electrodes as Potential Biosensing Platforms: Towards Enzymatic Modeling of 3D-Printed Structures. *Nanoscale* **2019**, *11*, 12124.
(201) López Marzo, A. M.; Mayorga-Martinez, C. C.; Pumera, M. 3D-Printed Graphene Direct Electron Transfer Enzyme Biosensors. *Biosens. Bioelectron.* **2020**, *151*, 111980.
(202) Ito, M.; Yamashita, Y.; Tsuneda, Y.; Mori, T.; Takeya, J.; Watanabe, S.; Ariga, K. 100°c-Langmuir-Blodgett Method for Fabricating Highly Oriented, Ultrathin Films of Polymeric Semiconductors. *ACS Appl. Mater. Interfaces* **2020**, *12* (50), 56522−56529.
(203) Srisombat, L.; Jamison, A. C.; Lee, T. R. Stability: A Key Issue for Self-Assembled Monolayers on Gold as Thin-Film Coatings and Nanoparticle Protectants. *Colloids Surfaces A Physicochem. Eng. Asp.* **2011**, *390* (1−3), 1−19.
(204) Yan, Y.; Björnmalm, M.; Caruso, F. Assembly of Layer-by-Layer Particles and Their Interactions with Biological Systems. *Chem. Mater.* **2014**, *26* (1), 452−460.
(205) Wu, C. Y.; Hsieh, H.; Lee, Y. C. Contact Photolithography at Sub-Micrometer Scale Using a Soft Photomask. *Micromachines* **2019**, *10* (8), 547.
(206) Rose, M. A.; Bowen, J. J.; Morin, S. A. Emergent Soft Lithographic Tools for the Fabrication of Functional Polymeric Microstructures. *ChemPhysChem* **2019**, *20* (7), 909−925.
(207) Fruncillo, S.; Su, X.; Liu, H.; Wong, L. S. Lithographic Processes for the Scalable Fabrication of Micro- And Nanostructures for Biochips and Biosensors. *ACS Sensors* **2021**, *6* (6), 2002−2024.

https://doi.org/10.1021/acsmeasuresciau.3c00034
ACS Meas. Sci. Au 2023, 3, 404−433

(208) Traub, M. C.; Longsine, W.; Truskett, V. N. Advances in Nanoimprint Lithography. *Annu. Rev. Chem. Biomol. Eng.* **2016**, *7*, 583−604.
(209) Arrigan, D. W. M. Nanoelectrodes, Nanoelectrode Arrays and Their Applications. *Analyst* **2004**, *129*, 1157−1165.
(210) Derkus, B. Applying the Miniaturization Technologies for Biosensor Design. *Biosens. Bioelectron.* **2016**, *79*, 901−913.
(211) Laczka, O.; Baldrich, E.; Muñoz, F. X.; Del Campo, F. J. Detection of Escherichia Coli and Salmonella Typhimurium Using Interdigitated Microelectrode Capacitive Immunosensors: The Importance of Transducer Geometry. *Anal. Chem.* **2008**, *80* (19), 7239−7247.
(212) Soraya, G. V.; Chan, J.; Nguyen, T. C.; Huynh, D. H.; Abeyrathne, C. D.; Chana, G.; Todaro, M.; Skafidas, E.; Kwan, P. An Interdigitated Electrode Biosensor Platform for Rapid HLA-B*15:02 Genotyping for Prevention of Drug Hypersensitivity. *Biosens. Bioelectron.* **2018**, *111*, 174−183.
(213) Martín, A.; Kim, J.; Kurniawan, J. F.; Sempionatto, J. R.; Moreto, J. R.; Tang, G.; Campbell, A. S.; Shin, A.; Lee, M. Y.; Liu, X.; Wang, J. Epidermal Microfluidic Electrochemical Detection System: Enhanced Sweat Sampling and Metabolite Detection. *ACS Sensors* **2017**, *2* (12), 1860−1868.
(214) Franssila, S. Etching. *Introd. to Microfabr.* **2010**, 127−141.
(215) Zanouk, R.; Park, B. Y.; Madou, M. J. Fabrication of Microelectrodes Using the Lift-Off Technique. In *Microfluidic Techniques Reviews and Protocols*; Minteer, S. D., Ed.; Humana Press, 2003; p 247.
(216) Pal, R. K.; Pradhan, S.; Narayanan, L.; Yadavalli, V. K. Micropatterned Conductive Polymer Biosensors on Flexible PDMS Films. *Sensors Actuators B. Chem.* **2018**, *259*, 498−504.
(217) Ma, D.; Chon, S.; Cho, S.; Lee, Y.; Yoo, M.; Kim, D.; Lee, D. Y.; Lim, J. K. A Novel Photolithographic Method for Fabrication of Fl Exible Micro-Patterned Glucose Sensors. *J. Electroanal. Chem.* **2020**, *876*, 114720.
(218) Yu, M.; Li, Y. T.; Hu, Y.; Tang, L.; Yang, F.; Lv, W. L.; Zhang, Z. Y.; Zhang, G. J. Gold Nanostructure-Programmed Flexible Electrochemical Biosensor for Detection of Glucose and Lactate in Sweat. *J. Electroanal. Chem.* **2021**, *882*, 115029.
(219) Qin, D.; Xia, Y.; Whitesides, G. M. Soft Lithography for Micro- and Nanoscale Patterning. *Nat. Protoc.* **2010**, *5* (3), 491−502.
(220) Baraket, A.; Lee, M.; Zine, N.; Sigaud, M.; Yaakoubi, N.; Trivella, M. G.; Zabala, M.; Bausells, J.; Jaffrezic-Renault, N.; Errachid, A. Diazonium Modified Gold Microelectrodes onto Polyimide Substrates for Impedimetric Cytokine Detection with an Integrated Ag/AgCl Reference Electrode. *Sensors Actuators, B Chem.* **2013**, *189*, 165−172.
(221) Kaur, G.; Tomar, M.; Gupta, V. Development of a Microfluidic Electrochemical Biosensor: Prospect for Point-of-Care Cholesterol Monitoring. *Sensors Actuators B. Chem.* **2018**, *261*, 460−466.
(222) Shen, M. C.; Lai, J. C.; Hong, C. Y.; Wang, G. J. Electrochemical Aptasensor for Detecting Der P2 Allergen Using Polycarbonate-Based Double-Generation Gold Nanoparticle Chip. *Sens. Bio-Sensing Res.* **2017**, *13*, 75−80.
(223) Lin, W. P.; Wang, W. J.; Lee, C. H.; Jan, F. J.; Wang, G. J. A Two-in-One Immunoassay Biosensor for the Simultaneous Detection of Odontoglossum Ringspot Virus and Cymbidium Mosaic Virus. *Sensors Actuators B Chem.* **2022**, *350*, 130875.
(224) Ahn, J.; Kwon, S.; Jung, S.; Lee, W. S.; Jeong, J.; Lim, H.; Shin, Y. B.; Lee, J. J. Fabrication of Pyrrole-Based Electrochemical Biosensor Platform Using Nanoimprint Lithography. *Adv. Mater. Interfaces* **2018**, *5* (8), 1−5.
(225) Zanut, A.; Cian, A.; Cefarin, N.; Pozzato, A.; Tormen, M. Nanoelectrode Arrays Fabricated by Thermal Nanoimprint Lithography for Biosensing Application. *Biosensors* **2020**, *10* (8), 90.
(226) Presnova, G.; Presnov, D.; Krupenin, V.; Grigorenko, V.; Trifonov, A.; Andreeva, I.; Ignatenko, O.; Egorov, A.; Rubtsova, M. Biosensor Based on a Silicon Nanowire Field-Effect Transistor Functionalized by Gold Nanoparticles for the Highly Sensitive Determination of Prostate Specific Antigen. *Biosens. Bioelectron.* **2017**, *88*, 283−289.
(227) Lee, J. H.; Chae, E. J.; Park, S. j.; Choi, J. W. Label-Free Detection of γ-Aminobutyric Acid Based on Silicon Nanowire Biosensor. *Nano Convergence* **2019**, 13.
(228) Dawson, K.; Baudequin, M.; O'Riordan, A. Single On-Chip Gold Nanowires for Electrochemical Biosensing of Glucose. *Analyst* **2011**, *136* (21), 4507−4513.
(229) Virgilio, F.; Prasciolu, M.; Ugo, P.; Tormen, M. Development of Electrochemical Biosensors by E-Beam Lithography for Medical Diagnostics. *Microelectron. Eng.* **2013**, *111*, 320−324.
(230) Hondred, J. A.; Stromberg, L. R.; Mosher, C. L.; Claussen, J. C. High-Resolution Graphene Films for Electrochemical Sensing via Inkjet Maskless Lithography. *ACS Nano* **2017**, *11* (10), 9836−9845.
(231) Hondred, J. A.; Breger, J. C.; Alves, N. J.; Trammell, S. A.; Walper, S. A.; Medintz, I. L.; Claussen, J. C. Printed Graphene Electrochemical Biosensors Fabricated by Inkjet Maskless Lithography for Rapid and Sensitive Detection of Organophosphates. *ACS Appl. Mater. Interfaces* **2018**, *10* (13), 11125−11134.
(232) Cummins, G.; Desmulliez, M. P. Y. Inkjet Printing of Conductive Materials: A Review. *Circuit World* **2012**, *38* (4), 193−213.
(233) Adly, N.; Feng, L.; Krause, K. J.; Mayer, D.; Yakushenko, A.; Offenhäusser, A.; Wolfrum, B. Flexible Microgap Electrodes by Direct Inkjet Printing for Biosensing Application. *Adv. Biosyst.* **2017**, *1* (3), 1600016.
(234) Grob, L.; Rinklin, P.; Zips, S.; Mayer, D.; Weidlich, S.; Terkan, K.; Weiß, L. J. K.; Adly, N.; Offenhäusser, A.; Wolfrum, B. Inkjet-Printed and Electroplated 3d Electrodes for Recording Extracellular Signals in Cell Culture. *Sensors* **2021**, *21* (12), 3981.
(235) Díaz-Amaya, S.; Zhao, M.; Lin, L. K.; Ostos, C.; Allebach, J. P.; Chiu, G. T. C.; Deering, A. J.; Stanciu, L. A. Inkjet Printed Nanopatterned Aptamer-Based Sensors for Improved Optical Detection of Foodborne Pathogens. *Small* **2019**, *15* (24), 1−14.
(236) Nguyen, T. N. H.; Nolan, J. K.; Cheng, X.; Park, H.; Wang, Y.; Lam, S.; Lee, H.; Kim, S. J.; Shi, R.; Chubykin, A. A.; Lee, H. Fabrication and Ex Vivo Evaluation of Activated Carbon-Pt Microparticle Based Glutamate Biosensor. *J. Electroanal. Chem.* **2020**, *866*, 114136.
(237) Nesaei, S.; Song, Y.; Wang, Y.; Ruan, X.; Du, D.; Gozen, A.; Lin, Y. Micro Additive Manufacturing of Glucose Biosensors: A Feasibility Study. *Anal. Chim. Acta* **2018**, *1043*, 142−149.
(238) Secor, E. B. Principles of Aerosol Jet Printing. *Flex. Print. Electron.* **2018**, *3* (3), 035002.
(239) Parate, K.; Rangnekar, S. V.; Jing, D.; Mendivelso-Perez, D. L.; Ding, S.; Secor, E. B.; Smith, E. A.; Hostetter, J. M.; Hersam, M. C.; Claussen, J. C. Aerosol-Jet-Printed Graphene Immunosensor for Label-Free Cytokine Monitoring in Serum. *ACS Appl. Mater. Interfaces* **2020**, *12* (7), 8592−8603.
(240) Zips, S.; Grob, L.; Rinklin, P.; Terkan, K.; Adly, N. Y.; Weiß, L. J. K.; Mayer, D.; Wolfrum, B. Fully Printed μ-Needle Electrode Array from Conductive Polymer Ink for Bioelectronic Applications. *ACS Applied Materials and Interfaces.* **2019**, *11*, 32778−32786.
(241) Lopez-Larrea, N.; Criado-Gonzalez, M.; Dominguez-Alfaro, A.; Alegret, N.; del Agua, I.; Marchiori, B.; Mecerreyes, D. Digital Light 3D Printing of PEDOT-Based Photopolymerizable Inks for Biosensing. *ACS Appl. Polym. Mater.* **2022**, *4* (9), 6749−6759.
(242) Samper, I. C.; Gowers, S. A. N.; Rogers, M. L.; Murray, D. S. R. K.; Jewell, S. L.; Pahl, C.; Strong, A. J.; Boutelle, M. G. 3D Printed Microfluidic Device for Online Detection of Neurochemical Changes with High Temporal Resolution in Human Brain Microdialysate. *Lab Chip* **2019**, *19* (11), 2038−2048.
(243) Forouzanfar, S.; Pala, N.; Madou, M.; Wang, C. Perspectives on C-MEMS and C-NEMS Biotech Applications. *Biosens. Bioelectron.* **2021**, *180*, 113119.
(244) Hemanth, S.; Halder, A.; Caviglia, C.; Chi, Q.; Keller, S. S. 3D Carbon Microelectrodes with Bio-Functionalized Graphene for Electrochemical Biosensing. *Biosensors* **2018**, *8* (3), 70.

https://doi.org/10.1021/acsmeasuresciau.3c00034
ACS Meas. Sci. Au 2023, 3, 404−433

(245) Sharma, D.; Lee, J.; Shin, H. An Electrochemical Immunosensor Based on a 3D Carbon System Consisting of a Suspended Mesh and Substrate-Bound Interdigitated Array Nanoelectrodes for Sensitive Cardiac Biomarker Detection. *Biosens. Bioelectron.* **2018**, *107*, 10−16.
(246) Thiha, A.; Ibrahim, F.; Muniandy, S.; Dinshaw, I. J.; Teh, S. J.; Thong, K. L.; Leo, B. F.; Madou, M. All-Carbon Suspended Nanowire Sensors as a Rapid Highly-Sensitive Label-Free Chemiresistive Biosensing Platform. *Biosens. Bioelectron.* **2018**, *107*, 145−152.
(247) Tripathy, S.; Bhandari, V.; Sharma, P.; Vanjari, S. R. K.; Singh, S. G. Chemiresistive DNA Hybridization Sensor with Electrospun Nanofibers: A Method to Minimize Inter-Device Variability. *Biosens. Bioelectron.* **2019**, *133*, 24−31.
(248) Pavinatto, F. J.; Paschoal, C. W. A.; Arias, A. C. Printed and Flexible Biosensor for Antioxidants Using Interdigitated Ink-Jetted Electrodes and Gravure-Deposited Active Layer. *Biosens. Bioelectron.* **2015**, *67*, 553−559.
(249) Salazar, P.; Martín, M.; O'Neill, R. D.; González-Mora, J. L. Glutamate Microbiosensors Based on Prussian Blue Modified Carbon Fiber Electrodes for Neuroscience Applications: In-Vitro Characterization. *Sensors Actuators, B Chem.* **2016**, *235*, 117−125.
(250) Shi, W.; Lin, N.; Song, Y.; Liu, C.; Zhou, S.; Cai, X. A Novel Method to Directionally Stabilize Enzymes Together with Redox Mediators by Electrodeposition. *Biosens. Bioelectron.* **2014**, *51*, 244−248.
(251) Gupta, R. K.; Periyakaruppan, A.; Meyyappan, M.; Koehne, J. E. Label-Free Detection of C-Reactive Protein Using a Carbon Nanofiber Based Biosensor. *Biosens. Bioelectron.* **2014**, *59*, 112−119.
(252) Baraket, A.; Lee, M.; Zine, N.; Sigaud, M.; Bausells, J.; Errachid, A. A Fully Integrated Electrochemical Biosensor Platform Fabrication Process for Cytokines Detection. *Biosens. Bioelectron.* **2017**, *93*, 170−175.
(253) Brosel-Oliu, S.; Galyamin, D.; Abramova, N.; Muñoz-Pascual, F. X.; Bratov, A. Impedimetric Label-Free Sensor for Specific Bacteria Endotoxin Detection by Surface Charge Registration. *Electrochim. Acta* **2017**, *243*, 142−151.
(254) Ataide, V. N.; Mendes, L. F.; Gama, L. I. L. M.; De Araujo, W. R.; Paixaõ, T. R. L. C. Electrochemical Paper-Based Analytical Devices: Ten Years of Development. *Anal. Methods* **2020**, *12* (8), 1030−1054.
(255) Lamas-Ardisana, P. J.; Martínez-Paredes, G.; Añorga, L.; Grande, H. J. Glucose Biosensor Based on Disposable Electrochemical Paper-Based Transducers Fully Fabricated by Screen-Printing. *Biosens. Bioelectron.* **2018**, *109*, 8−12.
(256) Sun, X.; Wang, H.; Jian, Y.; Lan, F.; Zhang, L.; Liu, H.; Ge, S.; Yu, J. Ultrasensitive Microfluidic Paper-Based Electrochemical/Visual Biosensor Based on Spherical-like Cerium Dioxide Catalyst for MiR-21 Detection. *Biosens. Bioelectron.* **2018**, *105*, 218−225.
(257) Ming, T.; Cheng, Y.; Xing, Y.; Luo, J.; Mao, G.; Liu, J.; Sun, S.; Kong, F.; Jin, H.; Cai, X. Electrochemical Microfluidic Paper-Based Aptasensor Platform Based on a Biotin-Streptavidin System for Label-Free Detection of Biomarkers. *ACS Appl. Mater. Interfaces* **2021**, *13* (39), 46317−46324.
(258) Arduini, F.; Cinti, S.; Caratelli, V.; Amendola, L.; Palleschi, G.; Moscone, D. Origami Multiple Paper-Based Electrochemical Biosensors for Pesticide Detection. *Biosens. Bioelectron.* **2019**, *126*, 346−354.
(259) Cinti, S.; Moscone, D.; Arduini, F. Preparation of Paper-Based Devices for Reagentless Electrochemical (Bio)Sensor Strips. *Nat. Protoc.* **2019**, *14* (8), 2437−2451.
(260) Pursey, J. P.; Chen, Y.; Stulz, E.; Park, M. K.; Kongsuphol, P. Microfluidic Electrochemical Multiplex Detection of Bladder Cancer DNA Markers. *Sensors Actuators, B Chem.* **2017**, *251*, 34−39.
(261) Zupančič, U.; Jolly, P.; Estrela, P.; Moschou, D.; Ingber, D. E. Graphene Enabled Low-Noise Surface Chemistry for Multiplexed Sepsis Biomarker Detection in Whole Blood. *Adv. Funct. Mater.* **2021**, *31* (16), 1−11.
(262) Lee, G. H.; Lee, J. K.; Kim, J. H.; Choi, H. S.; Kim, J.; Lee, S. H.; Lee, H. Y. Single Microfluidic Electrochemical Sensor System for Simultaneous Multi-Pulmonary Hypertension Biomarker Analyses. *Sci. Rep.* **2017**, *7* (1), 1−8.
(263) Wu, Y.; Xue, P.; Kang, Y.; Hui, K. M. A Paper-Based Microfluidic Electrochemical Immunodevice Integrated with Nanobioprobes onto Graphene Film for Ultrasensitive Multiplexed Detection of Cancer Biomarkers A Paper-Based Microfluidic Electrochemical Immunodevice Integrated with Nanobioprobes On. *Anal. Chem.* **2013**, *85*, 8661−8668.
(264) Liao, Z.; Wang, J.; Zhang, P.; Zhang, Y.; Miao, Y.; Gao, S.; Deng, Y.; Geng, L. Recent Advances in Microfluidic Chip Integrated Electronic Biosensors for Multiplexed Detection. *Biosens. Bioelectron.* **2018**, *121*, 272−280.
(265) Adam, H.; Gopinath, S. C. B.; Md Arshad, M. K.; Adam, T.; Hashim, U.; Sauli, Z.; Fakhri, M. A.; Subramaniam, S.; Chen, Y.; Sasidharan, S.; Wu, Y. S. Integration of Microfluidic Channel on Electrochemical-Based Nanobiosensors for Monoplex and Multiplex Analyses: An Overview. *J. Taiwan Inst. Chem. Eng.* **2023**, *146*, 104814.
(266) Mathur, A.; Roy, S.; Nagabooshanam, S.; Wadhwa, S.; Dubey, S. Effect of Gap Size of Gold Interdigitated Electrodes on the Electrochemical Immunosensing of Cardiac Troponin-I for Point-of-Care Applications. *Sensors and Actuators Reports* **2022**, *4* (July), 100114.
(267) Singh, K. V.; Bhura, D. K.; Nandamuri, G.; Whited, A. M.; Evans, D.; King, J.; Solanki, R. Nanoparticle-Enhanced Sensitivity of a Nanogap-Interdigitated Electrode Array Impedimetric Biosensor. *Langmuir* **2011**, *27* (22), 13931−13939.
(268) Medina-Sánchez, M.; Ibarlucea, B.; Pérez, N.; Karnaushenko, D. D.; Weiz, S. M.; Baraban, L.; Cuniberti, G.; Schmidt, O. G. High-Performance Three-Dimensional Tubular Nanomembrane Sensor for DNA Detection. *Nano Lett.* **2016**, *16* (7), 4288−4296.
(269) McMahon, C. P.; Killoran, S. J.; O'Neill, R. D. Design Variations of a Polymer-Enzyme Composite Biosensor for Glucose: Enhanced Analyte Sensitivity without Increased Oxygen Dependence. *J. Electroanal. Chem.* **2005**, *580* (2), 193−202.
(270) Zain, Z. M.; O'Neill, R. D.; Lowry, J. P.; Pierce, K. W.; Tricklebank, M.; Dewa, A.; Ghani, S. A. Development of an Implantable D-Serine Biosensor for in Vivo Monitoring Using Mammalian d-Amino Acid Oxidase on a Poly (o-Phenylenediamine) and Nafion-Modified Platinum-Iridium Disk Electrode. *Biosens. Bioelectron.* **2010**, *25* (6), 1454−1459.
(271) Farooq, A.; Butt, N. Z.; Hassan, U. Circular Shaped Microelectrodes for Single Cell Electrical Measurements for Lab-on-a-Chip Applications. *Biomed. Microdevices* **2021**, *23* (3), 35.
(272) Dardano, P.; Rea, I.; De Stefano, L. Microneedles-Based Electrochemical Sensors: New Tools for Advanced Biosensing. *Curr. Opin. Electrochem.* **2019**, *17*, 121−127.
(273) Abdullah, H.; Phairatana, T.; Jeerapan, I. Tackling the Challenges of Developing Microneedle-Based Electrochemical Sensors. *Microchim. Acta* **2022**, *189* (11), 440.
(274) Min, J.; Baeumner, A. J. Characterization and Optimization of Interdigitated Ultramicroelectrode Arrays as Electrochemical Biosensor Transducers. *Electroanalysis* **2004**, *16* (9), 724−729.
(275) Yang, H.; Rahman, M. T.; Du, D.; Panat, R.; Lin, Y. 3-D Printed Adjustable Microelectrode Arrays for Electrochemical Sensing and Biosensing. *Sensors Actuators, B Chem.* **2016**, *230*, 600−606.
(276) Kim, S. K.; Hesketh, P. J.; Li, C.; Thomas, J. H.; Halsall, H. B.; Heineman, W. R. Fabrication of Comb Interdigitated Electrodes Array (IDA) for a Microbead-Based Electrochemical Assay System. *Biosens. Bioelectron.* **2004**, *20* (4), 887−894.
(277) Han, D.; Kim, Y. R.; Kang, C. M.; Chung, T. D. Electrochemical Signal Amplification for Immunosensor Based on 3D Interdigitated Array Electrodes. *Anal. Chem.* **2014**, *86* (12), 5991−5998.
(278) Zamzami, M.; Alamoudi, S.; Ahmad, A.; Choudhry, H.; Khan, M. I.; Hosawi, S.; Rabbani, G.; Shalaan, E. S.; Arkook, B. Direct Identification of Label-Free Gram-Negative Bacteria with Bioreceptor-Free Concentric Interdigitated Electrodes. *Biosensors* **2023**, *13* (2), 179.

(279) Liu, G.; Lv, Z.; Batool, S.; Li, M. Z.; Zhao, P.; Guo, L.; Wang, Y.; Zhou, Y.; Han, S. T. Biocompatible Material-Based Flexible Biosensors: From Materials Design to Wearable/Implantable Devices and Integrated Sensing Systems. *Small* **2023**, DOI: 10.1002/smll.202207879.
(280) Kassal, P.; Steinberg, M. D.; Steinberg, I. M. Wireless Chemical Sensors and Biosensors: A Review. *Sensors Actuators, B Chem.* **2018**, *266*, 228−245.
(281) Arakawa, T.; Tomoto, K.; Nitta, H.; Toma, K.; Takeuchi, S.; Sekita, T.; Minakuchi, S.; Mitsubayashi, K. A Wearable Cellulose Acetate-Coated Mouthguard Biosensor for in Vivo Salivary Glucose Measurement. *Anal. Chem.* **2020**, *92* (18), 12201−12207.
(282) García-Carmona, L.; Martín, A.; Sempionatto, J. R.; Moreto, J. R.; González, M. C.; Wang, J.; Escarpa, A. Pacifier Biosensor: Toward Noninvasive Saliva Biomarker Monitoring. *Anal. Chem.* **2019**, *91* (21), 13883−13891.
(283) Wiorek, A.; Parrilla, M.; Cuartero, M.; Crespo, G. A. Epidermal Patch with Glucose Biosensor: PH and Temperature Correction toward More Accurate Sweat Analysis during Sport Practice. *Anal. Chem.* **2020**, *92* (14), 10153−10161.
(284) Lee, H.; Song, C.; Hong, Y. S.; Kim, M. S.; Cho, H. R.; Kang, T.; Shin, K.; Choi, S. H.; Hyeon, T.; Kim, D. H. Wearable/Disposable Sweat-Based Glucose Monitoring Device with Multistage Transdermal Drug Delivery Module. *Sci. Adv.* **2017**, *3* (3), 1−9.
(285) Sempionatto, J. R.; Brazaca, L. C.; García-Carmona, L.; Bolat, G.; Campbell, A. S.; Martin, A.; Tang, G.; Shah, R.; Mishra, R. K.; Kim, J.; Zucolotto, V.; Escarpa, A.; Wang, J. Eyeglasses-Based Tear Biosensing System: Non-Invasive Detection of Alcohol, Vitamins and Glucose. *Biosens. Bioelectron.* **2019**, *137* (March), 161−170.
(286) Keum, D. H.; Kim, S. K.; Koo, J.; Lee, G. H.; Jeon, C.; Mok, J. W.; Mun, B. H.; Lee, K. J.; Kamrani, E.; Joo, C. K.; Shin, S.; Sim, J. Y.; Myung, D.; Yun, S. H.; Bao, Z.; Hahn, S. K. Wireless Smart Contact Lens for Diabetic Diagnosis and Therapy. *Sci. Adv.* **2020**, *6* (17), 1−13.
(287) Kim, J.; Kim, M.; Lee, M. S.; Kim, K.; Ji, S.; Kim, Y. T.; Park, J.; Na, K.; Bae, K. H.; Kim, H. K.; Bien, F.; Lee, C. Y.; Park, J. U. Wearable Smart Sensor Systems Integrated on Soft Contact Lenses for Wireless Ocular Diagnostics. *Nat. Commun.* **2017**, *8*, 14997.
(288) Kim, J.; Jeerapan, I.; Imani, S.; Cho, T. N.; Bandodkar, A.; Cinti, S.; Mercier, P. P.; Wang, J. Noninvasive Alcohol Monitoring Using a Wearable Tattoo-Based Iontophoretic-Biosensing System. *ACS Sensors* **2016**, *1* (8), 1011−1019.
(289) Gao, Y.; Nguyen, D. T.; Yeo, T.; Lim, S. B.; Tan, W. X.; Madden, L. E.; Jin, L.; Long, J. Y. K.; Aloweni, F. A. B.; Liew, Y. J. A.; Tan, M. L. L.; Ang, S. Y.; Maniya, S. D.; Abdelwahab, I.; Loh, K. P.; Chen, C.-H.; Becker, D. L.; Leavesley, D.; Ho, J. S.; Lim, C. T. A Flexible Multiplexed Immunosensor for Point-of-Care in Situ Wound Monitoring. *Sci. Adv.* **2021**, *7* (21), 1−16.
(290) Yu, Y.; Nassar, J.; Xu, C.; Min, J.; Yang, Y.; Dai, A.; Doshi, R.; Huang, A.; Song, Y.; Gehlhar, R.; Ames, A. D.; Gao, W. Biofuel-Powered Soft Electronic Skin with Multiplexed and Wireless Sensing for Human-Machine Interfaces. *Sci. Robot.* **2020**, *5* (41), 1−14.
(291) Bandodkar, A. J.; Gutruf, P.; Choi, J.; Lee, K.; Sekine, Y.; Reeder, J. T.; Jeang, W. J.; Aranyosi, A. J.; Lee, S. P.; Model, J. B.; Ghaffari, R.; Su, C.-J.; Leshock, J. P.; Ray, T.; Verrillo, A.; Thomas, K.; Krishnamurthi, V.; Han, S.; Kim, J.; Krishnan, S.; Hang, T.; Rogers, J. A. Battery-Free, Skin-Interfaced Microfluidic/Electronic Systems for Simultaneous Electrochemical, Colorimetric, and Volumetric Analysis of Sweat. *Sci. Adv.* **2019**, *5* (1), eaav3294.
(292) Zhao, J.; Lin, Y.; Wu, J.; Nyein, H. Y. Y.; Bariya, M.; Tai, L. C.; Chao, M.; Ji, W.; Zhang, G.; Fan, Z.; Javey, A. A Fully Integrated and Self-Powered Smartwatch for Continuous Sweat Glucose Monitoring. *ACS Sensors* **2019**, *4* (7), 1925−1933.
(293) Xiong, Z.; Achavananthadith, S.; Lian, S.; Edward Madden, L.; Ong, Z. X.; Chua, W.; Kalidasan, V.; Li, Z.; Liu, Z.; Singh, P.; Yang, H.; Heussler, S. P.; Kalaiselvi, S. M. P.; Breese, M. B. H.; Yao, H.; Gao, Y.; Sanmugam, K.; Tee, B. C. K.; Chen, P. Y.; Loke, W.; Lim, C. T.; Chiang, G. S. H.; Tan, B. Y.; Li, H.; Becker, D. L.; Ho, J. S. A Wireless and Battery-Free Wound Infection Sensor Based on DNA Hydrogel. *Sci. Adv.* **2021**, *7* (47), 1−12.
(294) De la Paz, E.; Maganti, N. H.; Trifonov, A.; Jeerapan, I.; Mahato, K.; Yin, L.; Sonsa-ard, T.; Ma, N.; Jung, W.; Burns, R.; Zarrinpar, A.; Wang, J.; Mercier, P. P. A Self-Powered Ingestible Wireless Biosensing System for Real-Time in Situ Monitoring of Gastrointestinal Tract Metabolites. *Nat. Commun.* **2022**, *13* (1), 1−11.
(295) Kalantar-Zadeh, K.; Berean, K. J.; Ha, N.; Chrimes, A. F.; Xu, K.; Grando, D.; Ou, J. Z.; Pillai, N.; Campbell, J. L.; Brkljača, R.; Taylor, K. M.; Burgell, R. E.; Yao, C. K.; Ward, S. A.; McSweeney, C. S.; Muir, J. G.; Gibson, P. R. A Human Pilot Trial of Ingestible Electronic Capsules Capable of Sensing Different Gases in the Gut. *Nat. Electron.* **2018**, *1* (1), 79−87.
(296) Xu, J.; Cheng, C.; Li, X.; Lu, Y.; Hu, S.; Liu, G.; Zhu, L.; Wang, N.; Wang, L.; Cheng, P.; Su, B.; Liu, Q. Implantable Platinum Nanotree Microelectrode with a Battery-Free Electrochemical Patch for Peritoneal Carcinomatosis Monitoring. *Biosens. Bioelectron.* **2021**, *185*, 113265.

https://doi.org/10.1021/acsmeasuresciau.3c00034
ACS Meas. Sci. Au 2023, 3, 404−433